

Evaluation of the performance of SVR and ANN Models in Sea Water Level Prediction for the Izmir Coast of the Aegean Sea

Yavuz Karsavran ^{a*}

^a *Istanbul Şişli Vocational School, Architectural Restoration Program, Istanbul, Turkey*
*e-mail: karsavran@itu.edu.tr (*Corresponding Author)*

Abstract

Prediction of sea water level is a very important phenomenon for making future projections for flood control, human living conditions and coastal planning. However, it is not easy to estimate sea water level due to the influence of atmospheric conditions. Thus, Artificial Neural Networks (ANN) and Support Vector Regression (SVR) methods are used for the prediction of seawater level of Izmir Coast based on the time series data. Coefficient of determination (R^2) and root mean square error (RMSE) are applied as model evaluation criteria in this study. 19 months of seawater level data in the time series were used in this study. The results show that the ANN model can predict the water level with R^2 of 0.84 and 0.68 for 1st and 2nd days, respectively, while the SVR model can predict the water level with R^2 of 0.83 and 0.69 for 1st and 2nd days, respectively.

Keywords: ANN; SVR; sea level prediction; Izmir Menteş coast; Aegean Sea.

1. INTRODUCTION

Seawater levels have increased remarkably around the World because of climate change and human efforts (Yesudian and Dawson, 2021; Jin et al., 2023; Karsavran, 2023). The ecological habitat and economy of coastal regions have been devastatingly influenced by sea level rise (Bernstein et al., 2019; Karsavran, 2023). Therefore, accurate estimation of sea level change is important for coastal areas with increasing populations (Jin et al., 2023; Karsavran, 2023).

Alpar et al. (1997) researched the meteorological effects on sea level along the coast of Izmir. Similarly, Çoşkun and Balas (2018) studied the effect of meteorological conditions on sea level changes in Izmir Bay. The possible impact of different sea level rises on the population of Izmir was explored (Aksoy et al., 2017). In addition, the effect of sea level rise on coastal floods in Izmir Bay was simulated with a soft computer program (Türkseven et al., 2023).

Artificial intelligence (AI) methods offer exceptional noise tolerance and learning performance over traditional methods. For this reason, AI methods are chosen in the examination of coastal areas (Guillou and Chapalain, 2021; Karsavran, 2023). Likewise, Song et al. (2022) reported that sea water level prediction with neural networks was

successfully used in studies. For example, Imani et al. (2018) used machine learning to predict water level forecasts in Chiayi Beach.

ANN was first applied to predict sea water level by Röske (1997). A neural network method used to estimate the sea water level of the Yellow Sea (Zhao et al., 2019). Besides, Karsavran and Erdik (2021) applied ANN and SVR methods to estimate the sea level of the Bosphorus. SVR and neural network systems were used to estimate sea level fluctuations in Peninsular West Malaysia (Balogun et al., 2021). Additionally, the sea level of the coastal region of China was predicted by neural network methods (Jin et al., 2023). Lastly, Karsavran (2023) used ANN and SVR to forecast the sea level of Sinop.

Even though there are many studies in this field, there is a need to compare the sea level prediction performances of ANN and SVR methods in the Izmir coast. ANN and SVR models are employed to predict the sea water level in this study. Additionally, we assess the future vision of sea level oscillations of Izmir coast.

2. MATERIALS AND METHODS

2.1 Artificial Neural Network

ANN is a small group of individually connected processing units that carry information to interconnects. The multilayer perceptron (MLP), used for predictions in engineering and science, is made up of at least three interconnected layers of neurons (Chau and Cheng, 2002). The first layer is the input layer to receive external data, and the last layer is the output layer to produce MLP results (Karsavran et al., 2023).

The backpropagation algorithm implements two stages of the data flow. First, inputs move to the network from input layer to the output layer. Finally, the network produces an output vector that encounters the desired target vector and an error is estimated using the predetermined error function. At that point, the error signals are back-propagated from the output layer to the previous layers to update their weights based on the Equation 1:

$$\Delta w_{ij}(n) = \alpha' \Delta w_{ij}(n-1) - \varepsilon \left(\frac{\partial E}{\partial w_{ij}} \right) \quad (1)$$

$\Delta(n)$ and $\Delta w_{ij}(n-1)$ are the weight gets among the input and hidden layers during the n th and $(n-1)$ th steps, α' is the momentum factor that increases the training and aids blocking oscillations, and ε is the learning rate that rises the possibility of preventing the training process from being ambushed in a local minimum instead of a global minimum (ASCE Task Committee, 2000; Karsavran et al., 2023).

2.2 Support Vector Regression

SVR is a statistical learning based neural network method used in various engineering regression problems (Patil et al., 2012). SVR has a hyperplane-driven machine learning algorithm to partition data from one dimension into higher dimensional space (Alshouny et al., 2022). It solves the regression problems with Equation 2:

$$f(x) = \sum_{i=1}^n w_i \phi_i(X) + b \quad (2)$$

w =weight, $\phi_i(X)$ = Kernel function and b =bias. The optimal objective function is shown in Equation 3:

$$\min R = \frac{1}{2} w^2 + C \sum_{i=1}^n (\xi_i + \xi_i^*) \quad (3)$$

The constraint conditions are depicted in Equation 4:

$$\text{Subject_to} \left\{ \begin{array}{l} f(x_i) - y_i \leq \varepsilon + \xi_i \\ y_i - f(x_i) \leq \varepsilon + \xi_i^* \\ \xi_i \geq 0, \xi_i^* \geq 0, i = 1, 2, \dots, n \end{array} \right\} \quad (4)$$

ε = allowable error, C= cost factor, ξ_i and ξ_i^* are relaxation numbers. Both will be greater than zero if there are some prediction errors, otherwise both will be zero (Lin et al., 2020; Karsavran and Erdik, 2021).

2.3 Model Evaluation Criteria

Model performances were obtained according to two different numerical error statistics. These are the root mean square error (RMSE) and coefficient of determination (R^2) given in Equation 5 and Equation 6, respectively (Erdik et al., 2009; Wang et al., 2009).

$$RMSE = \sqrt{\frac{1}{n} \sum_{i=1}^n (WL_f(i) - WL_0(i))^2} \quad (5)$$

$$R^2 = \left[\frac{\frac{1}{n} \sum_{i=1}^n (WL_0(i) - WL_0')(WL_f(i) - WL_f')}{\sqrt{\frac{1}{n} \sum_{i=1}^n (WL_0(i) - WL_0')^2} \cdot \sqrt{\frac{1}{n} \sum_{i=1}^n (WL_f(i) - WL_f')^2}} \right]^2 \quad (6)$$

where $WL_0(i)$ and $WL_f(i)$ are observed and forecasted sea water level, respectively. WL_0' and WL_f' depicts their averages, and n is the number of data.

2.4 Data And Study Area

This research is established on measurements of the Mentés tide measuring station on the coast of Izmir (Figure 1). The sea level data are obtained from the Turkish Sea Level Monitoring System (TUDES, <https://tudes.harita.gov.tr/>), provided at 15-minute time intervals.



Figure 1. The location of the Menteş Tide Gauge Station.

The sea level data used in this study were taken at 15-minute time intervals for 19 months, from June 2020 to January 2022, and were used as is (Figure 2). Missing data were imputed using the linear interpolation method. In this study, 70% of the total data was used for training and the remaining 30% was used for testing all models (Seo et al., 2015; Karsavran, 2023). The same training and testing data were used for each model run and data splitting was done randomly.

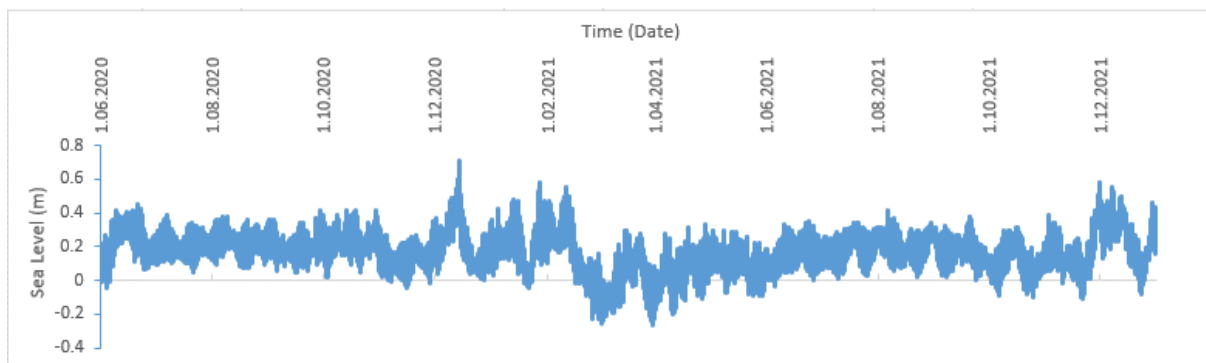


Figure 2. Time series of seawater level in Menteş station.

3. RESULTS AND DISCUSSIONS

In this study, SVR and ANN performances compared for the next 4 days for sea water level prediction of the Izmir coast. First of all, ANN is used to make a decision on the input set combination of the models. The comparison of input sets regarding the prediction results of the ANN model for the next day (t+1) at Menteş Station is depicted in Table 1. Using two values WL(t) and WL(t-1) increased the model performance with an R^2 value of 0.84, while using the next three values (WL(t), WL(t-1)) and WL(t-2) could not increase the performance of the ANN model. As a result, WL(t) and WL(t-1) were used as input sets in all models.

Table 1. ANN model performance for t+1 sea level according to input sets

| Input Set | Output Set | RMSE (m) | R^2 |
|-----------------------------------|------------|----------|-------|
| WL(t) | WL(t+1) | 0.051 | 0.83 |
| WL(t)WL(t-1) | WL(t+1) | 0.051 | 0.84 |
| WL(t)WL(t-1)WL(t-2) | WL(t+1) | 0.051 | 0.84 |
| WL(t)WL(t-1)WL(t-2)WL(t-3) | WL(t+1) | 0.051 | 0.83 |
| WL(t)WL(t-1)WL(t-2)WL(t-3)WL(t-4) | WL(t+1) | 0.051 | 0.83 |

After deciding on the input set, sea water level was estimated for 1, 2, 3 and 4 day lead times using the ANN model containing the Vanilla-Standard back-propagation algorithm. Logsig, tansig and purelin activation functions of hidden and output neurons are used. As a result, R^2 is estimated 0.84 and 0.68 for lead times 1 and 2 days, respectively (Table 2).

The Radial Basis Function (RBF) Kernel is employed to predict the water level with specified lead times in SVR. Most studies on the use of SVR in coastal modeling and prediction have shown that RBF has positive performance (Karsavran and Erdik, 2021; Karsavran, 2023). Accordingly, RBF was applied as the Kernel function and the C parameter of the Kernel is 1000 in this study. In addition, ϵ and σ , which affect the accuracy of the SVR model, are chosen as 0.1 and 0.33, respectively. Finally, R^2 is estimated 0.83 and 0.69 for lead times 1 and 2 days, respectively (Table 2).

Finally, SVR and ANN models have similar performances in predicting sea water level at Menteş Station near Izmir. While, the ANN model predicts sea water level with $R^2 = 0.84, 0.68, 0.53$ and 0.41 , the SVR model estimates $R^2 = 0.83, 0.69, 0.53$ and 0.42 for lead times 1,2,3 and 4 days, respectively. The similarity of ANN and SVR model results is due to the short duration of the data measured at the station. Additionally, there is no overfitting in either model. Accordingly, the SVR and ANN models have good performance in sea level prediction for 1 and 2 day lead times in Izmir coast. However, these models are not ideal to be applied for 3 and 4 day lead times due to the dramatic drop in forecast performance.

This research can be used for short-term projections of sea level along the coast of Izmir. Besides, the results and approach proposed in this study may help the analysis of such phenomena in the future.

Table 2. Model performances with respect to lead time prediction WL(t+L)

| Inputs (t = day) | Prediction (t = day) | ANN | | SVM | |
|---------------------|-------------------------|-------------|-------|-------------|-------|
| | | RMSE (m) | R^2 | RMSE (m) | R^2 |
| WL(t)WL(t-1) | WL(t+1) | 0.051 | 0.84 | 0.051 | 0.83 |
| WL(t)WL(t-1) | WL(t+2) | 0.071 | 0.68 | 0.071 | 0.69 |
| WL(t)WL(t-1) | WL(t+3) | 0.087 | 0.53 | 0.086 | 0.53 |
| WL(t)WL(t-1) | WL(t+4) | 0.097 | 0.41 | 0.097 | 0.42 |



4. CONCLUSIONS

In this study, SVR and ANN models were applied to predict the sea level of Izmir coasts for 1, 2, 3 and 4 day lead times. Both models have similar performances in sea level prediction. They have good performance to predict sea level for 1 and 2 day lead times, unlike 3 and 4 day lead times. Thus, both SVR and ANN models can be applied in sea level forecasts for short-term lead times of 1 and 2 days for the coast of Izmir.

Artificial intelligence based SVR and ANN models can be preferred for emergency sea level rise warning system in the future. The results presented here may provide new information for predicting sea level. Particularly, the models preferred in this study can be used for other coasts of the Aegean Sea and the Mediterranean regions, including but not limited to Çanakkale, Muğla and Aydın.

Acknowledgements

Thanks to Professor Tarkan Erdik for his support in this study. Also, thanks to TUDES for providing the data.

References

- Aksoy, H., Demirel, H., & Seker, D.Z., 2017. Exploring possible impacts of sea level rise: the case of Izmir, Turkey. *International Journal of Global Warming*, 13(3-4), 398-410.
- Alpar, B., Burak, S., & GAZİOĞLU, C., 1997. Effect of weather system on the regime of sea level variations in İzmir Bay. *Journal of Black Sea/Mediterranean Environment*, 3(2).
- Alshouny, A., Elnabwy, M.T., Kaloop, M.R., Baik, A., Miky, Y., 2022. An integrated framework for improving sea level variation prediction based on the integration Wavelet-Artificial Intelligence approaches. *Environmental Modelling & Software*, 152, 105399.
- ASCE Task Committee, 2000. Artificial neural networks in hydrology; I: Preliminary concepts. *J Hydrol Eng* 5(2),115–123. [https:// doi.org/ 10.1061/ \(ASCE\) 1084- 0699\(2000\)5: 2\(115\)](https://doi.org/10.1061/(ASCE)1084-0699(2000)5:2(115)).
- Balogun, A.L., Adebisi, N., 2021. Sea level prediction using ARIMA, SVR and LSTM neural network: assessing the impact of ensemble Ocean-Atmospheric processes on models' accuracy. *Geomatics, Natural Hazards and Risk* 12(1): 653-674.
- Bernstein, A., Gustafson, M.T., Lewis, R., 2019. Disaster on the horizon: The price effect of sea level rise. *J. Financ. Econ.* 134, 253–272. doi: 10.1016/j.jfineco.2019.03.013.
- Chau, K.W., Cheng, C.T., 2002. Real-time prediction of water stage with artificial neural network approach. In *Australian Joint Conference on Artificial Intelligence*, (pp. 715-715). Springer, Berlin, Heidelberg. doi: 10.1007/3-540-36187-1_64.
- Çoşkun, E., & Balas, L., 2018. Sea Level Changes in Izmir Bay. *Int. J. Eng. Res. Dev.*, 14(9), 68-73.
- Erdik, T., Savci, M.E., & Sen, Z., 2009. Artificial neural networks for predicting maximum wave runup on rubble mound structures. *Expert Systems with Applications*, 36(3, part 2), 6403-6408.
- Guillou, N., Chapalain, G., 2021. Machine learning methods applied to sea level predictions in the upper part of a tidal estuary. *Oceanologia* 63(4), 531-544.
- Imani, M., Kao, H.C., Lan, W.H., & Kuo, C.Y., 2018. Daily sea level prediction at Chiayi coast, Taiwan using extreme learning machine and relevance vector machine. *Global and planetary change* 161, 211-221.
- Jin, H., Zhong, R., Liu, M., Ye, C., Chen, X., 2023. Using EEMD mode decomposition in combination with machine learning models to improve the accuracy of monthly sea level predictions in the coastal area of China. *Dynamics of Atmospheres and Oceans* 102,101370.
- Karsavran, Y., Erdik, T., 2021. Artificial Intelligence Based Prediction of Seawater Level: A Case Study for Bosphorus Strait. *International Journal of Mathematical, Engineering and Management Sciences*, 6(5), 1242.
- Karsavran, Y., 2023. Comparison of ANN and SVR based models in sea level prediction for the Black Sea coast of Sinop. *Turkish Journal of*

Maritime and Marine Sciences, 1-8. doi: 10.52998/trjmms.1342164.

Karsavran, Y., Erdik, T., & Ozger, M., 2023. An improved technique for streamflow forecasting between Turkish straits. *Acta Geophysica*, 1-12. <https://doi.org/10.1007/s11600-023-01216-z>.

Lin, G.Q., Li, L.L., Tseng, M.L., Liu, H.M., Yuan, D.D., Tan, R.R., 2020. An improved moth-flame optimization algorithm for support vector machine prediction of photovoltaic power generation. *Journal of Cleaner Production*, 253, 119966. doi: 10.1016/j.jclepro.2020.119966.

Patil, S.G., Mandal, S., Hegde, A.V., 2012. Genetic algorithm based support vector machine regression in predicting wave transmission of horizontally interlaced multilayer moored floating pipe breakwater. *Adv. Eng. Software* 45, 203–212. doi: 10.1016/j.advensoft.2011.09.026.

Röske, F., 1997. Wasserstandsvorhersage mittels neuronaler Netze. *Deutsche Hydrografische Zeitschrift* 49, 71-99.

Seo, Y., Kim, S., Kisi, O., & Singh, V. P., 2015. Daily water level forecasting using wavelet decomposition and artificial intelligence techniques. *Journal of Hydrology* 520, 224-243.

Song, C., Chen, X., Xia, W., Ding, X., Xu, C., 2022. Application of a novel signal decomposition prediction model in minute sea level prediction. *Ocean Engineering* 260, 111961.

Türkseven, O.D., Kısacık, D., Baykal, C., & Güler, I., 2023. Soft Measures Against to Coastal Flooding as A Result of Expected Sea Level Rise in Izmir Bay.

Wang, W.C., Chau, K.W., Cheng, C.T., & Qiu, L., 2009. A comparison of performance of several artificial intelligence methods for forecasting monthly discharge time series. *Journal of Hydrology*, 374(3-4), 294-306. <https://doi.org/10.1016/j.jhydrol.2009.06.019>.

Yesudian, A.N., Dawson, R.J., 2021. Global analysis of sea level rise risk to airports. *Clim. Risk Manag.* 31, 100266. doi: 10.1016/j.crm.2020.100266.

Zhao, J., Fan, Y., Mu, Y., 2019. Sea level prediction in the yellow sea from satellite altimetry with a combined least squares-neural network approach. *Mar. Geodes.* 42(4), 1–23. doi: 10.1080/01490419.2019.1626306.



Using Artificial Intelligence Algorithms to Detect Hate Speech in Social Media Posts

Aytaç Uğur Yerden^a, Kadir Turgut^b

^aDepartment of Industrial Engineering, Istanbul Gedik University, Istanbul, TURKIYE e-mail: aytac.yerden@gedik.edu.tr

^bDepartment of Computing, Istanbul Gedik University, Istanbul, TURKIYE e-mail: kadiring@hotmail.com

Abstract

Detecting hate speech on social media is of great importance to prevent negative impacts on people and communities and to remove such content. However, detecting hate speech is a complex and challenging process due to linguistic and cultural diversity. Therefore, it is important to develop powerful and effective machine learning algorithms. Since detecting such content using traditional methods can be time-consuming and costly, it is stated that artificial intelligence-based machine learning algorithms have great potential in this regard. The aim of this study is to evaluate the performance of artificial intelligence-based machine learning algorithms used in detecting posts containing hate speech on social media. The study focuses on the problem of detecting and managing hate speech on social media platforms. In this study, we will compare the performances of different algorithms and determine the most suitable methods. Additionally, the effects of the dataset and feature extraction methods on algorithm performance will be analyzed. Algorithms are often based on natural language processing techniques and try to detect hate speech by learning features in texts. The performance of these algorithms can vary depending on factors such as language, culture, the attributes they use, and the training dataset, so a comprehensive analysis is required. In the research, the performance of the algorithms used in detecting hate speech was compared with the dataset and feature extraction methods. In this process, the algorithms' linguistic and cross-cultural effectiveness, feature selection and representation, false positive and false negative rates, and overall accuracy will be analyzed.

Keywords: Social Media; Hate Speech; Artificial Intelligence.

1. INTRODUCTION

Social media offers people great freedom to share their thoughts, ideas and feelings. These platforms provide social benefits by facilitating communication and information exchange between people [1]. However, with the widespread use of social media, negative effects such as hate speech have also emerged. Hate speech is expressions of intolerance and hostility towards a specific group, community or individuals [2]. Such expressions can lead to discrimination, violence and social tension in various societies and countries [3].

Detection and management of posts containing hate speech has become an important problem for social media platforms [4]. With traditional methods (e.g., manual review by moderators), detecting and managing such posts can

be time-consuming and costly [5]. Therefore, AI-based machine learning algorithms have great potential to automatically detect and manage hate speech on social media [6].

In this study, the performance evaluation of artificial intelligence-based machine learning algorithms used in detecting posts containing hate speech on social media is discussed. The performance of various algorithms will be compared with the dataset and feature extraction methods used for hate speech detection [7].

As a result, this study, which focuses on the performance evaluation of artificial intelligence-based machine learning algorithms in detecting posts containing hate speech on social media, can be seen as an important step to prevent the spread of hate speech and make social media environments safer.

2. MATERIAL AND METHOD

This study on the performance evaluation of artificial intelligence-based machine learning algorithms in detecting posts containing hate speech on social media aims to use various machine learning and deep learning methods to automatically detect hate speech. The flow diagram of the method used is shown in Figure 1. This section provides a detailed description of the methods and techniques used.

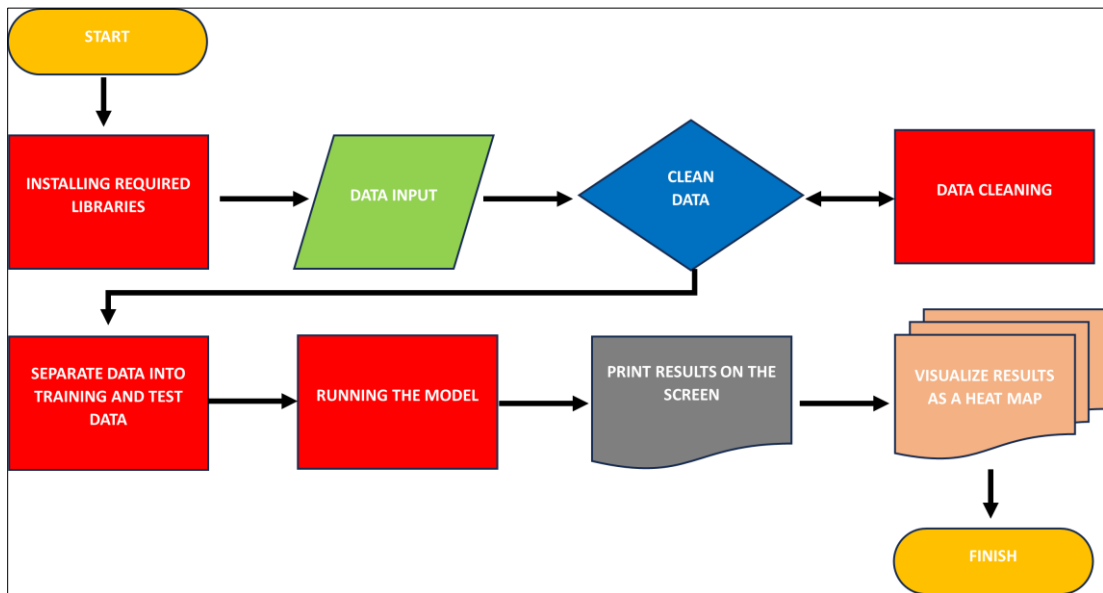


Figure 1. Flow Diagram.

2.1 Data collection and preprocessing

The dataset that forms the basis of this study consists of social media posts that contain and do not contain hate speech. The dataset is the Twitter hate speech dataset obtained from the kaggle.com platform. When determining the dataset, accounts and pages that specifically focused on topics related to hate speech were examined. In the pre-processing step, texts were cleaned to reduce noise and prepared for feature extraction.

2.2 Feature extraction

To detect hate speech using machine learning and deep learning methods, features need to be extracted from texts.

2.3 Classification models

Various machine learning and deep learning algorithms have been used to classify posts that contain and do not contain hate speech. These algorithms are Support Vector Machines, Multi-Layer Perceptron, Decision Trees, Multinomial Naive Bayes, K-Nearest Neighbor, Gradient Boosting, Logistic Regression and Random Forest models.

2.4 Model training and performance evaluation

The dataset is divided into training, validation, and testing subsets for model training and performance evaluation [8]. Classification models were trained on the training dataset and hyperparameter tuning was performed on the validation dataset [9]. To evaluate model performance, various metrics were used on the test dataset. These metrics include AUC-ROC Score, F1-score, Recall, Precision and Accuracy the value under the area curve [10].

2.5 Algorithms

In this section, Support Vector Machines, Multi-Layer Perceptron, Decision Trees, Multinomial Naive Bayes, K-Nearest Neighbor, Gradient Boosting, Logistic Regression and Random Forest algorithms are briefly described.

3. FINDINGS AND DISCUSSION

In this section, first of all, 8 different algorithms were run one by one and it was aimed to reach a successful result.

A high Accuracy, Precision, Recall, F1 Score and AUC-ROC Score indicates that the model is performing well. Low Precision indicates that the number of false positive predictions is high, while low Recall indicates that the number of false negative predictions is high. Ideally, the aim is to achieve a high F1 Score with high Precision and Recall.

Accuracy: Shows the correct rate of all predictions.

Precision: Shows how many of the samples predicted as positive are actually positive.

Recall: Shows how many of the true positive samples were predicted as positive.

F1 Score: Takes the harmonic average of the Precision and Recall value and provides a balanced performance measure.

AUC-ROC Score: Indicates the probability of the classifier correctly sorting a random positive and negative sample.

According to all these results, the performance of the model in detecting tweets containing hate speech can be evaluated. High accuracy indicates the proportion of samples classified correctly. However, Precision, Recall and F1 Score values should also be checked for balance. In particular, attention should be paid to the Precision value to reduce the false alarm rate (false positive) in detecting hate speech. Recall indicates how many true positives were classified correctly, while F1 Score provides a balance between Precision and Recall. AUC-ROC Score indicates the model's ability to distinguish classes; A value close to 1 indicates perfect discrimination.

3.1 Decision Trees (DT) Performance Evaluation

The metric values shown in Table 1 are the results of the performance test conducted with the Decision Trees (DT) algorithm on the twitter-hate-speech dataset.

Table 1. Decision Trees (DT) Metric Values.

| Metric | Value |
|---------------|--------------------|
| AUC-ROC Score | 0.7534795173887220 |
| F1 Score | 0.5628604382929643 |
| Recall | 0.5350877192982456 |
| Precision | 0.5936739659367397 |
| Accuracy | 0.9407164085718754 |

3.2 Gradient Boosting Performance Evaluation

The metric values shown in Table 2 are the results of the performance test conducted with the gradient boosting algorithm on the twitter-hate-speech dataset.

Table 2. Gradient Boosting Metric Values.

| Metric | Value |
|---------------|---------------------|
| AUC-ROC Score | 0.63908761291809610 |
| F1 Score | 0.42737896494156924 |
| Recall | 0.28070175438596490 |
| Precision | 0.89510489510489510 |
| Accuracy | 0.94634756765211950 |

3.3 K-Nearest Neighbour (KNN) Performance Evaluation

The metric values shown in Table 3 are the results of the performance test conducted with the K-Nearest Neighbor (KNN) algorithm on the twitter-hate-speech dataset.

Table 3. K-Nearest Neighbor (KNN) Metric Values.

| Metric | Value |
|---------------|---------------------|
| AUC-ROC Score | 0.59716663120661680 |
| F1 Score | 0.32363636363636360 |
| Recall | 0.19517543859649122 |
| Precision | 0.94680851063829790 |
| Accuracy | 0.94181135617081180 |

3.4 Logistic Regression (LR) Performance Evaluation

The metric values shown in Table 4 are the results of the performance test conducted with the Logistic Regression (LR) algorithm on the twitter-hate-speech dataset.

Table 4. Logistic Regression (LR) Metric Values.

| Metric | Value |
|---------------|--------------------|
| AUC-ROC Score | 0.6665841112381763 |

| | |
|-----------|--------------------|
| F1 Score | 0.4911717495987159 |
| Recall | 0.3355263157894737 |
| Precision | 0.9161676646706587 |
| Accuracy | 0.9504145158767402 |

3.5 Multi-Layered Perceptron (MLP) Performance Evaluation

The metric values shown in Table 5 are the results of the performance test conducted with the Multi-Layered Perceptron (MLP) algorithm on the twitter-hate-speech dataset.

Table 5. Multi-Layered Perceptron (MLP) Metric Values.

| Metric | Value |
|---------------|--------------------|
| AUC-ROC Score | 0.7899180429598504 |
| F1 Score | 0.6103183315038420 |
| Recall | 0.6096491228070176 |
| Precision | 0.6109890109890110 |
| Accuracy | 0.9444705146253715 |

3.6 Multinomial Naive Bayes (MNB) Performance Evaluation

The metric values shown in Table 6 are the results of the performance test conducted with the Multinomial Naive Bayes (MNB) algorithm on the twitter-hate-speech dataset.

Table 6. Multinomial Naive Bayes (MNB) Metric Values.

| Metric | Value |
|---------------|---------------------|
| AUC-ROC Score | 0.66793325532122380 |
| F1 Score | 0.49597423510466987 |
| Recall | 0.33771929824561403 |
| Precision | 0.9333333333333330 |
| Accuracy | 0.95104020021898950 |

3.7 Random Forest (RF) Performance Evaluation

The metric values shown in Table 7 are the results of the performance test conducted with the Random Forest (RF) algorithm on the twitter-hate-speech dataset.

Table 7. Random Forest (RF) Metric Values.

| Metric | Value |
|---------------|--------------------|
| AUC-ROC Score | 0.7381120182973857 |
| F1 Score | 0.6171107994389902 |
| Recall | 0.4824561403508772 |
| Precision | 0.8560311284046692 |
| Accuracy | 0.9572970436414828 |

3.8 Support Vector Machines (SVM) Performance Evaluation

The metric values shown in Table 8 are the results of the performance test conducted with the Support Vector Machines (SVM) algorithm on the twitter-hate-speech dataset.

Table 8. Support Vector Machines (SVM) Metric Values.

| Metric | Value |
|---------------|--------------------|
| AUC-ROC Score | 0.7036963777559109 |
| F1 Score | 0.5675265553869500 |
| Recall | 0.4100877192982456 |
| Precision | 0.9211822660098522 |
| Accuracy | 0.9554199906147348 |

3.9 Support Vector Machines (SVM) Performance Evaluation

Metric values of all algorithms used in performance evaluation tests are shown in Figure 2.

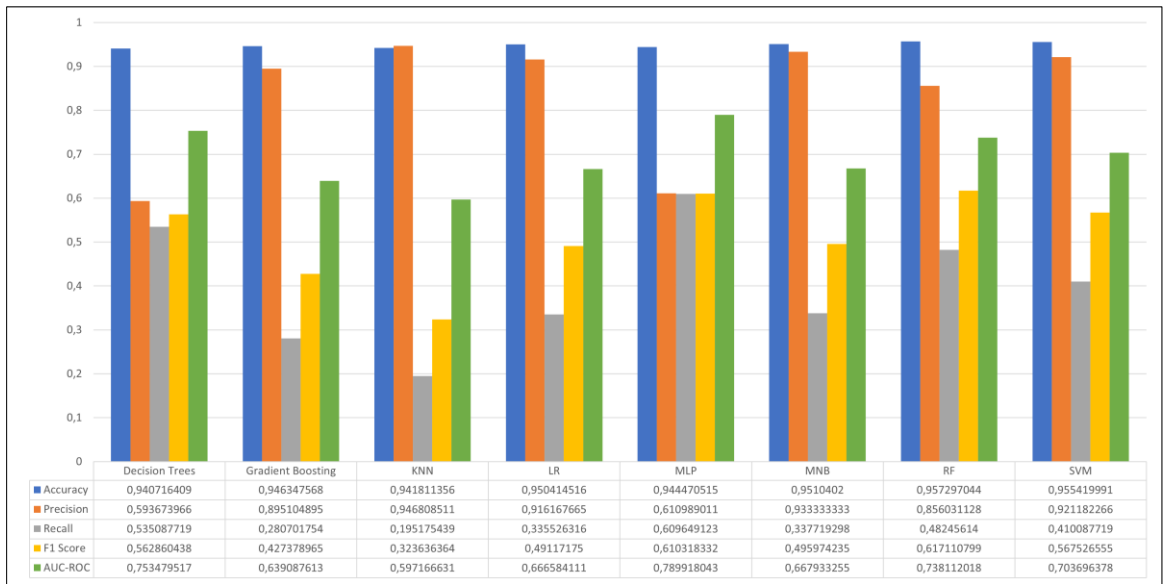


Figure 2. Metric Values of All Algorithms.

Accuracy values of all algorithms used in performance evaluation tests are shown in Figure 3.

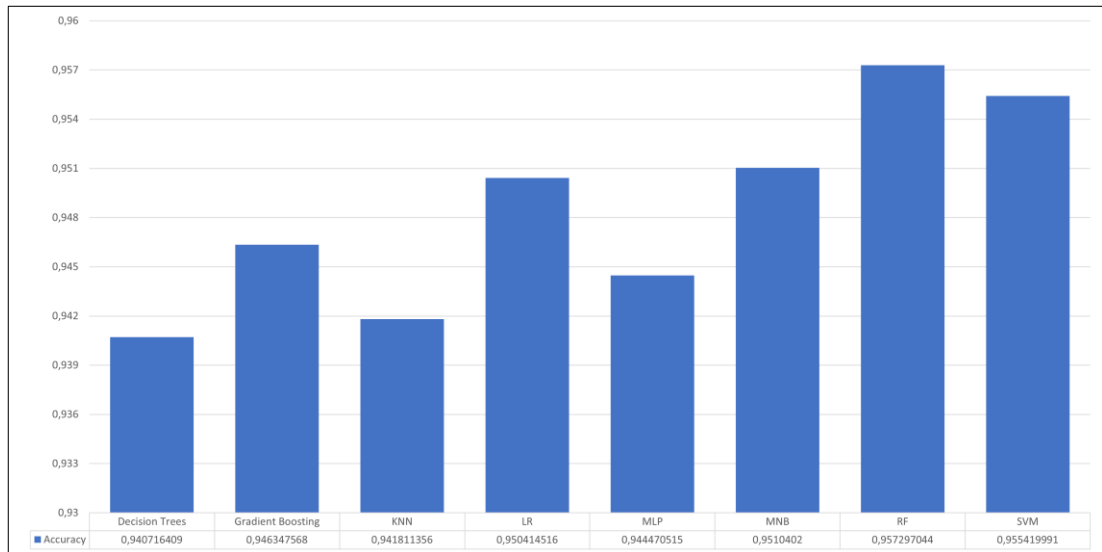


Figure 3. Accuracy Values of All Algorithms.

While Random Forest (RF) has the highest accuracy value, the lowest accuracy value belongs to the Decision Trees (DT) algorithm.

4. CONCLUSION

This study focused on evaluating the performance of various machine learning algorithms in classifying tweets containing hate speech on Twitter. These algorithms include Support Vector Machines, Multi-Layer Perceptron, Decision Trees, Multinomial Naive Bayes, K-Nearest Neighbor, Gradient Boosting, Logistic Regression and Random Forest. For each of these algorithms, their performance was evaluated according to AUC-ROC Score, F1 Score, Recall, Precision and Accuracy metrics. For each algorithm, pre-processing, model definition, training, evaluation and interpretation of the results stages were carried out.

The findings show that, overall, these algorithms have fairly high Accuracy rates. This shows that most of the models' predictions are in line with the actual values and indicates that the models are generally successful. On the other hand, it has been observed that Recall and F1 scores are generally lower, indicating that the models have some difficulties in detecting true positive cases.

Precision metrics show that the models retain a very low rate of false positives (false alarms), while low Recall values indicate that a significant portion of true positive cases are missed. This indicates that models need to be improved, especially in terms of detecting positive cases. F1 scores show that the models deliver balanced but not perfect performance between Precision and Recall.

Although AUC-ROC Score values show that the classification performances of the models are above average, they indicate that no model exhibits perfect performance. This suggests that models may be more prone to certain types of errors and therefore should be used with caution in certain scenarios.

To briefly summarize the performance of each algorithm:

Decision Trees (DT): It made successful predictions with high Accuracy, but remained weak in certain classifications with low Precision and Recall values.

Gradient Boosting: It attracted attention with its high Accuracy and Precision, but its low Recall value caused some true positive cases to be missed.

K-Nearest Neighbor (KNN): Showed high Accuracy and Precision, but missed most of the true positive cases with very low Recall value.

Logistic Regression (LR): Made reliable predictions with high Accuracy and good Precision, but missed some positive cases with low Recall rate.

Multilayer Detectors (MLP): Showed high Accuracy, but Precision, Recall and F1 Score values remained lower.

Multinomial Naive Bayes (MNB): It made successful predictions with very high Accuracy and Precision, but could not detect some positive situations with its low Recall value.

Random Forest (RF): Showed good overall performance with highest Accuracy and good Precision, but missed some positive cases with low Recall rate.

Support Vector Machines (SVM): Showed the second highest Accuracy and Precision, but missed some positive cases with a low Recall rate.

In conclusion, this study shows that various machine learning algorithms can be used effectively to detect content containing hate speech on Twitter. However, it is also clear that each algorithm has its own advantages and limitations and must therefore be carefully selected and implemented. In order for algorithms to be used more effectively and responsibly, they need to be constantly improved and implemented in accordance with ethical standards. Further improving these algorithms and testing them on different data sets may produce more effective results in detecting and blocking content containing hate speech. Therefore, it was concluded that algorithms should be combined or improved to develop a more balanced and effective model. These findings may provide guidance for the development of more powerful and balanced models that can detect hate speech on Twitter.

Although the algorithms examined in this study make an important step forward in the field of hate speech detection, continuous development and careful thought are required in this field. Detection of hate speech is not only a technological issue, but also a social, cultural and ethical responsibility.

Future Studies: This study lays an important foundation for future studies in this field and reveals the potential of machine learning applications in managing social media content. Future studies could focus on datasets in different languages, the changing nature of social media, and the evolution of hate speech.

Acknowledgements

This research is a part of the master's thesis prepared by the researcher at Istanbul Gedik University.

Funding

There are no financial interests in this study.

Declaration of Competing Interest

There is no conflict of interest in this study.

References

- [1] Kaplan, A.M. and Haenlein, M. (2010). Users of the world, unite! The challenges and opportunities of social media. *Business Horizons*, 53(1), 59-68.
- [2] Allport, G. W. (1954). *The nature of prejudice*. Cambridge, MA: Addison-Wesley.
- [3] Perry, B. (2001). *In the name of hate: Understanding hate crimes*. New York: Routledge.
- [4] Chetty, N., and Alathur, S. (2018). Hate speech review in the context of online social networks. *Aggression and Violent Behavior*, 40, 108-118.
- [5] Davidson, T., Warmsley, D., Macy, M., and Weber, I. (2017). Automated hate speech detection and the problem of offensive language. In *Proceedings of the 11th International Conference on Web and social media, ICWSM 2017*, pp. 512-515.

- [6] Schmidt, A., and Wiegand, M. (2017). A survey on hate speech detection using natural language processing. In Proceedings of the Fifth International Workshop on Natural Language Processing for social media (pp. 1-10).
- [7] Fortuna, P., and Nunes, S. (2018). A survey on automatic detection of hate speech in text. *ACM Computing Surveys (CSUR)*, 51(4), 1-30.
- [8] Kohavi, R. (1995). A study of cross-validation and bootstrap for accuracy estimation and model selection. In Proceedings of the 14th International Joint Conference on Artificial Intelligence (pp. 1137-1143). Morgan Kaufmann.
- [9] Bergstra, J., and Bengio, Y. (2012). Random search for hyper-parameter optimization. *Journal of machine learning research*, 13(Feb), 281-305.
- [10] Sokolova, M., and Lapalme, G. (2009). A systematic analysis of performance measures for classification tasks. *Information Processing and Management*, 45(4), 427-437.

Dielectric and Optical Properties of $\text{Eu}_x(\text{Bi}_{1-x})\text{Sr}_2\text{CaCu}_2\text{O}_{6.5}$ ($x=0.3$ and 1) Samples

Utku Canci Matur^{a*}, Özden Aslan Çataltepe^b, Sevcan Tabanlı^c

^aIstanbul Gedik University, Energy Technologies Application and Research Center, Istanbul, Turkey, utku.canci@gedik.edu.tr
(*Corresponding Author)

^bFaculty of Engineering, Istanbul Gedik University, 34876, Istanbul, Türkiye, ozden.aslan@gedik.edu.tr

^cDepartment of Physics Engineering, Istanbul Technical University, 34469, Istanbul, Türkiye, tabanlisevcan@itu.edu.tr

Abstract

Eu-based copper oxide layered ceramics have some interesting dielectric properties depending on its stoichiometric ratios and elements used in ceramics. In this study, optical properties of $\text{EuSr}_2\text{CaCu}_2\text{O}_{6.5}$ and $\text{Eu}_{0.3}\text{Bi}_{0.7}\text{Sr}_2\text{CaCu}_2\text{O}_{6.5}$ samples and dielectric property of $\text{EuSr}_2\text{CaCu}_2\text{O}_{6.5}$ sample were investigated for the first time. Negative real permittivity for $\text{EuSr}_2\text{CaCu}_2\text{O}_{6+x}$ sample was observed at temperature with 373 K and higher temperatures and below than the cross over frequency with 14 Hz. Moreover, it is determined that Eu^{3+} concentration in the material affects the relative emission intensity.

Keywords Eu-based ceramics; Optical properties of Eu-based ceramics; Dielectric properties of Eu-based ceramics.

1. INTRODUCTION

Materials with negative or colossal ($\epsilon' \geq 10^3$) dielectric constant attract the attention of the scientific world due to the next generation technological applications. The variation the dielectric properties of the material by changing its stoichiometric ratio or elements in the materials make the material interesting for scientist. In the literature, dielectric properties of some materials doped with europium such as europium trioxide doped lead boro-tellurite glasses [1], $(\text{Eu,Ca})\text{Cu}_3\text{Ti}_4\text{O}_{12}$ ceramics [2], Eu_2O_3 -doped calcium copper titanium oxide samples [3] having with giant and positive real dielectric constant were investigated by researchers. Z.Güven Özdemir and her research group were studied dielectric properties of $\text{Eu}_x(\text{Bi}_{1-x})\text{Sr}_2\text{CaCu}_2\text{O}_{6.5}$ ceramics (where $x=0, 0.3, 0.5, 0.7$) between 1 Hz and 40 MHz from room temperature to 433 K for the first time[4,5]. Also, the research group determined the dielectric properties of $\text{EuBa}_2\text{Ca}_2\text{Cu}_3\text{O}_{9-x}$ (Eu-1223) and $\text{EuBa}_2\text{Cu}_3\text{O}_{7+x}$ (Eu-123) samples [4,5]. In this article, real dielectric constants of the materials investigated by Güven Özdemir and et al. were reviewed in details. Also, this paper reports the measurements of the optical properties of $\text{EuSr}_2\text{CaCu}_2\text{O}_{6.5}$ coded as (Eu_1Bi_0) -212 and $\text{Eu}_{0.3}\text{Bi}_{0.7}\text{Sr}_2\text{CaCu}_2\text{O}_{6.5}$ coded as $(\text{Eu}_{0.3}\text{Bi}_{0.7})$ -212 and dielectric property of the (Eu_1Bi_0) -212 sample for the first time. It was reported that negative real permittivity for $\text{EuSr}_2\text{CaCu}_2\text{O}_{6+x}$ sample was observed at temperature with 373 K and higher temperatures and below than the cross over frequency with 14 Hz.

The rare earth ions are very effective ions in many optical materials due to a large number of the absorption and

emission bands arising from the transitions between the energy levels [6]. For this reason, many researchers interested in trivalent Eu ions as a luminescence centers in intense red emission which comes from its $^5D_0 \rightarrow ^7F_2$ transition [7,8]. Luminescent materials (or phosphors) as Eu ions and doped Eu ions are good candidates for many technological applications such as fluorescent lightings [9], computer screens [10], lasers [11], temperature sensors [12], solar cells [13], fingerprint detections [14] and biological fluorescence probes [15]. White light can be produced by appropriate combination of the primary colors (red, green and blue). Eu-doped luminescent materials are commercially used as red phosphors for white light production in LEDs due to the intense red emission of Eu^{3+} [16,17]. In the study, the optical properties ($\text{Eu}_{0.3}\text{Bi}_{0.7}$)-212 and (Eu_1Bi_0)-212 samples were investigated for the first time and it was determined that the higher luminescence intensity occurs due to the higher mole concentration of the europium

2. DIELECTRIC PROPERTIES OF Eu- BASED CuO_2 LAYERED MATERIALS

The substances with negative dielectric constant (NDC) [18,19] can be utilized as electromagnetic shielding, optical power limiting, perfect absorber, microelectronic implements such as capacitors, memory devices etc. Also, the materials with NDC have a promising potential for metamaterials applications. The importance of metamaterials (MMs) is to have a negative index of refraction [6,20]. In this context, Eu-based copper oxide materials have not only negative dielectric constant (NDC) but also high dielectric constant depending on mole ratio of Eu elements in the sample and temperatures operating. Eu-123 [21] and ($\text{Eu}_{0.7}\text{Bi}_{0.3}$) $\text{Sr}_2\text{CaCu}_2\text{O}_{6.5}$ coded as ($\text{Eu}_{0.7}\text{Bi}_{0.3}$)-212 [4] ceramics belonging to the Eu-based copper oxide family have the NDC. Eu-123 sample was investigated at room temperature under the magnetic field varying from 0–0.4 T as shown in Figure 1[21].

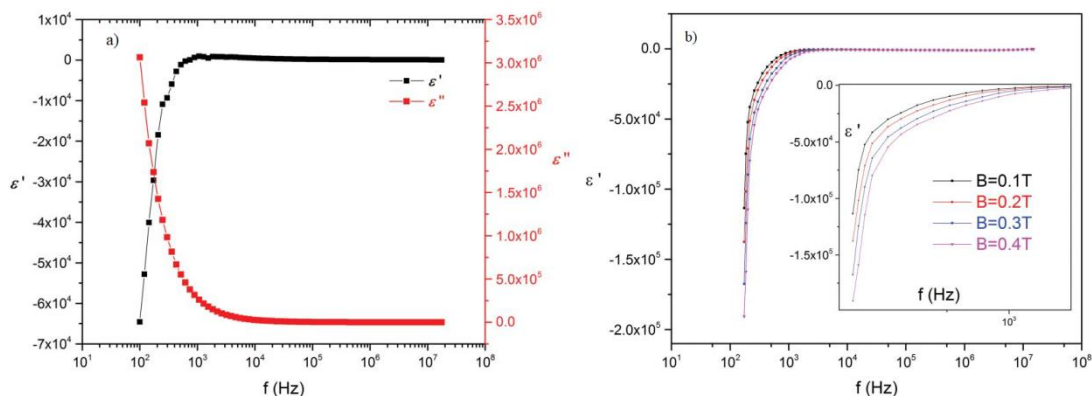


Figure 1. a) The real and imaginary components of complex dielectric function. b) The effect of magnetic field on the real part of complex dielectric function of Eu-123[21].

As is seen Figure 1 that the real part of complex dielectric function (ϵ') of the Eu-123 sample has negative values for low frequencies up to 1 kHz. On the other, when the magnetic field is applied to the sample, the magnitude of ϵ' increases and NDC property extends to 10 kHz at room temperature [21].

($\text{Eu}_{0.7}\text{Bi}_{0.3}$)-212 sample displays the negative real permittivity (NRP) which was observed at 353 K and the higher temperatures as shown in Figure 2 [4].

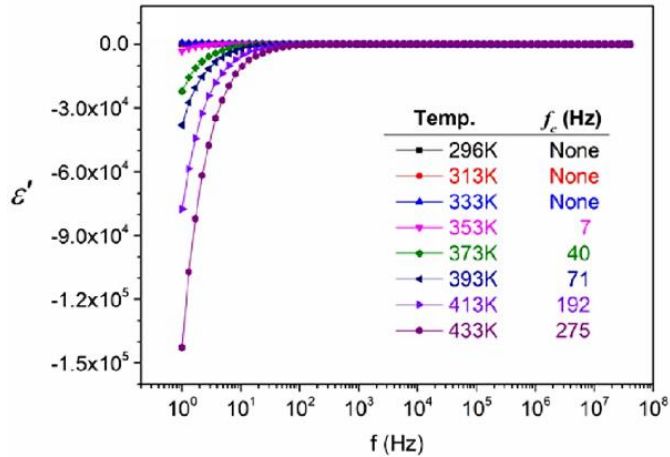


Figure 2. The frequency dependence of the real part of complex permittivity of (Eu_{0.7}Bi_{0.3})-212 material at all temperatures operated [4].

Güven Özdemir and et al. determined that Eu-1223 [22] and (Eu_{0.5}Bi_{0.5})-212 [5] samples have very high dielectric constant ($\epsilon \geq 10^3$), and they suggested that the materials investigated can be good candidate for next generation electronics and large scale integrated microelectronics technology (Figure 3). The effect of temperature on dielectric properties of Eu-1223 was investigated within the range of 5 Hz–13 MHz frequencies and 298 K–408 K temperatures. It was determined that at each temperature, the Eu-1223 sample has high dielectric constants. Also, Eu-1223 material acts as a very high dielectric material, which are greater than 103, up to 300 kHz for 408 K [22].

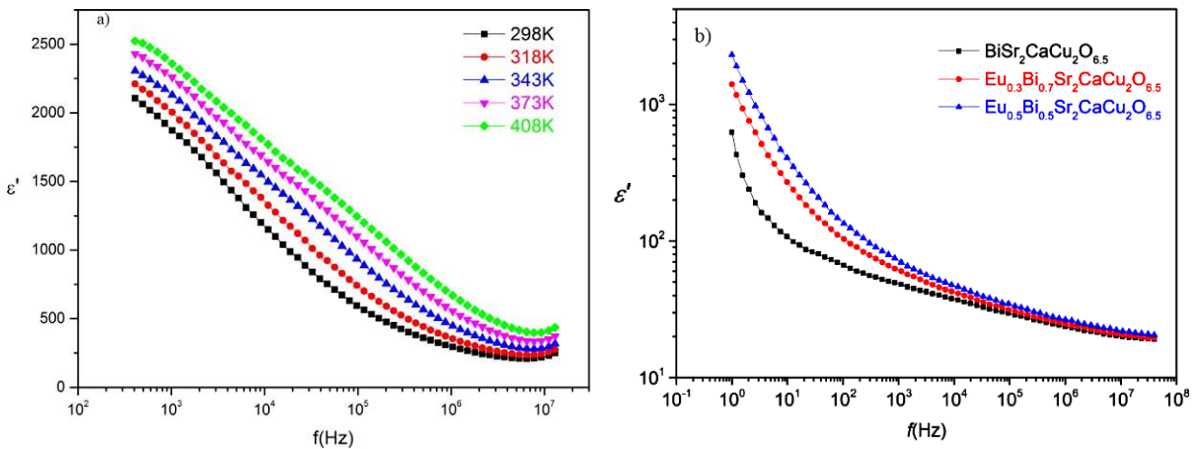


Figure 3. a) Frequency dependence of the real components of the complex dielectric functions at different temperatures for Eu-1223 material [3]. b) for the (Eu_xBi_{1-x})-212 samples (x=0, 0.3, 0.5) at room temperature [2].

It was determined by dielectric measurements that (Eu_{0.5}Bi_{0.5})-212 sample exhibits a higher dielectric constant and lower dielectric loss relative to (Eu₀Bi₁)-212. In this context, partial europium substitution into BiSr₂CaCu₂O_{6.5} system was proposed as an effective dopant for producing better dielectric material with the lower dielectric loss.

3. SYNTHESIZES OF $\text{Eu}_x(\text{Bi}_{1-x})\text{Sr}_2\text{CaCu}_2\text{O}_{6.5}$ SAMPLES

To prepare of Eu substituted Bi based materials ($\text{Eu}_x\text{Bi}_{1-x}\text{Sr}_2\text{CaCu}_2\text{O}_{6.5}$ where $x=0.3$ and 1) which were synthesized by conventional solid-state reaction, $\text{Eu}_2\text{O}_3(99.99\%)$, $\text{Bi}_2\text{O}_3(99.99\%)$, $\text{SrO}(99.99\%)$, $\text{CaO}(99.99\%)$ and $\text{CuO}(99.99\%)$, powders supplied from Sigma Aldrich were used. Powders in appropriate stoichiometric ratios were ground in an agate mortar for 2 h. The pressure of approximately 10^9 Pa was applied for pressing the resultant powder and the pellet obtained was place in Al_2O_3 crucible and heated at a rate of $1^\circ\text{C}/\text{min}$ to 950°C for 24 h in an atmospheric environment. For fine powder mixture, the material was ground for 15 min and then it was again pressed. At the end of process, the pellet was sintered at 950°C for 24 h in an atmospheric environment [5].

4. RESULTS AND DISCUSSION

4.1. Dielectric Property of (Eu_1Bi_0) -212 material

NOVO Control Broadband Dielectric/Impedance analyzers with Quatro Cryo system in the temperature interval between 296–433 K within frequency range 1 Hz and 40 MHz was used to take impedance measurements. In the study, dielectric property of the (Eu_1Bi_0) -212 sample was measured by impedance analyzer for the first time. Negative real permittivity for (Eu_1Bi_0) -212 material was observed at temperature with 373 K and higher temperatures and below than the cross over frequency with 14 Hz as shown in Figure 4.

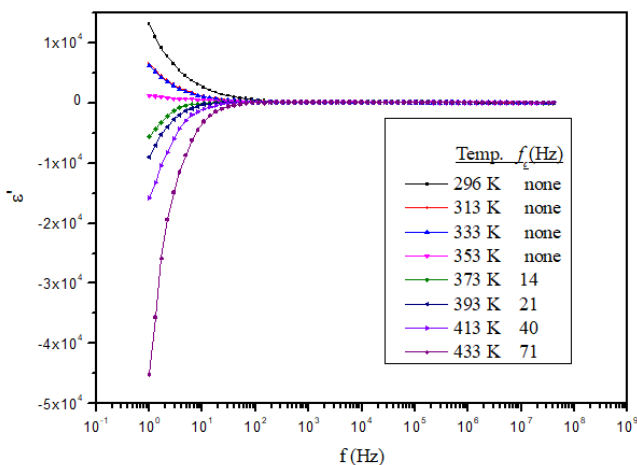


Figure 4. Frequency dependence of the real components of the sample at different temperatures for (Eu_1Bi_0) -212 material.

It was determined that substitution of europium for bismuth in the stoichiometric ratio higher than 0.5 enables negative real permittivity at temperatures of 353 K and above [4].

4.2. Optical Properties of (Eu_1Bi_0) -212 and $(\text{Eu}_{0.3}\text{Bi}_{0.7})$ -212 Samples

The optical properties of (Eu_1Bi_0) -212 and $(\text{Eu}_{0.3}\text{Bi}_{0.7})$ -212 samples were investigated in the article for the first time. The emission spectra were collected using a monochromator (Princeton Instruments - model SP2500i) and Silicon detector (Acton series: SI-440) for the detection of the optical region luminescence. The samples were excited with a continuous wave (CW) laser operating at 485 nm. All measurements were performed at room temperature.

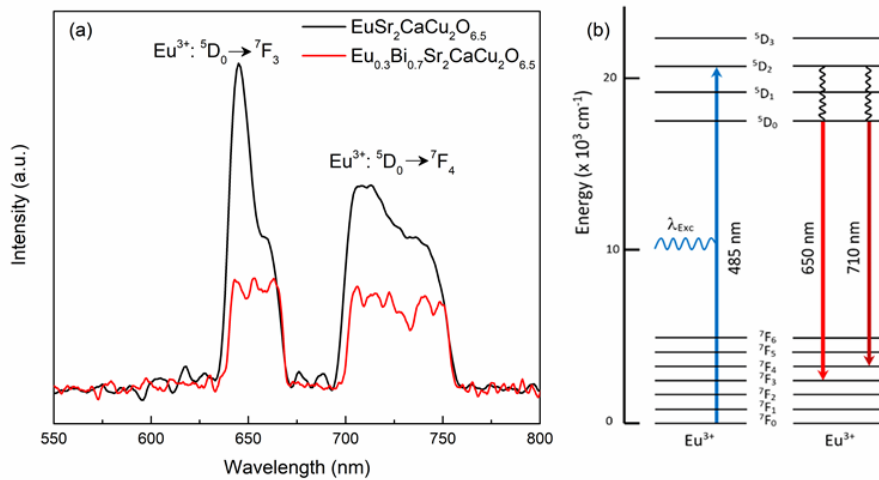


Figure 5. (a) The luminescence spectra of the (Eu_1Bi_0) -212 (black line) and $(\text{Eu}_{0.3}\text{Bi}_{0.7})$ -212 (red line) samples under 485 nm laser excitation with CW laser, (b) the energy level diagram of Eu^{3+} and possible paths.

Figure 5 (a) shows the luminescence spectra of the (Eu_1Bi_0) -212 and $(\text{Eu}_{0.3}\text{Bi}_{0.7})$ -212 samples under 485 nm laser excitation with CW laser. The red emission of Eu^{3+} is located at around 650 nm associated with ${}^5\text{D}_0 \rightarrow {}^7\text{F}_3$ transition. The dark-red emission located between 700 nm and 750 nm due to the ${}^5\text{D}_0 \rightarrow {}^7\text{F}_4$ transition. The energy level diagram of Eu^{3+} and possible paths under 485 nm excitation is also given in Figure 5 (b). Eu^{3+} ions are first excited to ${}^5\text{D}_2$ level under 485 nm laser excitation and then decay into ${}^5\text{D}_0$ level by non-radiative relaxation process. The electrons decay radiatively from ${}^5\text{D}_0$ level to the ${}^7\text{F}_3$ and ${}^7\text{F}_4$ level to produce red and dark-red emissions, respectively. The reduction of the relative emission intensity of ${}^5\text{D}_0 \rightarrow {}^7\text{F}_3$ and ${}^5\text{D}_0 \rightarrow {}^7\text{F}_4$ transitions can be due to not only Eu^{3+} concentration but also structure of the host matrix.

5. CONCLUSION

In this study, the luminescence spectra, and real parts of dielectric function for (Eu_1Bi_0) -212 and $(\text{Eu}_{0.3}\text{Bi}_{0.7})$ -212 materials have been investigated for the first time. As is known, the dielectric function describes the response of the materials to the electromagnetic radiation mediated through the interaction of photons and the electrons and it depends upon the electronic band structure of the material. Also, the real part of the dielectric constant determines some optical property of a material [23]. In this context the luminescence spectra of the (Eu_1Bi_0) -212 and $(\text{Eu}_{0.3}\text{Bi}_{0.7})$ -212 materials give the comparison of the concentration of the europium element in the materials investigated. The higher luminescence intensity occurs due to the higher mole concentration of the europium. As is known, the mole concentration of the europium affects the dielectric properties of the materials. Hence, europium as dopants ions makes the materials a promising candidate for some electronic devices needing color red on their displays [24]. NRP for (Eu_1Bi_0) -212 sample was observed at temperature with 373 K and higher temperatures and below than the cross over frequency with 14 Hz for the first time. Moreover (Eu_1Bi_0) -212 and $(\text{Eu}_{0.3}\text{Bi}_{0.7})$ -212 materials which displays dielectric properties depending on temperatures operating and Eu-concentration, may be utilized for some chemical sensors, light emitting devices or solar energy conversion.

Conflicts of interest

There are no conflicts of interest in this work.

References

- [1] Devaraja C., Jagadeesha Gowda G. V., Eraiah B., A. M. Talwar, Dahshan A., Nazrin S.N., Structural, conductivity and dielectric properties of europium trioxide doped lead boro-tellurite glasses, *J Alloy Compd*, 898 (2022) 162967, <https://doi.org/10.1016/j.jallcom.2021.162967>
- [2] Doležal V., Jakeš V., Petrášek J., Ctibor P., Jankovský O., Rubešová K., Sedmidubský D., Dielectric properties of (Eu,Ca)Cu₃Ti₄O₁₂ ceramics prepared by a sol-gel method, *J Phys Chem Solids*, 178 (2023), <https://doi.org/10.1016/j.jpcs.2023.111334>
- [3] Evangeline T G, Annamalai A R, Ctibor P., Effect of Europium Addition on the Microstructure and Dielectric Properties of CCTO Ceramic Prepared Using Conventional and Microwave Sintering, *Molecules*, 28(4) (2023)1649; <https://doi.org/10.3390/molecules28041649>
- [4] Kılıç M., Özdemir Z., Karabul Y., Karataş Ö., Çataltepe Ö. A., Negative real permittivity in (Bi_{0.3}Eu_{0.7})Sr₂CaCu₂O_{6.5} ceramic, *Phys. B: Condens. Matter*, 584 (2020) 412080.
- [5] Özdemir Z.G., Kılıç M., Karabul Y., Erdönmez S., İçelli O., The influence of the partially europium substitution on the AC electrical properties of BiSr₂CaCu₂O_{6.5} ceramics, *Process. Appl. Ceram.*, 13 (4) (2019) 323-332.
- [6] Omar N. A. S, Fen Y. W., Matori K. A, Zaid M. H. M., Norhafizah M. R, Nurzilla M., Zamratul M.I.M., Synthesis and optical properties of europium doped zinc silicate prepared using low cost solid state reaction method, *J. Mater. Sci.: Mater. Electron.*, 27 (2) (2016) 1092-1099.
- [7] Cincovic M.M., Jankovic B., Milicevic B., Antic Z. and Whiffen R.K., Dramicanin M.D., The comparative kinetic analysis of the non-isothermal crystallization process of Eu³⁺ doped Zn₂SiO₄ powders prepared via polymer induced sol–gel method, *Powder Technol.*, 249, (2013) 497-512.
- [8] Rojas S.S., Souza J.E.D., Yukimitu K., Hernandez A.C., Structural, thermal and optical properties of CaBO and CaLiBO glasses doped with Eu³⁺, *J. Non- Cryst. Solids*, (398) (2014) 57-61.
- [9] Kido J., Hayase H., Hongawa K., Nagai K., Okuyama K., Bright red light-emitting organic electroluminescent devices having a europium complex as an emitter, *Appl. Phys. Lett.*, 65 (1994) 2124-2126.
- [10] Kumari P. and Manam J., Enhanced red emission on co-doping of divalent ions (M²⁺= Ca²⁺, Sr²⁺, Ba²⁺) in YVO₄: Eu³⁺ phosphor and spectroscopic analysis for its application in display devices, *Spectrochim. Acta A Mol. Biomol. Spectrosc.*, 152 (2016)109-118.
- [11] Hebert T., Wannemacher R., Lenth W., Macfarlane R., Blue and green cw upconversion lasing in Er: YLiF₄, *Appl. Phys. Lett.*, 57 (1990) 1727-1729.
- [12] Dey R., Rai V.K., Yb³⁺ sensitized Er³⁺ doped La²O₃ phosphor in temperature sensors and display devices, *Dalton Trans.*, 43 (2014) 111-118.
- [13] Shalav A., Richards B., Trupke T., Krämer K., Güdel H.-U, Application of NaYF₄: Er³⁺ up-converting phosphors for enhanced near-infrared silicon solar cell response, *Appl. Phys. Lett.*, 86 (2005) 013505.
- [14] Wang J., Wei T., Li X., Zhang B., Wang J., Huang C., Yuan Q., Near-Infrared-Light-Mediated Imaging of Latent Fingerprints based on Molecular Recognition, *Angew. Chem.*, 126 (2014) 1642-1646.
- [15] Tsukube H., Shinoda S., Lanthanide complexes in molecular recognition and chirality sensing of biological substrates, *Chem. Rev.*, 102 (2002) 2389-2404.
- [16] Hu Y., Zhuang W., Ye H., Zhang S., Fang Y., Huang X., Preparation and luminescent properties of (Ca_{1-x}, Sr_x) S: Eu²⁺ red-emitting phosphor for white LED, *J. Lumin.*, 111, (2005) 139-145.
- [17] Haque M.M., Kim D.K., Luminescent properties of Eu³⁺ activated MLa₂(MoO₄)₄ based (M= Ba, Sr and Ca) novel red-emitting phosphors, *Mater. Lett.*, 63 (2009) 793-796.
- [18] Ramakrishna S. A., Grzegorzczak T.M., *Physics and Applications of Negative Refractive Index Materials*, 1st ed. Washington: CRC Press, (2008).
- [19] Hou Q., Sun K., Xie P., Yan K., Fan R., Liu Y., Ultrahigh dielectric loss of epsilon-negative copper granular composites, *Mater. Lett.*, 169 (2016) 86–89.
- [20] Shelby R.A., Smith D.R., Schultz S., Experimental verification of a negative index of refraction, *Science*, 292 (2001) 77–79.
- [21] Özdemir Z., Kılıç M., Karabul Y., Çataltepe Ö. A., İçelli O., Onbaşı U., Structural and dielectric properties of Europium based copper oxide layered perovskite material, *Ferroelectrics*, 510 (1) (2017)121-131.
- [22] Özdemir Z., Kılıç M., Karabul Y., Mısırlıoğlu B., Çataltepe Ö. A., İçelli O., Synthesis and characterization of EuBa₂Ca₂Cu₃O_{9-x}: The influence of temperature on dielectric properties and charge transport mechanism, *Mater. Sci. Semicond. Process*, 63 (2017) 196-202.
- [23] Tripathy S.K., Pattanaik A., Optical and electronic properties of some semiconductors from energy gaps, *Opt. Mater.*, 53 (2016) 123-133.
- [24] Yashodha S. R., Dhananjaya N., Manohara S. R., Yogananda H. S., Investigation of photoluminescence and dielectric properties of europium-doped LaOCl nanophosphor and its Judd–Ofelt analysis, *J. Mater. Sci.: Mater. Electron.*, 32,(2021) 11511–11523.



The Liquefaction Behavior of Leachate-Contaminated of Sand under Cyclic Loads

Aytaç Yaşargün^{a*}, Ayfer Erken^b

^aCivil Engineering Faculty, Istanbul Technical University, Maslak 34467, Istanbul, Turkey
e-mail: yasargunaytac@itu.edu.tr (*Corresponding Author)

^bCivil Engineering Faculty, Istanbul Technical University, Maslak 34467, Istanbul, Turkey
e-mail: erken@itu.edu.tr

Abstract

Uncontrolled solid waste affects the stress-strain behavior of the sand as well as causes an environmental problem. In this research, the effect of leachate on the dynamic behavior of sand has been studied and the results were compared with clean sand with different saturation degrees. The modified split molds at 50 mm diameter and 100 mm height were used to prepare the leachate-contaminated sand. Both contaminated and clean sand samples were prepared by dry pluviation method. After preparation, the sand samples in the modified mold were put in the leachate wastewater to keep for different cure times. Then they were installed on the dynamic triaxial test system at 0.1 Hz and the same cyclic stress ratio. During the saturation process to prevent the structure of contaminated sands from being disturbed, samples were not passed through CO₂ and distilled water. Stress-controlled cyclic tests were conducted at on both clean and contaminated sand consolidated at 100 kPa isotropically. After consolidation phase the measured B values varied between 0.45-0.93. Results show that leachate-contaminated sands are more liquefiable depending on cure time at the same saturation value and saturated clean sand samples and partially saturated leachate-contaminated sand samples show similar liquefaction behavior under the same cyclic ratio.

Keywords: Leachate; Critical Deformation Level; Contaminated Sand; Dynamic Behavior; Curing Time.

1. INTRODUCTION

The storage of solid waste is one of the important environmental problems. According to 2022 data, 14.1% of the domestic solid waste collected in Turkey is currently stored as unsanitary disposal by municipalities, and this amount is approximately 4.27 million tons/year [1]. The wrong storage of urban waste effects soil layers, ground and underground water. In sanitary landfill sites, the waste water leachate contamination affects the engineering properties of soil layers underlying solid waste landfill. Leachates disrupt the properties of soil within the chemical content. In practice, impermeable clay barriers have been used to minimize the infiltration of leachates in sanitary landfills. For this reason, clay soil contamination with leachate has been studied by many researchers. Tuncan et al.,1988 conducted a series of laboratory tests on clay soils mixed and cured with leachate to study the unconfined compressive strength, stress-strain relationship, and permeability [2].

The unconfined compression strength increased with increasing leachate wastewater ratio for short curing periods and decreased with longer curing periods. Roque and Didier, 2006 studied the effect of demineralized water and acid leachate on the hydraulic conductivity of fine-grained soils. Hydraulic conductivity increased due to the

chemical reactions of the acidic leachate [3]. Another hydraulic conductivity characteristics of soils including fines have been studied by Nayak et al. (2007) Contaminated specimens were prepared by mixing soil with leachate in the amounts of 5%, 10% and 20% by weight. The results indicated a small reduction in maximum dry density and an increase in hydraulic conductivity [4]. Brandl, 1992 treated silty clays with different chemicals to determine the effect of chemicals on the plasticity index. The results indicated that the plasticity index decreased as hydraulic conductivity increased [5]. Although there are many studies conducted with clays contaminated with waste-water leachate, there is a lack of research on how leachate affects the dynamic properties of sands. The effect of sand exposed to different pollutants on the dynamic behavior has been studied by many researchers. Naeini and Shojaedin (2014) used Firoozkuh sand containing 4%, 8%, and 12% crude oil by weight leaked from oil pipelines and tanks and revealed that contamination levels up to 8% increased liquefaction resistance, but beyond this threshold, higher contamination levels led to a decrease in liquefaction resistance [6]. Rajabi and Sharifipour (2018) research short term and long term influence on small strain shear modulus (G_{max}) of hydrocarbon contaminated sand [7]. Hosseini and Hajiani Buserian (2019) studied the behavior of circular foundations resting on oil-contaminated sand under cyclic loading. Hosseini, and Hajiani Boushehrian, 2019 conducted experimental and numerical analysis and developed equations that predict the number of loading periods to achieve the required settlement based on the contaminated layer thickness and contamination percentage [8]. Nasiri et al. (2023) conducted tests to explore the time-dependent dynamic and static properties (shear modulus, damping ratio, and friction angle) of sands contaminated with 6% crude oil and with a relative density of 60% [9].

In this study, the effect of the leachate on the dynamic behavior of sand has been studied leaking from the unsanitary disposal or carelessly constructed clay barriers in sanitary landfills. The contaminated samples prepared in modified molds and cured for periods ranging from 3 to 299 days, and partly saturated clean sand samples prepared in standard molds were tested in the cyclic triaxial test system undrained to analyze the liquefaction behavior of samples. Firstly, the clean sand was prepared in standard and modified mold. Thus the behavioral effect was examined when exposed to dynamic loading under the same conditions. Then, the clean and leachate-contaminated samples were consolidated under 100 kPa pressure for one day, and then the day after, dynamic experiments were carried out by applying a constant strain in the range of $\pm\sigma_{dev}/2\sigma'_{con} = 0.28-0.30$. As a result, the liquefaction behavior and critical deformation levels of the samples under the influence of contamination were compared with clean sands.

2. MATERIAL AND METHODS

2.1 Akpınar Sand

Sands used in this study have been obtained from Akpınar district in İstanbul, Turkey. The soil is poorly graded sand (SP). Table 1 gives the index properties of sand. The grain size distribution of sand is presented in Figure 1. The specific gravity of Akpınar sand is 2.69, the minimum void ratio is 0.558 and the maximum void ratio is 0.874.

Table 1. Soil properties of Akpınar sand.

| Soil Properties | Value |
|------------------------------|-------|
| Specific Gravity | 2.69 |
| Maximum void ratio | 0.874 |
| Minimum void ratio | 0.558 |
| D50 (mm) | 0.30 |
| D10 (mm) | 0.23 |
| Coefficient of Uniformity Cu | 1.434 |
| Coefficient of Curvature, Cc | 0.96 |
| Fines Content, FC | 0 |

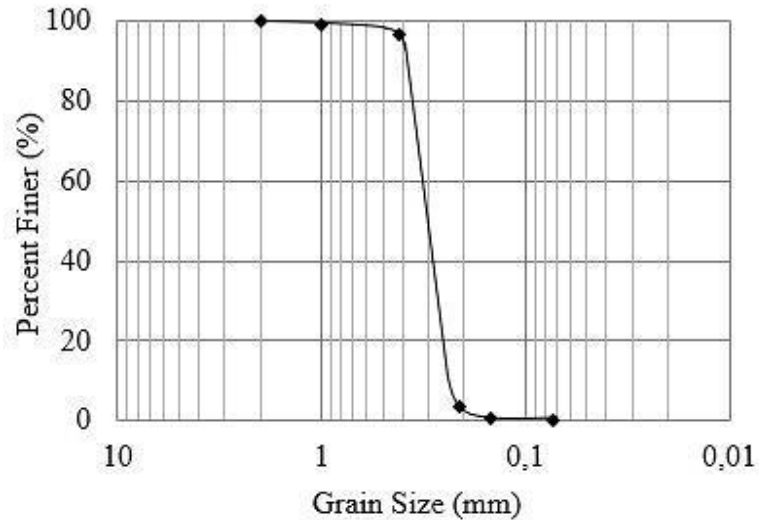


Figure 1. Grain size distribution of Akpınar sand.

2.2 Leachate Wastewater

Leachate wastewater obtained from the site of the Kemberburgaz sanitary landfill in Istanbul has been used in this research. The composition of leachate which is given in Table 2 was determined from tests conducted in Istanbul Technical University Environmental Laboratory. Sample 1 is the composition of young leachate about one week and sample 2 is old leachate about 22 months.

The chemical composition of leachate will vary depending on the age of the landfill. If a leachate sample is collected during the acid phase decomposition the pH value will be low and the concentrations of BOD₅, COD, and nutrients will be high. Meanwhile the composition of leachate on the methane phase BOD₅, COD, and nutrients value will be significantly lower [10].

In this research, the pH value calculated at the one-week sample increased from 7.30 to 9.25 at the 22-month sample. The value of chemical oxygen demand obtained at the one-week sample decreased from 37665 to 3595 in the 22-month sample.

Table 2. The composition of leachate.

| Parameter | Unit | Sample 1 (One Week) | Sample 2 (22 Months) |
|---------------------------------|------------------------|------------------------|-------------------------|
| pH | - | 7.30 | 9.25 |
| Total Solids | Mg/l | 29710 | 15350 |
| Total Volatile Solids | Mg/l | 13055 | 2670 |
| Total Dissolved Solids | Mg/l | 27950 | 12320 |
| Total Volatile Dissolved Solids | Mg/l | 13510 | 1385 |
| Alkalinity | Mg/l CaCO ₃ | 14300 | 7740 |
| COD | Mg/l | 37665 | 3595 |
| Soluble. COD | Mg/l | 30000 | 1570 |
| BOD ₅ | Mg/l | 24450 | 400 |
| T.P | Mg/l | 30 | 10 |
| TKN | Mg/l | 2780 | 1120 |
| NH ₃ -N | Mg/l | 2550 | 820 |
| Chloride | Mg/l | 3266 | 4190 |
| Sulfate | Mg/l | 120 | 356 |
| Ca Hardness | Mg/l CaCO ₃ | 6919 | 110 |
| Total. Hardness | Mg/l CaCO ₃ | 8595 | 1808 |
| Ca | Mg/l | 2773 | 44 |
| Mg | Mg/l | 409 | 468 |
| Na | Mg/l | 2590 | 2853 |
| K | Mg/l | 1700 | 1700 |
| Fe | Mg/l | 41.2 | 184 |
| Ni | Mg/l | 0.82 | 1.16 |
| Cr | Mg/l | 0.64 | 0.76 |
| Zn | Mg/l | 1.27 | 3.04 |

2.3 Sample Preparation of Contaminated Sand

Dynamic tests have been conducted on laboratory sand samples. Sand samples have been prepared in a modified split mold. The diameter of the mold is 50mm and the height is 100mm. Mold has a bottom and upper cap (Figure 2). Both caps are perforated. To study the effect of wastewater leachate on the dynamic behaviour of sand, samples have been prepared at the same relative density but varied saturation degrees. The relative densities of sand samples change from 50% to 60% (Table 3). Sand samples have been prepared by the dry pluviation method in 3 layers [11]. The funnel has been used to pour the sand into the mold in every layer. Sand samples contaminated by 100% leachate wastewater have been used in this research and the results compared clean sand sample results.



Figure 2. Modified steel mold 3-D view and prepared sample in the modified steel mold.

2.4 Samples Curing

Contaminated sand samples were prepared at 100% cure ratio. The curing time was started by dipping the sand samples into the leachate pool, covering the upper level of the mold, as seen in Figure 3. It was observed that some of the air bubbles in the samples get out as a result of the leachate entering through the drainage holes into the samples prepared by dry pluviation. An increase in gaseous emissions occurred due to chemical reaction in the leachate tank. In order to prevent the methane gas accumulation, the gas outlet valve was periodically opened to release trapped air. During this process, samples were stored in the leachate tank for different curing times at 3 days, 10 days, 103 days, 146 days, and 299 days.

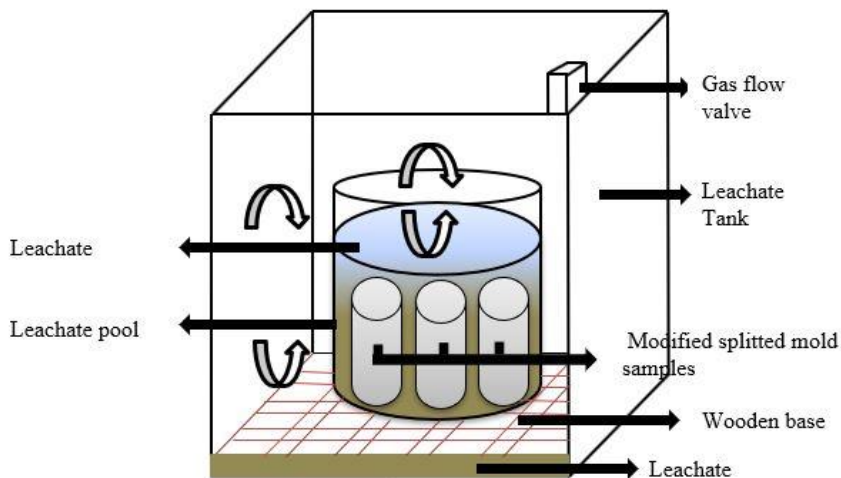


Figure 3. Leachate Tank Schema.

2.5 Cyclic Triaxial Test System

The stress-controlled cyclic triaxial test was used to evaluate the cyclic behaviour of undisturbed and reconstituted laboratory sand samples. DTC 311 - 0094 model, developed by the Japanese company "Seiken Inc" located in Istanbul Technical University, Soil Mechanics Laboratory, was used. The size of triaxial test samples varies between 5 cm and 7.5 cm in diameter, and 10 cm to 15 cm in height. In the apparatus, a pneumatic stress-controlled system is capable of generating cyclic axial triaxial stresses at frequencies between 0.001 Hz and 2 Hz. The testing system individually enables the measure and the record of axial vertical load, axial vertical displacement, pore water pressure; and the specimen volume change. The stress-strain relationships of the sand specimens can be determined under isotropic and anisotropic conditions by applying sinusoidal loads. It is possible to measure the initial elastic modulus of sands with the gap sensors connected to the top of the triaxial cell and monotonic loading with different loading rates.

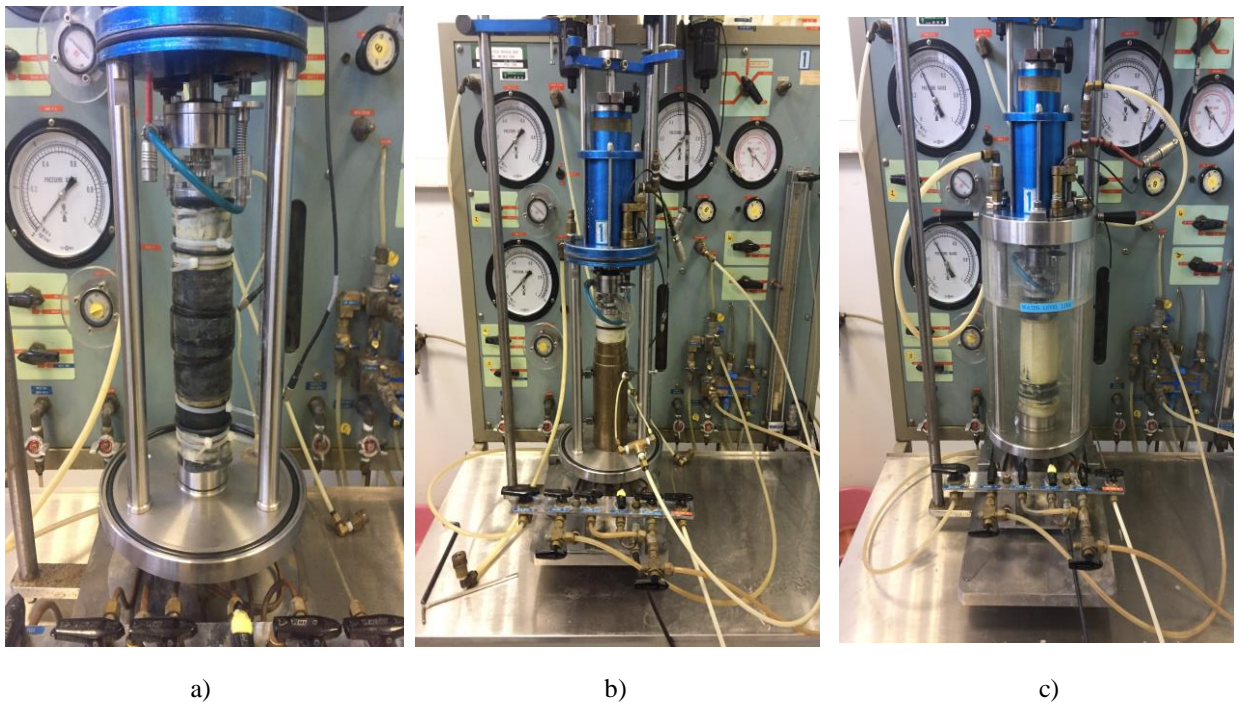


Figure 4. Cyclic-triaxial test system a) modified mold set-up b) standard mold set-up c) consolidated set-up.

The leachate-contaminated sand samples prepared with the modified splitted mold shown in Figure 4.a and the clean sand samples prepared in the standart mold shown in Figure 4.b placed in the cyclic triaxial test system. Both specimens with 5 cm diameter and 10 cm height were isotropically consolidated to the 100 kPa in the triaxial cell and the backpressures ranging between 200-300 kPa were applied one day to provide saturation (Figure 4.c). The calculated B values were between 45-93 %. After the consolidation process, a cyclic axial load was applied under the undrained condition (CU). The frequency of the cyclic load was 0.1 Hz during the tests. The cyclic test properties of sand samples are given in Table 3.

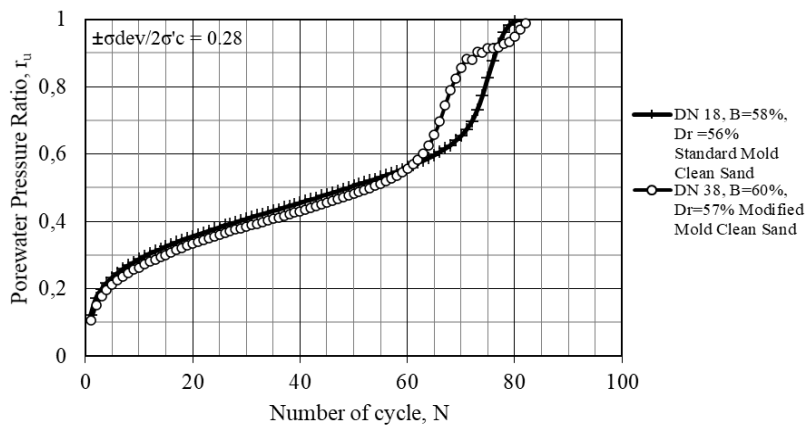
Table 3. Cyclic test properties of sand.

| Test No | Cure Ratio (%) | $\pm\sigma_{dev}/2\sigma'_{con}$ | N $\varepsilon=\pm 2.5\%$ | N $\varepsilon=\pm 0.5\%$ | Cure Time (days) | Dr (%) | B (%) | σ_{ef} (kPa) |
|---------|----------------|----------------------------------|------------------------------|------------------------------|------------------|--------|-------|---------------------|
| DN13 | 0 | 0.28 | 98 | 91 | - | 60 | 0.52 | 100 |
| DN18 | 0 | 0.28 | 82 | 76 | - | 56 | 0.58 | 100 |
| DN38 | 0 | 0.28 | 77 | 69 | - | 57 | 0.60 | 100 |
| DN40 | 0 | 0.28 | 32 | 24 | - | 57 | 0.93 | 100 |
| DN52 | 0 | 0.30 | 52 | 42 | - | 53 | 0.72 | 100 |
| DN29 | 100 | 0.30 | 248 | 238 | 146 | 56 | 0.45 | 100 |
| DN31 | 100 | 0.30 | 35 | 23 | 103 | 57 | 0.60 | 100 |
| DN58 | 100 | 0.30 | 34 | 17 | 299 | 55 | 0.57 | 100 |
| DN72 | 100 | 0.28 | 59 | 50 | 3 | 50 | 0.65 | 100 |
| DN87 | 10 | 0.28 | 90 | 82 | 10 | 60 | 0.53 | 100 |

3. RESULT AND DISCUSSIONS

3.1 Comparison of the Clean Sand Prepared with Modified and Standard Mold

As seen in Figure 5, in order to examine the effect of the sample preparation mold on the structure, a dynamic load at $\pm\sigma_{dev}/2\sigma'_{con} = 0.28$ stress level was applied to the clean sand samples prepared in the standard and the modified mold under the same conditions. The comparison focused on the relationship between porewater pressure ratio and number of cycles, as well as dynamic axial deformation and number of cycles. The DN18 sample was prepared in a standard mold and $Dr = 56\%$ and $B = 0.58$ value were obtained. The DN38 sample was prepared in a modified sample preparation mold, and in order to be in similar conditions to the contaminated samples, it was soaked in a clean water tank for 24 hours before being set-up to the dynamic triaxial test cell. The DN38 sample was consolidated to 100 kPa under the same conditions as the DN18 sample, and Dr was obtained as 57% and the B value was measured as 0.60 . Figure 5. shows the relationship between the pore water pressure ratio and the number of cycles for the DN18 sample prepared in the standard mold with a Skempton-B value of 0.58 and the modified mold with a Skempton-B value of 0.60 . Both show similar behavior up to $N=60$ cycles. Likewise, in the dynamic deformation – number of cycles shown in Figure 6, at the $\varepsilon=\pm 2.5\%$ deformation level defined as the failure criterion, the porewater pressure ratio of the DN38 sample up to $N = 77$ cycles is $r_u = 0.95$, and the porewater pressure ratio of the DN18 sample up to $N = 82$ cycles is $r_u = 1.00$. It has been observed that the dynamic behaviours of sand samples prepared in the standard mold and the modified mold are generally similar.

**Figure 5.** DN 18- DN38 Pore water pressure – Number of cycle.

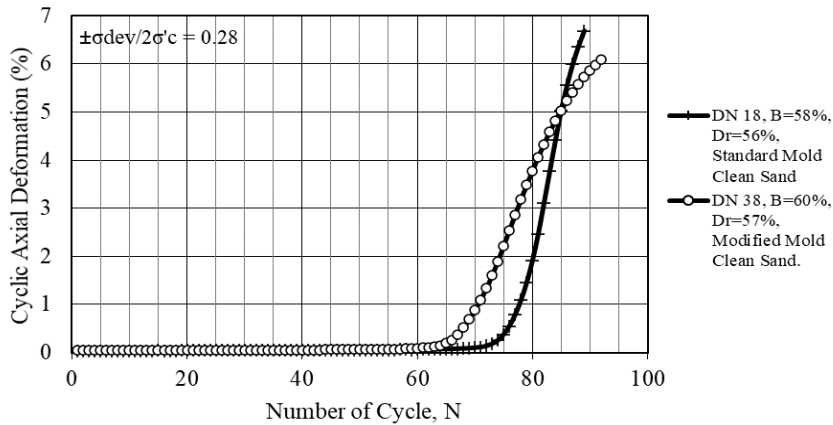


Figure 6. DN 18 - DN38 Cyclic axial deformation – Number of cycle.

3.2 Comparing the Cyclic Triaxial Test Results of Clean and Contaminated Sand

Figure 7 shows the relationship between the pore water pressure and the number of cycles and figure 8 shows the cyclic axial deformation and the number of cycles of clean sand samples. To study the effect of contamination on pore water generation and the cyclic axial deformation, $\pm\sigma_{dev}/2\sigma'_{con}=0.28-0.30$ dynamic stress level was applied to the sand samples prepared at the relative density varied from $Dr=\%50$ to $Dr=\%60$.

According to figure 8 the clean DN13 sample, which has the same saturation value as the contaminated DN87 sample with $t=10$ days curing time, reached failure deformation levels at $N=90$ and $N=98$ cycle numbers, respectively with a similar movement. As seen in Figure 7 the pore water pressure ratio is $ru=1.00$ in both samples at this level. Leachate-contaminated DN69 sample with curing time of $t=45$ days and the saturation value $B=0.51$ reaches $\epsilon=\pm 2.5\%$ dynamic axial deformation level at $N=69$ cycles and the pore water pressure ratio at this cycle was measured $ru=0.98$. The contaminated and clean sand samples with similar saturation degrees, DN69 sample with $t=45$ days curing time liquefied first, then DN87 sample with $t=10$ days curing time, and finally clean DN13 sample shows liquefaction behaviour. As the curing time increase pore water pressure generation and cyclic axial strain increment occur at a lower number of cycles.

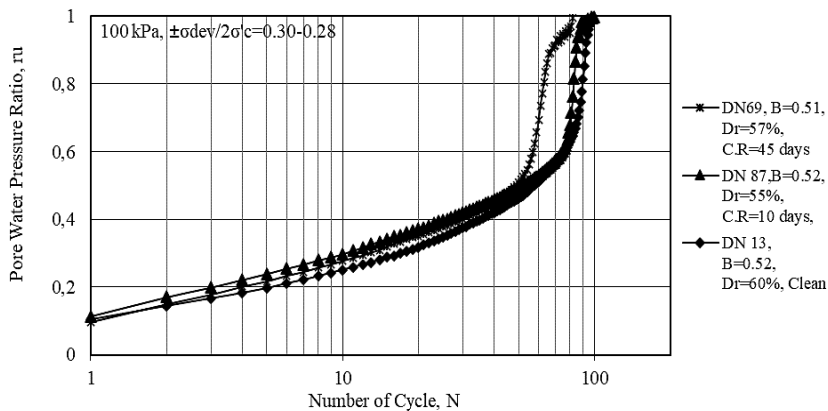


Figure 7. DN69, DN87, DN13 Pore water pressure – Number of cycle.

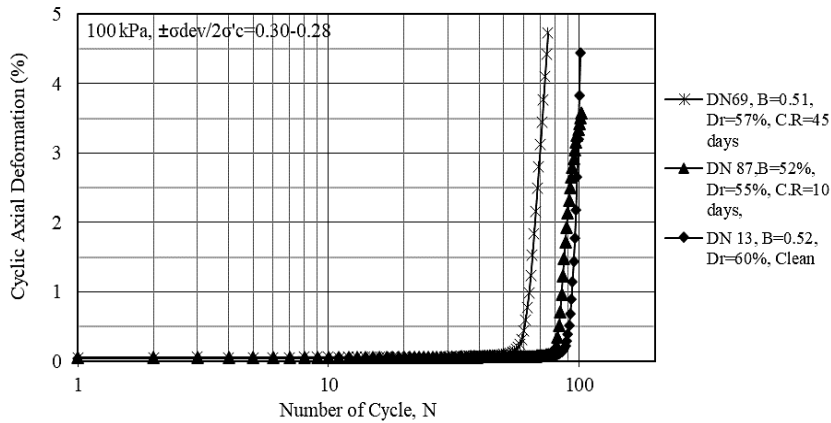


Figure 8. DN69, DN87, DN13 Cyclic axial deformation – Number of cycle.

Another study to compare the contaminated and clean sand samples is given in Figure 9 and Figure 10 below. The saturation value of the clean DN40 sample is $B=0.93$ and the relative density is $Dr=55\%$, the saturation value of the DN31 sample with $t=103$ days curing time is $B=0.60$ and the relative density is $Dr=57\%$ and DN58 sample with $t=299$ days of curing time saturation value was calculated $B=0.57$ and relative density $Dr=52\%$. Dynamic tests were carried out at the stress level $\pm\sigma_{dev}/2\sigma'_c=0.30-0.28$ on the samples that were kept for one day under 100 kPa consolidation pressure.

As shown in Figure 10 clean sand sample with a saturation value of $B=0.93$ reaches the end of $N=32$ cycles, DN31 sample with $t=103$ days and saturation value of $B=0.60$ at $N=35$ cycles, and DN58 sample with a saturation value of $B=0.57$ and cure time of $t=299$ days reached at the end of $N=34$ cycles $\epsilon=\pm 2.5\%$ dynamic axial deformation level. Clean and contaminated sand samples at different saturation values reach a similar number of cycles caused to liquefaction. The pore water pressure ratio reaches all samples $r_u = 1.00$ at the end of the test (Figure 9). Partially saturated contaminated sands exposed to long-term contamination liquefy at a similar number of cycles with clean sand at a saturation degree of $B=0.93$.

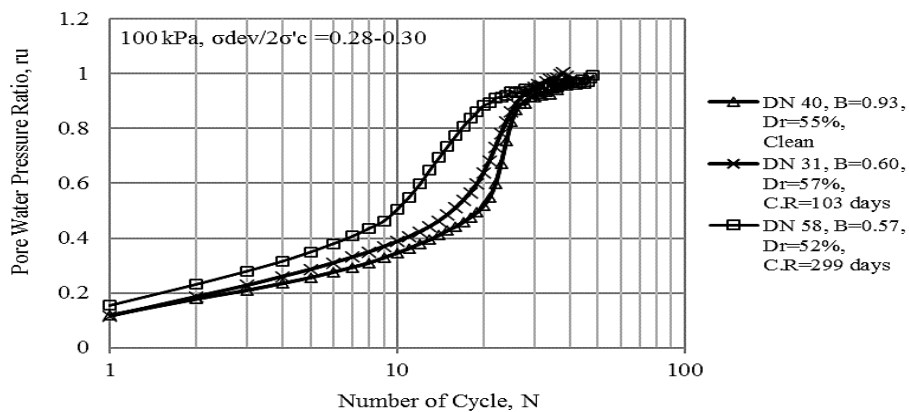


Figure 9. DN40, DN31, DN58 Pore water pressure – Number of cycle.

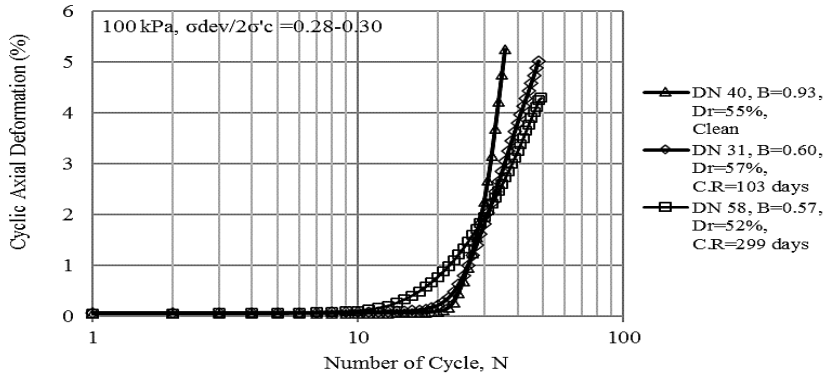


Figure 10. DN40, DN31, DN58 Cyclic axial deformation – Number of cycle.

3.3 Determination of Critical Deformation Values of Clean and Contaminated Sand

When the shear stresses on soils are large enough to generate axial unit stresses and pore water pressures, the axial unit impacts in the soil increase due to the softening of the soil. There is a deformation level at which axial strains and pore water pressure begin to increase rapidly as the effective stress decreases [12-13]. This level, which occurs before the failure deformation, is defined as the critical deformation level. The critical deformation level is determined by where the tangents drawn from the mean effective stress and axial strain cycles intersect, indicating the point of critical deformation.

In this part of the research, the critical deformation level is determined by both partly saturated clean and contaminated sand. For this purpose, three partly saturated sand samples were used and tested $\pm\sigma_{dev}/2\sigma'_c=0.30-0.28$ cyclic ratio. Figure 11 shows the axial strain percentage and mean effective stress relation partially saturated clean sand at Skempton-B value at 0.73, Figure 12 shows the same relation with leachate-contaminated sand at B value 0.6 and short-period curing time (3 days) and Figure 13 illustrate the axial strain percentage and mean effective stress long-period curing time (146 days) at B value 0.45. As shown in the figure, the point where the tangents intersect is defined as the critical deformation level. The behaviors of the both contaminated and clean samples were similar and the critical deformation value is estimated $\epsilon_c = \pm 0.50\%$. It seems that contamination has no effect on changing the critical deformation value.

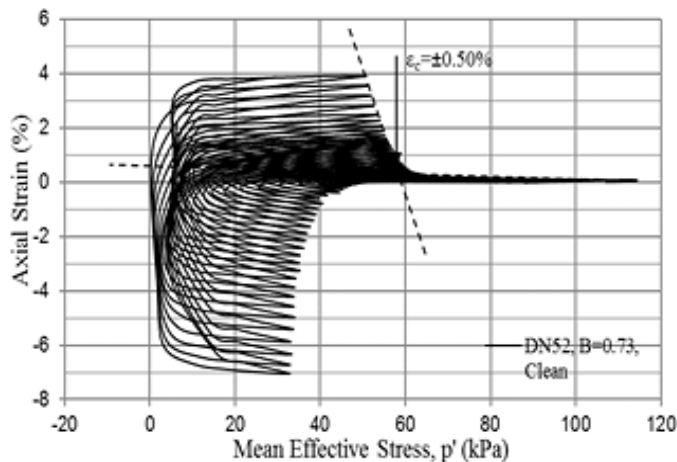


Figure 11. DN52, Axial strain – Mean effective Stress.

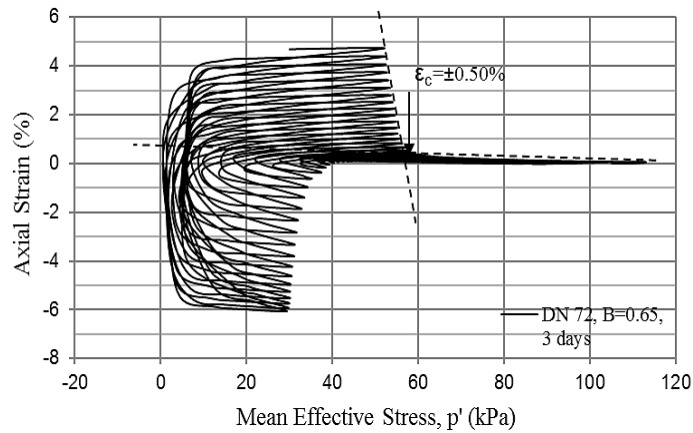


Figure 12. DN72, Axial strain – Mean effective Stress.

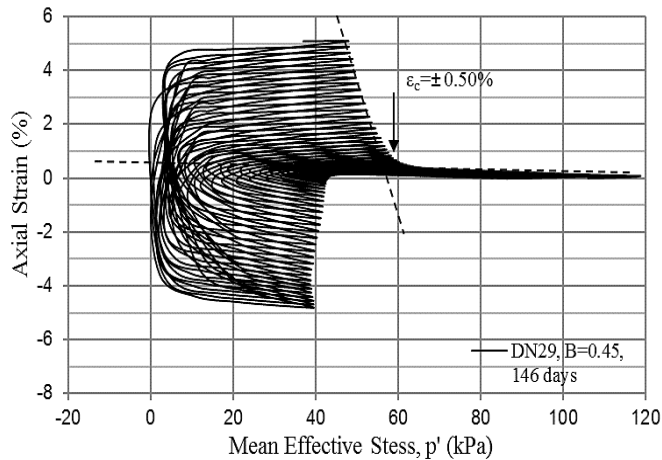


Figure 13. DN29, Axial strain – Mean effective Stress.

4. CONCLUSION

In this study, the effects of leachate on the dynamic behavior of sand were investigated. Clean sand samples and leachate-contaminated sand samples at different curing time were prepared and consolidated at 100kPa pressure for one day were tested. Experiments were carried out at different saturation values at a constant dynamic stress level in the dynamic triaxial test system, and the effect of leachate on liquefaction was investigated by comparing the behavior of clean sand samples with contaminated sand samples. According to the experiments conducted, it was observed that contaminated sands from partially saturated samples having similar saturation value and relative density were more liquefiable than clean sands, and contamination (curing time) in the samples increased the liquefaction potential. It has been previously demonstrated by many researchers that decreasing saturation, increases the liquefaction resistance of clean sands through studies conducted with partially saturated sands in a dynamic triaxial test system [14-15-16-17]. In these studies, researchers revealed that saturated samples were more liquefiable than partially saturated samples.

This study indicates that sand samples contaminated with leachate exhibit higher liquefaction susceptibility compared to clean sand samples, and a longer curing period leads to a rise in liquefaction potential. It has also been observed that long-term contaminated sand at saturation value between $B=0.57-0.60$ liquefies at a nearly same number of cycles with clean sand at saturation value $B=0.93$ show similar behavior.

Considering the critical deformation levels, it was calculated that the critical deformation value in clean and contaminated partially saturated samples at different saturation values was approximately $\varepsilon_c = \pm 0.50\%$. Although the contamination effect increases the liquefaction potential, there is no variation observed in terms of critical deformation behavior. However, it is thought that it affects the liquefaction behavior of leachate contaminated sand samples by physical effect due to the precipitation of organic and inorganic materials it contains, rather than the chemical and biological reaction of leachate components.

Acknowledgements

This research is a part of the Ph.D. thesis prepared by the researcher at Istanbul Technical University.

References

- [1] Turkish Statistical Institute. (2023). Municipal Solid-waste Statistics Report (Report No: 49570). Ankara -Turkiye, 14 Kasım 2023.
- [2] Tuncan M., Khan L., and Pamukçu S. (1988) The effect of leachate on geotechnical properties of clay liner. Hazardous and industrial Waste- Proceedings of the Twentieth mid-Atlantic Industrial waste Conference, 133-144.
- [3] A.J. Roque, and G. Didier, "Calculating Hydraulic Conductivity of Fine Grained Soils to Leachates Using Linear Expression," *Engineering Geology*, 85(2006):147-157
- [4] Nayak S., Sunil B.M., and Shrihari S. (2007) Hydraulic and compaction characteristics of leachate-contaminated lateric soil. *Engineering Geology*, 94, 137-144
- [5] H. Brandl, "Mineral Liners for Hazardous Waste Containment," *Geotechnique*, 1992 42(1):57-65.
- [6] Naeini S, Shojaedin M (2014) Effect of oil contamination on the liquefaction behavior of sandy soils. *Int J Environ Chem Ecol Geol Geophys Eng* 8:289–292. <https://doi.org/10.5281/zenodo.2660830>
- [7] Rajabi H, Sharifpour M (2017) An experimental characterization of shear wave velocity (V_s) in clean and hydrocarboncontaminated sand. *Geotech Geol Eng* 35(6):2727–2745. <https://doi.org/10.1007/s10706-017-0274-0>
- [8] Hosseini, A., & Hajiani Boushehrian, A. (2019). Laboratory and numerical study of the behavior of circular footing resting on sandy soils contaminated with oil under cyclic loading. *Scientia Iranica*, 26(6), 3219-3232. doi: 10.24200/sci.2018.5427.1267
- [9] Masoud Nasiri, Mohammad Hajiazizi, Pornkasem Jongpradist & Ahmad R. Mazaheri (2024) Time-Dependent Behavior of Crude Oil-Contaminated Sands Under Static and Dynamic States, *Soil and Sediment Contamination: An International Journal*, 33:3, 353-374, DOI: 10.1080/15320383.2023.2204981
- [10] G. Tchobanoglous, H. Theisen, S.A. Vigil, "Integrated Solid Waste Management – *Engineering Principles and Management Issues*," 1993, Chapter 11-5, p.417-419.
- [11] Japanese Geotechnical Society Standard. "Preparation of soil specimens for triaxial tests". Tokyo, Japan, JGS 0520-2020, 2015
- [12] Z. Kaya, A. Erken, "Cyclic and post-cyclic monotonic behavior of Adapazari soils," *Soil Dynamics and Earthquake Engineering* Volume 77, 2015, Pages 83-96.
- [13] Z. Kaya, A. Erken, H. Cilsalar, "Characterization of Elastic and Shear Moduli of Adapazari Soils by Dynamic Triaxial Tests and Soil-Structure Interaction with Site Properties," *Soil Dynamics and Earthquake Engineering* Volume 151, 2021, 106966.
- [14] Kamata, T., Tsukamoto, Y., & Ishihara, K. (2009). Undrained shear strength of partially saturated sand in triaxial tests. *Bulletin of the New Zealand Society for Earthquake Engineering*, 42(1), 57–62. <https://doi.org/10.5459/bnzsee.42.1.57-62>
- [15] Zhang, Bo & Muraleetharan, Kanthasamy & Liu, Chunyang. (2016). Liquefaction of Unsaturated Sands. *International Journal of Geomechanics*. 16. D4015002. 10.1061/(ASCE)GM.1943-5622.0000605.
- [16] Arab, A., Belkhatir, M. & Sadek, M. Saturation Effect on Behaviour of Sandy Soil Under Monotonic and Cyclic Loading: A Laboratory Investigation. *Geotech Geol Eng* 34, 347–358 (2016). <https://doi.org/10.1007/s10706-015-9949-6>.
- [17] Chakraborty, P., Roshan, A.R. & Das, A. Evaluation of Dynamic Properties of Partially Saturated Sands Using Cyclic Triaxial Tests. *Indian Geotech J* 50, 948–962 (2020). <https://doi.org/10.1007/s40098-020-00433-3>

Utilization of Engineering Management Principles in the Adoption of Solar Energy in Iraq

Ahmed K. Alboahmed^a, Tuğbay Burçin Gümüş^{b*}

^a *Engineering Management Programme, Istanbul Gedik University, Istanbul, Turkey. aalbohamed@gmail.com*

^b *Department of Industrial Engineering, Istanbul Gedik University, Istanbul, Turkey. burcin.gumus@gedik.edu.tr (*Corresponding Author)*

Abstract

This article explores the application of engineering management principles to overcome energy challenges in developing countries, focusing on Iraq's energy sector. It examines the current situation, challenges, and potential of solar energy in Iraq. The article introduces the topic, reviews relevant literature, and discusses the evolution of Iraq's electricity sector. It highlights challenges and proposes solar energy as a solution. The study evaluates the state of solar energy in Iraq, emphasizing its contextual suitability and potential impact. The research methodology, data analysis, and key findings are outlined, ensuring rigor and validity. The role of engineering management principles in adopting solar energy is explored. The conclusion summarizes research outcomes, offering recommendations for policymakers, stakeholders, and researchers to enhance solar energy benefits in Iraq.

Keywords: Energy Sector; Engineering Management Principles; Solar, Challenges; Adoption; Iraq.

1. INTRODUCTION

This article delves into Iraq's persistent energy challenges, examining the potential of solar energy adoption and how engineering management principles can be instrumental in this transformation. Challenges include war-induced infrastructure damage, overreliance on fossil fuels, and issues like illegal grid trespassing. The article posits that solar energy, with Iraq's abundant sunlight, can revolutionize the energy landscape, bolster economic stability, and align with global environmental goals. The study aims to provide a comprehensive overview of Iraq's energy sector, highlight the advantages of solar power, employ user-based data analysis, and propose a roadmap for solar energy adoption using engineering management principles.

On a global scale, there's an urgent push towards renewable energy sources, particularly solar, as emphasized by international organizations and agreements. The literature review traces the historical evolution of global electric power generation, underscoring the increasing significance of renewable energy [21]. According to Vijayan et al. (2023), engineering management practices play an important role in solar energy projects in developing countries. The adoption and application of engineering management principles in the context of these countries needs to be carefully examined, considering their unique characteristics and challenges. It emphasizes the vital importance of

effectively utilizing engineering management principles for the successful execution and management of solar energy initiatives in such environments [22]. The article puts forth a hypothesis suggesting a robust link between engineering management principles and increased solar energy adoption in Iraq, leading to enhanced living standards and environmental sustainability. The methodology employs a multi-method approach, combining a thorough literature review with a case study in Iraq, incorporating a questionnaire. The research framework involves a comprehensive examination of literature, engagement with end users and experts, and statistical analysis of collected data. Acknowledging limitations such as geopolitical instability, infrastructural constraints, economic challenges, and cultural factors, the study proposes a holistic and multidisciplinary approach to overcome.

In conclusion, the article aspires not only to explore possibilities but to drive a transformative shift by advocating for the responsible adoption of eco-friendly energy sources in Iraq, with a specific focus on solar energy and the strategic application of engineering management principles.

1.1 *Electricity Sector In Iraq*

Iraq's electricity sector faces challenges due to a demand-supply gap, chronic underinvestment, and aging infrastructure. Political instability, corruption, and military conflicts have further strained the sector. Despite these issues, Iraq is taking steps to rehabilitate infrastructure, diversify energy sources, and attract foreign investment. The government's efforts aim to improve reliability, support economic growth, and position Iraq as a key player in the regional energy landscape [10].

In Iraq, electricity consumption is divided across sectors, with the residential category being the largest consumer. The rise in population and urbanization has increased household connections to the grid, leading to a surge in reliance on electricity for daily needs [20]. However, this concentration in the residential sector strains the national power grid, causing frequent shortages and impacting residents' access to essential services. Iraq heavily depends on fossil fuels for electricity, contributing to environmental issues and financial burdens [18]. To address these challenges, Iraq is actively pursuing strategies, including diversifying energy sources, promoting energy efficiency, and investing in renewable projects, aiming to enhance reliability, reduce environmental impact and ensure.

Iraq's electricity sector faces numerous challenges:

- a. *Supply Demand Imbalance*: Meeting the increasing electricity demand is a critical challenge due to population growth, urbanization, and industrial expansion, causing a surge in consumption.
- b. *Infrastructure Deficiencies*: Decades of conflict, neglect, and underinvestment have deteriorated Iraq's electricity infrastructure, leading to reduced efficiency and substantial power losses, impacting healthcare, education, and economic activities.
- c. *Political Instability and Security Concerns*: Frequent government changes, disputes, and security issues hinder long-term planning and discourage investment. Attacks on infrastructure disrupt electricity supply, affecting essential services and deterring foreign investment [9].
- d. *Corruption and Mismanagement*: Corruption diverts funds from infrastructure development, leading to an overburdened power grid. Mismanagement affects project quality, causing frequent outages, straining essential services, and diverting resources from vital public services and infrastructure.

- e. *Lack of Investment:* Despite international support, a significant funding gap hinders modernization and expansion efforts. Security concerns and bureaucratic complexities deter private sector investment, leaving Iraq with outdated infrastructure and frequent power disruptions.
- f. *Environmental Concerns:* Heavy reliance on fossil fuels contributes to environmental degradation, air pollution, and climate change impacts. Iraq's commitment to cleaner energy sources is hampered by current sector composition [7].
- g. *Regulatory and Governance Issues:* Inefficient regulatory frameworks and governance mechanisms create uncertainty and impede modernization efforts. Inefficient pricing methods and subsidies strain public finances, and widespread illegal electricity network use results in substantial state revenue loss.
- h. *Regional and International Dynamics:* Dependence on neighbouring nations for electricity due to limited domestic resources, coupled with geopolitical complexities, leads to energy insecurity, disrupting daily life and economic planning. Iraq needs to diversify energy sources, invest in infrastructure, and engage diplomatically for stable energy relations [2].

1.2 Solar Energy In Iraq

1.2.1 Overview on Iraq's Solar Electricity Capacity

Iraq, with its abundant sunshine, is strategically positioned for solar power harnessing, particularly in the southern and western regions with high solar irradiance levels. The government has initiated various solar projects, including a 750 MW plant in Al-Samawah and a 300 MW project in Al-Dibdibah, aiming to diversify the energy mix, reduce emissions, and decrease reliance on fossil fuels [13]. However, challenges such as political instability, security concerns, infrastructure investments, and regulatory frameworks must be addressed for successful solar sector development. Despite obstacles, Iraq aims for 30% of national demand to be met by renewables, including solar, by 2030 [10].

1.2.2 Potentials of Solar Energy in Iraq

Iraq boasts significant potential for solar energy due to its strategic location, abundant sunshine, and distinctive country attributes:

1.2.2.1 Abundant Solar Irradiance

Situated in the Sun Belt region, Iraq enjoys exceptional solar energy potential, particularly during its long, hot summers. The region experiences consistent sunlight, clear skies, and intense solar radiation, creating an optimal environment for efficient solar power systems. With high solar insolation and extended daylight hours, Iraq is well-positioned for substantial electricity generation from solar sources [2].

1.2.2.2 Optimal Land Availability

Iraq's extensive flatlands in the southern and western regions provide ideal conditions for large-scale solar energy projects. These flat areas offer ample space for solar panel installations, contributing to meeting the country's growing electricity demands. The desert landscapes minimize land-use conflicts, facilitating the deployment of solar installations without significant disruptions. The flat terrain ensures uninterrupted sunlight exposure, maximizing energy production and supporting energy security and sustainability objectives [2].

1.2.2.3 Low Precipitation

Iraq's climate, characterized by low annual precipitation levels and minimal cloud cover, enhances its solar energy potential. Clouds can impede solar panel performance by scattering and blocking sunlight, resulting in inconsistent energy generation. However, Iraq's arid regions with clear skies experience fewer obstacles between the sun and solar panels, ensuring optimal sunlight absorption and a more predictable energy generation pattern. This reliability benefits both energy consumers and providers [2].

Capitalizing on these factors, Iraq has a unique opportunity to transition towards a sustainable and resilient energy future, diminishing reliance on fossil fuels, mitigating environmental impact, and fostering economic development. Successful implementation necessitates supportive policies, substantial infrastructure investments, capacity building, and collaborative efforts among stakeholders [12]. With a comprehensive strategy, Iraq can fully unlock the potential of solar power, paving the way for a sustainable and resilient energy future.

1.2.3 Potentials of Solar Power in Addressing Iraq's Electricity Challenges

The myriad challenges facing Iraq's electricity sector, a comprehensive strategy is imperative. This must encompass infrastructure rehabilitation, energy diversification, policy reforms, good governance, regional cooperation, and climate change adaptation. Successfully addressing these issues promises enhanced energy security, improved citizen well-being, and sustainable socio-economic development. The main challenges faced are also outlined in Figure 1.

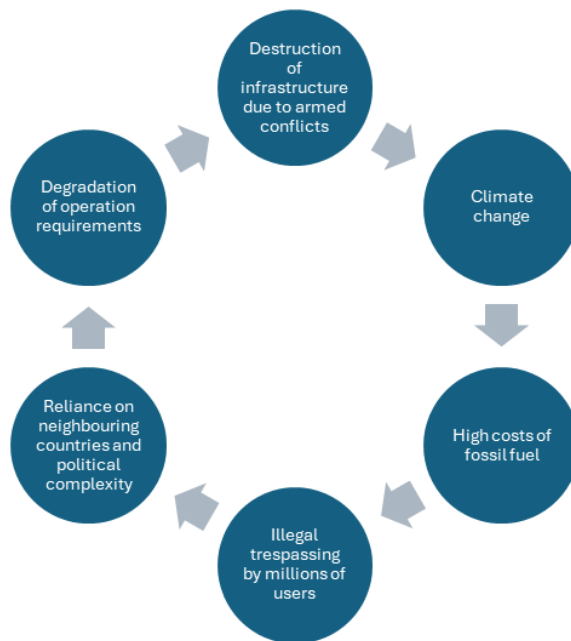


Figure 1. Key Challenges Analyzed [1].

It is imperative to consider that a successful implementation hinges on establishing a robust framework encompassing supportive policies, substantial investments in research and development, enhanced capacity building initiatives, and fostering collaborative partnerships among stakeholders [1]. With a comprehensive and multifaceted strategy in place, Iraq can confidently stride towards a sustainable, secure, and resilient energy future, contributing to a globally responsible and eco-conscious tomorrow.

2. METHODOLOGY

The term "multi-method study" refers to a study where many distinct research methodologies are employed to address related questions effectively. "Different paradigms each focus attention on different aspects of the situation, and so multimethod research is necessary to deal effectively with the full richness of the real world" [14].

To uphold ethical and scientific standards while conducting rigorous research and producing dependable results, a systematic approach was employed. This approach included meticulous questionnaire design, effective web-based distribution, a combination of secondary and primary data collection methods, and an extensive data analysis phase [16]. The focus was on addressing the intricate challenges associated with the transition to renewable energy in Iraq.

The research process followed can be explained in the below three key phases:

Phase #1: Questionnaire Design:

The 15-questions questionnaire was thoughtfully designed to be easy-to-understand, non-suggestive to any certain opinions, topic-relevant yet comprehensive enough to gather credible information on respondents' personal information, educational backgrounds, habits of electricity consumption, and attitude and positions on solar energy.

Phase #2: Questionnaire Finalization and Data Collection:

During the data collection phase, A pilot testing involving individuals with data expertise was conducted to improve the questionnaire quality. Before the 150 questionnaires were distributed, resulting in 123 valid responses. The adopted approach was a web-based dissemination for ease of access, minimal time and effort, customization, data verification, real-time analysis, cost-efficiency, and environmental friendliness.

Phase #3: Data Processing:

Data analysis stands as a pivotal phase in the research journey, playing a crucial role in translating collected data into meaningful insights. This integral step encompasses both qualitative and quantitative findings, serving as a linchpin in the comprehensive research process by bridging the gap between theoretical concepts and practical application. The resulting outcome not only furnishes well-grounded conclusions but also offers valuable insights. Moreover, the process places emphasis on acknowledging the complexity of the transition to renewable energy by considering a multitude of perspectives and opinions.

2.1 Unveiling Perspectives on Renewable Energy Adoption

The planned areas of investigation through the survey commence by emphasizing the collective responsibility of individuals in preserving the environment. Subsequently, it underscores the increasing significance of adopting alternative, clean, and renewable energy sources over fossil fuel systems. The transition is posited to contribute to enhancing the quality of life for future generations, mitigating the degradation of human habitats, and preserving the natural environment. The survey queries individuals about the environmental impact of incorporating energy-saving practices into their daily routines. Additionally, it draws attention to the economic and environmental superiority of technologies facilitating energy conservation [8]. While emphasizing the potential contribution of insulating household surfaces to environmental amelioration, the survey scrutinizes the extent of efforts by government bodies, support organizations, and the private sector in raising awareness regarding the benefits of clean energy utilization. Participants are prompted to express their opinion on the most suitable renewable energy source for investment in Iraq and whether governmental support, particularly in subsidizing the costs of renewable energy technologies, would incentivize citizens to adopt them. The questionnaire also delves into the participants' perspectives on the adequacy of governmental, support agencies', and the private sector's initiatives in promoting the benefits of utilizing alternative clean and renewable energy sources. Moreover, respondents are asked to consider the financial feasibility of long-term investments in installing renewable energy sources, particularly solar energy,

thereby providing a comprehensive exploration of attitudes and considerations regarding sustainable energy practices in Iraq.

3. Results Generation

The empirical data gathered was analysed using SPSS 22. The analysis aimed to gauge energy users' habits and perceptions regarding solar energy in Iraq, contributing to the overarching research topic. SPSS is a widely recognized and extensively employed statistical software that provides a comprehensive platform for data management and statistical analysis [4]. Descriptive statistics were employed to summarize and present the key features of the dataset, offering insights into the central tendencies and variability of the collected data. With 150 respondents following a diverse and inclusive selection criterion, the questionnaire captured insights from individuals of varied ages, sexes, education levels, employment statuses, and electric power user relationships. Notably, the high response rate of 82%, with 123 participants, underscores the research's significance and the effectiveness of the data collection approach. The scrutinized data allowing for meaningful findings, pattern identification, and informed conclusions. This marks a crucial point in the research journey, transitioning from data collection to actionable insights, with the robust participation rate bolstering the credibility and reliability of the research. Key Statistical Indicators included the Repose Ratio, Reliability, Likert Scale, Respondents Backgrounds, Standard Deviation, Mean Value, Variance, and Rank Correlation.

| | |
|--|-----|
| $\text{Response ratio} = \frac{123}{150} * 100 = 82\%$ | (1) |
|--|-----|

3.1 Reliability Test

The reliability coefficient, also known as Cronbach's Alpha, can be calculated using statistical tools like SPSS [11]. Ranging from 0 to 1, a higher value indicates greater reliability in the survey tools and items. In this research, Cronbach's Alpha is 0.806, signifying strong reliability and reasonably high internal consistency. Notably, a reliability coefficient of 0.70 or above is considered satisfactory.

Table 1. Questionnaire Reliability Statistics

| Reliability Statistics | |
|-------------------------------|--------------|
| Cronbach's Alpha | No. of Items |
| 0.806 | 12 |

3.2 Employment Status

A total of 123 valid responses were obtained for the survey. The participants' employment status distribution is as Figure 2: 22% were students, 37.4% were employed, 26% were self-employed or freelancers, 4.1% were retired, and 10.6% were homemakers. The largest demographic group consists of employed individuals, constituting 37.4% of the total respondents. Following closely, the second-largest group comprises self-employed individuals and freelancers, accounting for 26%, while students represent the third-largest group with a percentage of 22. The proportion of retired participants is 4.1%, whereas homemakers constitute 10.6% of the total responses. Cumulative percentages represent the total proportion of participants within each category.

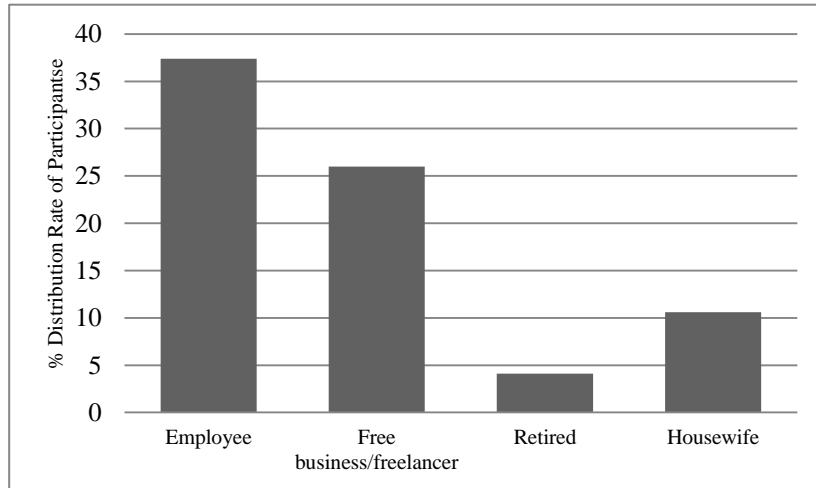


Figure 2. Respondents Employment Status.

3.3 Respondents Educational Levels

The distribution of participants' educational levels is as Figure 3: 48.8% of respondents hold a bachelor's degree (BSC), constituting the largest educational category. Following closely, participants with a master's degree (MSC) make up the second-largest group with a percentage of 13.0. Those with a Doctorate (PHD) represent 9.8% of the respondents. Individuals with diplomas constitute another significant group, comprising 14.6% of the total respondents. Additionally, participants who graduated from high school account for 13.8% of the distribution. Overall, there is a diverse participation in terms of educational backgrounds among the respondents who completed the survey. This distribution aligns with the typical pattern of academic qualifications.

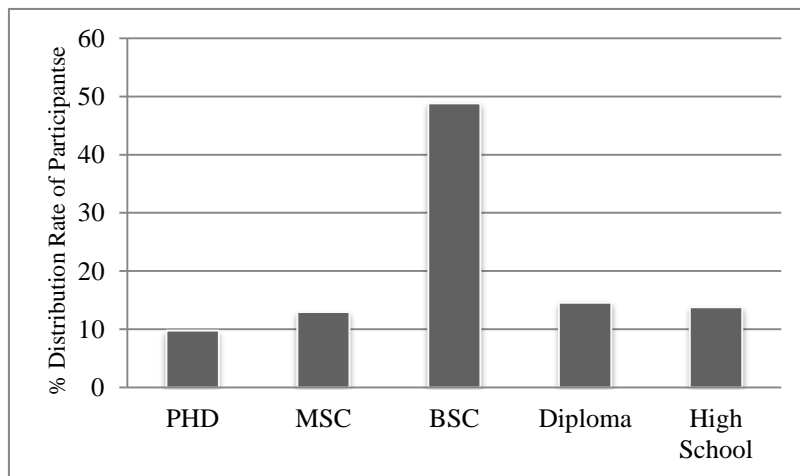


Figure 3. Respondents Educational Level.

3.4 Mean Value

The mean, within the context of mathematical and statistical analysis, denotes the average value derived from a given set of numerical data. Calculation of the mean involves various methods, with the most prevalent being the arithmetic mean. This method entails the summation of all individual values within the dataset, followed by division by the total number of observations [15]. In the specific context of our questionnaire items, mean values

were computed for each item, reflecting the respondents' collective evaluation of the presented statements. These mean values ranged from 4.32 to 3.53, showcasing the spectrum of responses and the degree of agreement or disagreement among the participants. The variability in mean values across different questionnaire items provides insights into the nuances of perceptions or attitudes towards the aspects under investigation, contributing to a more comprehensive understanding of the dataset.

3.5 Standard Deviation

The standard deviation serves as a metric for quantifying the extent of dispersion or variability within a dataset concerning its mean. It is derived by taking the square root of the variance. The standard deviation offers valuable insights into the degree of deviation of individual data points from the dataset's average, providing a measure of the data's overall spread [19]. In the context of comparing datasets or examining the consistency within a dataset, understanding the dispersion of values around the mean becomes crucial. The standard deviation allows for the assessment of the typical distance between individual data points and the mean, thereby indicating the overall stability or variability of the dataset [3]. For the specific questionnaire items under consideration, the computed standard deviation values ranged from 0.739 to 1.188. These values signify the degree of deviation of individual responses from the mean for each respective questionnaire item. A higher standard deviation suggests greater variability among responses, while a lower standard deviation indicates a more clustered distribution around the mean. These standard deviation values contribute to a nuanced understanding of the spread and distribution of responses, aiding in the interpretation of the dataset's reliability and consistency."

3.6 Rank Correlation

Rank correlation is a statistical approach assessing relationships between rankings of ordinal variables, which lack precise numerical values. This method, crucial in fields like social sciences and economics, helps measure agreement or disagreement between different sets of rankings [5]. It is particularly valuable for understanding relationships in data where the order of items holds significance.

Table 2. Statical Analysis of Questionnaire Items

| Question No. | Mean | Standard Error of Mean | Standard Deviation | Variance | Rank |
|--------------|------|------------------------|--------------------|----------|------------------|
| 1 | 4 | 0.084 | 0.932 | 0.869 | 7 th |
| 2 | 4.07 | 0.087 | 0.96 | 0.921 | 5 th |
| 3 | 3.76 | 0.107 | 1.188 | 1.411 | 14 th |
| 4 | 3.81 | 0.092 | 1.019 | 1.039 | 13 th |
| 5 | 3.81 | 0.084 | 0.926 | 0.858 | 12 th |
| 6 | 4.06 | 0.085 | 0.943 | 0.89 | 6 th |
| 7 | 3.95 | 0.077 | 0.857 | 0.735 | 8 th |
| 8 | 3.9 | 0.083 | 0.918 | 0.843 | 10 th |
| 9 | 3.94 | 0.072 | 0.803 | 0.644 | 9 th |
| 10 | 4.2 | 0.077 | 0.859 | 0.737 | 2 nd |
| 11 | 3.53 | 0.067 | 0.739 | 0.546 | 15 th |
| 12 | 4.15 | 0.075 | 0.827 | 0.683 | 3d |
| 13 | 4.32 | 0.075 | 0.833 | 0.694 | 1 st |
| 14 | 3.84 | 0.081 | 0.9 | 0.809 | 11 th |
| 15 | 4.14 | 0.076 | 0.843 | 0.71 | 4 th |

Table 2 presents the mean values and corresponding ranks for various questionnaire items, offering insights into the participants' perceptions regarding renewable energy adoption in Iraq. (Rank 1)"It is important that government

agencies increase the construction of renewable energy facilities to generate electric power" received the highest mean value of 4.32, securing the first rank. This indicates a strong consensus among respondents regarding the significance of governmental initiatives in expanding renewable energy infrastructure. (Rank 2) "In your personal opinion, please select the most appropriate source of renewable energy for investment in Iraq?" obtained a mean value of 4.20, ranking second. This underscores the participants' considerations on the optimal choice for renewable energy investment, providing valuable insights for policymakers and investors. (Rank 3) "Contribution from government agencies to subsidize the costs of renewable energy technologies will encourage citizens to use them" received a mean value of 4.15, securing the third rank. This suggests a positive perception of the role of financial incentives in promoting renewable technology adoption among citizens. (Rank 4) "In the long term, investing in installing renewable energy sources (solar) is more financially feasible" garnered a mean value of 4.14, positioning it in the fourth rank. This implies a general acknowledgment of the long-term financial viability associated with solar energy investments. (Rank 5) "Recently, it has been evident that it is getting increasingly important to adopt alternative clean and renewable energy sources instead of fossil-fuel systems" achieved a mean value of 4.07, ranking fifth. This reflects the growing awareness among participants regarding the imperative shift towards cleaner energy alternatives. (Rank 6) "Using energy-saving LED lights and home appliances is a better option in both economic and environmental aspects" attained a mean value of 4.06, securing the sixth rank. Participants generally acknowledge the dual benefits of economic savings and environmental impact associated with energy-efficient technologies. The analysis continues similarly for the remaining items, with mean values decreasing gradually. Overall, the rankings provide a clear hierarchy of priorities and preferences among respondents, offering valuable insights into public attitudes towards renewable energy adoption in Iraq. These findings can guide policymakers, energy planners, and stakeholders in formulating effective strategies for sustainable energy transitions.

3.7 Harmonizing Public Preferences with Engineering Management in Iraq's Sustainable Energy Transition

The outcomes of the survey not only underscore the public sentiment towards renewable energy adoption in Iraq but also provide a nuanced understanding of the factors influencing the preferences and priorities of the populace [6]. As governmental and societal interest increasingly converges toward embracing cleaner and sustainable energy alternatives, the integration of engineering management principles becomes pivotal in navigating the complexities of Iraq's energy transition. The survey's emphasis on the role of government agencies, financial incentives, and long-term feasibility aligns seamlessly with the overarching objective of effectively implementing engineering management strategies [17]. In steering the energy landscape towards greater reliance on renewable sources, engineering management principles offer a structured approach to address challenges, optimize resource allocation, and ensure the successful integration of solar energy and other sustainable solutions. As this transition unfolds, the insights gleaned from the survey stand poised to inform evidence-based decisions, facilitating a harmonized constructive collaboration between public aspirations and strategic engineering management in realizing Iraq's sustainable energy future.

3.8 Utilizing Engineering Management Principles in Iraq's Energy Transition

Engineering management is a multifaceted and expansive field with a wide range of principles and practices that can be approached and categorized in many ways, each shedding light on various aspects of the field. Seven key principles of engineering management were identified to support drawing a pathway for Iraq's energy sector transition towards solar source in Table 3.

Table 3. Engineering Management Principles and Solar Energy Transition in Iraq

| Engineering Management Principle | How To Utilize It |
|---|--|
| Integration of Engineering and Management | <ul style="list-style-type: none"> • Strategic Alignment: Develop a clear solar energy strategy that aligns with broader energy goals. • Cross-Functional Collaboration: Form interdisciplinary teams for comprehensive problem-solving. • Effective Communication: Establish robust channels for feedback and reporting to ensure seamless coordination. |
| Project Management | <ul style="list-style-type: none"> • Project Planning: Define clear objectives, scopes, and deliverables for solar power initiatives. • Resource Allocation: Efficiently allocate skilled personnel, equipment, and materials to maximize productivity. • Monitoring and Evaluation: Implement Key Performance Indicators for tracking project progress and ensuring quality. |
| Total Quality Management (TQM) | <ul style="list-style-type: none"> • Defining Quality Standards: Specify rigorous standards for adherence to solar components. • Quality Assurance: Enforce stringent quality control measures for procurement and installation. • Process Improvement: Implement continuous improvement processes and prioritize ongoing training initiatives. |
| Risk Management | <ul style="list-style-type: none"> • Risk Identification: Conduct thorough risk assessments to identify potential threats. • Risk Mitigation: Develop comprehensive strategies for identified risks, including diversification. • Risk Monitoring: Continuously monitor risks and reassess their potential impact to proactively manage challenges. |
| Cost Management | <ul style="list-style-type: none"> • Cost Estimation: Develop precise cost estimates, considering all aspects of the project. • Budget Allocation: Allocate financial resources judiciously, ensuring long-term financial sustainability. • Cost Control: Implement effective mechanisms to prevent cost overruns and optimize expenses. |
| Innovation and Technology Management | <ul style="list-style-type: none"> • Technology Assessment: Continuously assess emerging solar technologies to stay ahead. • Research and Development: Invest in Research and Development for adapting technologies to local conditions. • Pilot Projects: Implement pilot projects to test new technologies in real-world conditions and inform decision-making. |
| Ethics and Sustainability | <ul style="list-style-type: none"> • Environmental Impact Assessment: Conduct thorough assessments to mitigate any adverse effects. • Social Engagement: Involve local communities in the planning process to ensure equitable benefits. |
| Transparency and Accountability | <ul style="list-style-type: none"> • Maintain transparency in project financing, procurement, and operations. • Compliance with Regulations: Adhere rigorously to local and international regulations throughout the entire project lifecycle. |

In the conducted study several constraints and limitations were encountered and should be acknowledged for comprehensive understanding. Firstly, the research was conducted within a specified timeframe, limiting the scope and depth of data collection and analysis. Additionally, language constraint was present as the study relied solely on Arabic and English sources, potentially excluding valuable insights from other linguistic perspectives. Furthermore, the sampling method employed may introduce selection bias due to the overrepresentation of readily accessible or willing participants, thus limiting the generalizability of the findings to the broader population of energy users in Iraq. These constraints should be considered when interpreting the results and implications of the study, providing a nuanced understanding of its contributions and potentials for future research endeavours.

4. CONCLUSION AND RECOMMENDATIONS

Underscores a global shift towards solar energy, supported by regulated entities engaged in research and advocacy. Solar power's advantages, including cleanliness, renewable nature, and economic appeal, are universally recognized. In Iraq's context, abundant sunlight, economic benefits, and environmental advantages make solar energy a pertinent choice. The majority of surveyed respondents in Iraq endorse transitioning to solar power, favour energy conservation, and expect government leadership in solar initiatives. Engineering management principles, covering integration, project management, cost management, risk management, quality management, innovation and technology management, and ethics and sustainability, form a robust framework for successful energy transition.

In driving the transition towards increased reliance on solar energy in Iraq, each of the following stakeholders plays a crucial role, contributing uniquely to the success and sustainability of this transformative initiative. Government of Iraq is at the forefront of solar energy integration, responsible for developing a regulatory framework, establishing financial mechanisms, and allocating resources for national grid development. Concurrently, investments in research and development are crucial for enhancing solar technologies and ensuring long-term viability. Private Sector is crucial for developing and operating solar projects, investing in construction and maintenance. Collaboration with international firms is essential for technology transfer and expertise. Private entities engage with local communities to ensure social and environmental alignment, and public-private partnerships are explored for expanding solar capacity and enhancing investment opportunities, promoting sustainable energy growth. International Community, including entities like the United Nations, governments, and non-governmental organizations, supports Iraq's solar energy transition through financial aid and grants, facilitating infrastructure development and knowledge exchange. Collaboration with global research centres promotes mutual benefits and technological advancements. Participation in regional energy initiatives, particularly cross-border sharing of solar power, enhances regional energy security and sustainability.

Collaboration with Neighbouring Countries enhances local and regional energy security. Exploring cross-border energy trade agreements allows efficient use of surplus solar power for regional energy needs. Sharing best practices in solar energy integration fosters regional knowledge exchange. Establishing joint research and development programs promotes solar technology advancements, benefiting the entire region. A regional consortium for renewable energy fosters collaborative efforts to address energy challenges. Research and Academic Institutions lead innovation and education in renewable energy, conducting research for advanced solar technology, providing specialized education and training, collaborating internationally for knowledge exchange, and offering data-driven insights for evidence-based decision-making. Citizens' active involvement is crucial for the success of solar projects in Iraq. Their participation in energy conservation and community-based solar projects fosters a sense of ownership and sustainability. Advocating for sustainable energy policies and promoting solar power adoption further drives awareness and support for solar energy in Iraq.

The roadmap for the adoption of solar energy in Iraq presents a structured approach that emphasizes collaboration and sustainability over a defined period. It begins with Phase 1 focusing on establishing the necessary regulatory framework, infrastructure, and initial investments from both the government and private sector. Phase 2 sees the scaling up of solar energy projects, with increased support from the government and continued engagement with international partners. Phase 3 aims at achieving energy security and sustainability through further expansion of solar capacity, regional collaborations, and integration into the national grid. Finally, Phase 4 emphasizes the long-term sustainability and community involvement, highlighting the importance of stable regulatory environments, innovation, citizen participation, and advocacy for sustainable energy practices. Overall, the roadmap provides a comprehensive strategy for Iraq's transition to solar energy; It asserts the potential for a sustainable energy future while acknowledging the complexities involved.

Acknowledgements

This research is a part of the master's thesis prepared by the researcher at Istanbul Gedik University.

Funding

There are no financial interests in this study.

Declaration of Competing Interest

There is no conflict of interest in this study.

References

- [1] Abed, F. M., Al-Douri, Y., and Ghazi M.Y., Al-Shahery. (2014). Review on the energy and renewable energy status in Iraq: The outlooks. USA.
- [2] Al-Saffar, F., Salim S., Sallam, S., and Jamal, M., (2021). Iraqi Electricity Sector Overview, KAPITA Business Hub, Iraq. 7.
- [3] Chen, L., and Wang, G. (2019). "Engineering Management Strategies for Overcoming Barriers in the Adoption of Solar Energy: A Comparative Analysis." *Energy Policy*, 128, 123-134.
- [4] Dincer, I., and Acar, C. (2015). Review and evaluation of the solar and wind resource assessments. *Renewable and Sustainable Energy Reviews*, 52, 1107-1118.
- [5] Hair, J. F., Black, W. C., Babin, B. J., and Anderson, R. E. (2019). *Multivariate Data Analysis*. Pearson.
- [6] Hossain, M. S., & Rahman, S. (2021). "Engineering Management Strategies for the Sustainable Deployment of Solar Energy Technologies: A Case Study in Iraq." *Journal of Cleaner Production*, 289.
- [7] George, D., and Mallery, M., (2010), *SPSS for Windows Step by Step: A Simple Guide and Reference*, 17.0 Update, 10th Edition, Pearson, Boston
- [8] Ghazal, R., & Al-Naimi, S. (2020). "Engineering Management in the Context of Sustainable Energy: Challenges and Opportunities in the Middle East." *Journal of Engineering and Technology Management*, 56, 101571.
- [9] Gupta, R., and Patel, N. (2018). "Strategic Engineering Management for Overcoming Technological and Economic Barriers in Solar Energy Adoption." *Renewable and Sustainable Energy Reviews*, 82, 1245-1256.
- [10] Iraq's Ministry of Electricity Law, No. 53, 2017 - Chapter 4, Article 9, Point 2.
- [11] Istepanian, H., H., (2020). *Iraq Solar Energy: From Dawn to Dusk*. Al-Bayan Centre for Planning and Studies, Iraq
- [12] Kazan, E., and Çolak, M. (2020). "Engineering Management Principles in the Adoption of Solar Energy Technologies: A Case Study." *Renewable Energy*, 147, 235-245.
- [13] Li, Y., and Zhang, Z. (2020). "An Engineering Management Framework for Assessing the Viability of Solar Energy Integration into Existing Infrastructure." *Energy Reports*, 6, 1234-1245.
- [14] Mingers, J. (2001). *Combining IS Research Methods: Towards a Pluralist Methodology*. Warwick Business School. United Kingdom. 234.
- [15] Ott, L., and Longnecker, M. (2016). *An Introduction to Statistical Methods and Data Analysis*. Cengage Learning.
- [16] Rajasekar, S., Philominathan, P. and Chinnathambi, V., (2006). *Research Methodology*. Bharathidasan University, India.
- [17] Sharma, S., and Reddy, K. S. (2019). "Engineering Management Approaches for the Successful Implementation of Solar Energy Systems in Developing Countries." *Journal of Renewable Energy*, 75, 456-467.
- [18] Smith, J., and Brown, A. (2018). "Integration of Engineering Management Principles in the Implementation of Solar Energy Projects." *International Journal of Sustainable Energy Planning and Management*, 18(2), 45-60.
- [19] Tabachnick, B. G., and Fidell, L. S. (2019). *Using Multivariate Statistics*. Pearson.
- [20] Wang, L., and Li, J. (2017). "A Comprehensive Engineering Management Framework for Evaluating the Economic and Environmental Impacts of Solar Energy Projects." *Solar Energy*, 158, 789-801.
- [21] Wang, Y., and Zhang, L. (2019). "Engineering Management Strategies for Renewable Energy Implementation in Emerging Economies: Lessons from China's Transition." *Renewable and Sustainable Energy Reviews*, 112, 109-120.
- [22] Vijayan, D. & Koda, E. & Sivasuriyan, A. & Winkler, J. & Devarajan, P. & Kumar, R. & Jakimiuk, A. & Osinski, P. & Podlasek, A. & Vaverková, M.. (2023). *Advancements in Solar Panel Technology in Civil Engineering for Revolutionizing Renewable Energy Solutions-A Review*. *Energies*. 16. 6579. 10.3390/en16186579.



In-plant Logistics Issues and Methodologies Analysis: Case Study

Ozan ATEŞ^a

^a*Department of Industrial Engineering, Istanbul Gedik University, Turkey e-mail:ozan.ates@gedik.edu.tr (*Corresponding Author)*

Abstract

In-plant logistics, unlike other dimensions of logistics, has not been adequately analysed in the literature and practices. Internal logistics, which can be defined as material transportation movements that occur in a closed area by nature, has a high impact on cost, quality and customer satisfaction in the relevant field. Lean logistics is the logistics dimension of lean production. Since logistics activities, like production activities, are ongoing activities, the improvements to be made will have a great impact. This study is presented to both contribute to the gap in the literature and offer solutions to problems related to domestic logistics with a lean perspective. In this study, the solutions offered by a logistics company with problems related to internal logistics and the solutions offered by the author from a lean logistics perspective are included comparatively at the end of the study.

Keywords: In-plant logistics; lean philosophy; lean logistics; logistics.

1. INTRODUCTION

Unlike other dimensions of logistics, there are not enough studies in the literature on production logistics or In-plant logistics. However, logistics occupies an important place in production activities and directly affects the duration of production and product quality. Companies have entered into a process of simplification to get ahead in the competition. As part of this simplification process, one of the important sources of waste is the waste associated with material transportation. In this context, one of the important issues that come to the fore is how the logistics system should be in a lean production environment. Lean logistics is the logistics dimension of lean production. The simpler, more effective and efficient the logistics activities within the facility are the simpler, effective and efficient the activities within the facility (production, warehouse operations, etc.) will be. Because production logistics directly affects the duration and quality of production in terms of timely and damage-free transportation of the transported products (Ateş and Durmuşoğlu, 2023).

The concept of in-plant logistics relates to material handling within a large facility such as a factory or warehouse. Facility layout, stock areas in the warehouse, material handling vehicles, order picking strategies, operational rules for the movement of material transport vehicles, affecting internal logistics are factors (Özdağoğlu, 2003).

In-plant logistics, or In-plant logistics as it is commonly used, is an integral part of the activities within the facility. In this aspect, internal logistics; It differs in nature from logistics activities carried out outdoors with vehicles such as ships, trucks, trains or planes. One of the most important points of internal logistics system design is material handling systems. Different types and features of conveying systems can be used in a production system. Material handling is one of the types of waste that has no inherent value added. Choosing an appropriate material handling system here will ensure that this non-value-added process takes place with the least loss.

Material handling activity in a typical industrial enterprise; It includes 25% of all personnel in terms of the number of employees, 55% of the entire factory area in terms of space used, and 87% of the total production time in terms of processing time (Hiregoudar and Reddy, 2007). As can be seen from the relevant percentages, there is a wide area that can be improved and eliminated from waste. Material handling operations and the equipment used for them are complementary elements that must be taken into account in facility layout. It is not possible for them to separate. A change in the material handling system will change the facility layout, and in the same way, a change in the facility layout will change the material handling system (Stephens and Meyers, 2010).

In their study on in-plant logistics, Ateş and Durmuşoğlu found 34 studies on the subject between 2011 and 2022. 7 of these publications are about warehouse functions, 19 are about material transportation vehicles, and 14 are about cell layout - movement between cells. Some publications deal with more than one topic.

2. IN-PLANT LOGISTICS AND MATERIAL TRANSPORTATION

Various definitions are made regarding material transportation. Material handling is summarized by Tompkins (2003) as follows: “It is an activity that uses the right method to deliver the right amount of material at the right place, at the right time, in the right order, in the right position and at the right cost.” This definition explains that the material handling function should be viewed from a broader system perspective rather than a simple material handling activity (Heragu, 2008).

Another definition of material handling is made by the Material Handling Institute. “Material handling includes basic operations related to the movement of solid or semi-solid bulk, packaged or individual products by means of machinery within the boundaries of a work location” (Sule, 1994).

2. 1. Purposes of Material Transportation in In-plant Logistics

Material transportation cost includes a rate between 20% and 70% of the product cost, depending on the material transported. The aim of designing material handling systems should not only be to minimize design and operational costs, but also to create a system that supports other activities in the production area (Heragu, 2008). Sule (1994) stated that the need for material handling systems and careful planning can be attributed to two situations. First, material handling costs constitute a large part of production costs. The latter affects material handling, operations and facility design. In this case, the main purpose of material handling system design can be shown as reducing production costs through efficient transportation. More specifically, the objectives are stated by Sule (1994) as follows:

- Increasing material flow efficiency by ensuring the availability of materials when and where they are needed
- Reducing material handling costs
- Increasing the use of tools
- Improving safety and working conditions
- Simplifying the production process
- Increasing effectiveness

2. 2. Material Handling Principles in Internal Logistics

There are no hard-and-fast rules on how material handling should be carried out. But there are some basic principles. These principles exist in various numbers according to different sources. According to the Material Handling Industry of America, there are 10 principles regarding material handling as shown below (Url-1):

- Planning
- Standardization
- Work
- Ergonomics
- Unit load
- Space usage
- System
- Automation
- Environment
- Product cycle cost

2. 3. Types of Material Transport Vehicles in In-plant Logistics

There are a wide variety of material handling vehicles depending on production environments, production methods and the product to be produced. Heragu (2008) states that choosing a particular material handling vehicle; It states that it varies according to cost, shape, weight, size, volume of loads, space availability and types of stations. It is also stated that the following questions regarding the material handling vehicle become important at this point:

- Does it allow flexibility?
- Is it cheap and easy to maintain?
- Can it be integrated with existing systems?
- Does it significantly increase production efficiency?

The seven basic material handling vehicles can be classified as follows:

- Conveyors
- Pallet carriers
- Freight wagons
- Crane arms, cranes and hoists
- Robots
- AGVs
- Warehouse material handling vehicles (Heragu, 2008).

Selection of material transportation vehicles is also of great importance in designing the internal logistics system.

Using the right tool at the right time, in the right place, in the right way and for the right product is important for the correct design of the system. Basically, material transportation vehicles; It consists of forklifts, check trucks, pallet trucks, trains, conveyor networks and automatic guided vehicles (Kılıç, 2011).

Material transport vehicles can be classified in different ways, mostly similar, in different sources. Hiregoudar and Reddy (2007) classified material handling vehicles as follows:

- Conveyors
- Cranes
- Industrial trucks
- Positioning equipment
- Unit load generating equipment
- Identification and communication equipment

Johansson (1991) suggested that materials can be supplied to an assembly line in three different ways: continuous supply, batch shipment and kitting. Johansson based these three categories on two foundations. The first of these is that even all part types It is included or part of it is included. Secondly, is it based on the part number of the parts or whether it depends on the assembly product or not. These three line feeding types can be found in a system at the same time, but usually only one of them is included. In a study conducted by Johansson in 2006, a line-feeding system called sequential shipping was introduced method has been determined. In this system, parts coming from the supplier are placed on the line in the order of assembly (Sol, 2010).

Mainly for simplifying material handling systems Baudin offered the following steps:

- Creating plans for each part
- Creating the purchased parts market
- Creating distribution routes
- Creating pull signals
- Continuously improving the system (Baudin, 2004).

3. CASE STUDY

The case study is a study that compares the solutions found by the company in question regarding the internal logistics problems experienced by the company and the solutions offered by the author within the framework of the lean logistics perspective on this problem. The company started storage activities in 2000 and transportation activities in 2003. The company purchased self-owned vehicles in 2008 and started international transportation in 2010. In 2014, they expanded their logistics center from 20,000 m² to 150,000 m². They started railway transportation in 2016 with the purchase of 300 wagons. In 2018, they expanded their storage areas and started medical logistics activities. By starting intermodal transportation services in 2021, the number of self-owned vehicles increased to 350.

Today, FMCG products provide services in many areas, especially in e-commerce, healthcare, automotive and packaging sectors, and offer successful supply chain solutions to their customers, consisting of national and multinational world's leading brands and companies, to provide a competitive advantage in the market. They achieve double-digit growth every year with over 1,500 human resources and over 60 logistics centers across Turkey. The solutions they produced for the internal logistics problems experienced by the company and the solutions produced by the author from a lean logistics perspective are given comparatively in Table 1.

Table 1. In-plant Logistics Issues and Methodologies

| Issue | Firm's Solution | Author's Methodology |
|--|--|---|
| Faulty product transfers from bonded warehouse to free warehouse | Two solutions are offered. <ul style="list-style-type: none"> • Importing the entire invoice instead of carrying out the import transactions in parts • Checking the full/empty location in the warehouse after the transfer | Two solutions are suggested. <ul style="list-style-type: none"> • Product transfer is carried out under the control of an advanced software system (Use of RFID, bar code label) • Limiting partial imports with the software system |
| Incorrect performance of customs warehouse goods acceptance procedures | Weekly stock count | Transferring the goods acceptance delivery note to the software system and systematically comparing the physical products arriving with the delivery note by scanning the incoming products one by one (manually scanning the bar code with the RF terminal or automatic reading with the RFID system). |
| Difference between the ordered product and the products collected from the warehouse | Resolving the error by comparing the pallet scanning time and order quantities from the warehouse management system on a collector basis | Automatic transfer of orders to RF terminals via the system and a warning appears in the system if there is a difference between the order and the product collected. |
| Improperly performing goods acceptance product checks, not preparing a report for the faulty situation | Controlling the time between quantity entry times of pallet scanning information with the warehouse management system | If there is a difference as a result of the systematic comparison of the goods receipt and the physical incoming materials, if a new delivery note or report is not uploaded to the system, the process cannot continue, and the systematic taking of the products into stock is blocked. |
| Loading products into wrong vehicles | Giving a warning sound via the hand terminal if the bar code of the loaded product and the ramp bar code do not match. | If the scanning procedures are ignored, the loading of the products into the wrong vehicle will continue. Automating these reading processes with the RFID system will reduce errors. |

4. CONCLUSION

The concept expressed as internal logistics is a general concept that covers material transportation in a production facility and the movement of stored products within the warehouse. As long as physical production exists, logistics will inevitably exist in line with the need to deliver these products to customers. This study focused on logistics activities taking place within a facility. It is important to re-evaluate the activities in question from a simple perspective and eliminate unnecessary steps that cause waste.

In this context, the problems experienced by a logistics company are mostly related to warehouse activities. The five problems that emerged show that both the personnel cannot fully benefit from the software system and the software system in question cannot fully respond to all the problems of the company. It is a requirement of lean logistics to

avoid manual operations as much as possible, to do repetitive routine physical work with robots, and to do repetitive routine desk work with warehouse management systems. For this reason, improving the software system, installing advanced systems such as RFID systems if possible, and transferring the operations performed by pickers or forklifts to automatic material handling systems should be evaluated.

The company where the application work was carried out has a certain size and is a well-known brand in Turkey. However, the problems they experience show that they do not have sufficient knowledge about lean philosophy in general and lean logistics in particular. If the same situation of not having sufficient knowledge also occurs in other logistics dimensions such as Inbound or Outbound Logistics, it will be revealed that there are many areas where improvement can be made in the company. The gravity of the situation will be understood when other small and medium-sized enterprises that are not of this size are taken into consideration.

As a suggestion for future studies, it will be important to conduct studies that can guide companies in accelerating their transformation in lean logistics. The problems experienced by each company regarding internal logistics may differ depending on the areas in which they operate. However, a study can be conducted based on the common aspects of the internal logistics concept that covers all companies. If necessary, the study in question can be detailed specifically for businesses that have more problems with internal logistics.

Declaration of Competing Interest

The author confirms that there is no known conflict of interest or common interest with any institution/organization or person.

References

Ateş, O. and Durmuşoğlu, M. B. (2023). Methodology for the selection of fuzzy-based transportation method in industrial cells: case study. *Journal of the Faculty of Engineering and Architecture of Gazi University* 38:3 (2023) 1931-1944.

Baudin, M., (2004). *Lean logistics: The Nuts And Bolts of Delivering Materials and Goods*, Productivity Press, New York.

Heragu, S. S., 2008. *Facilities Design*, CRC Pressing, USA.

Hiregoudar, C. and Reddy, B. R., 2007. *Facility Planning & Layout Design: An industrial perspective*, Technical Publications Pune, India.

Kılıç, H. S. (2011) *The design of plant logistics in lean manufacturing environment*, Ph. D. Thesis, Istanbul Technical University, Istanbul.

Özdağoğlu, A. (2003) *Optimization of material handling systems*, Master Science Thesis, Dokuz Eylül University, Izmir.

Sol, E. (2010) *Comparison of kit delivery and line stocking, redesigning intra-logistics activities with a lean logistics point of view and implementation*, Master Science Thesis, Istanbul Technical University, Istanbul.

Stephens, M. P. and Meyers, F.E., 2010. Manufacturing Facilities: Design & Material Handling, Pearson, USA, page: 274.

Sule, D. R., 1994. Manufacturing Facilities, PWS Publishing Company, Boston.

Url-1 < <http://www.mhia.org/learning/glossary>>, Access date: 04.10.2010.



Biological Insights into Energy Storage Technologies

Fatma Ceren Kırmızıtaş^a, Burhan Baran Günder^b, Ali Köse^c *

^aResearch Assistant, Department of Animal and Food Science and Department of Mechanical Engineering, University of Delaware, USA
e-mail: ceren@udel.edu

^bBSc Student, Faculty of Engineering, Department of Mechanical Engineering, İstanbul Gedik University, Türkiye e-mail: 201007002@stu.gedik.edu.tr

^cResearch Assistant, Faculty of Engineering, Department of Mechanical Engineering, İstanbul Gedik University, Türkiye e-mail: ali.kose@gedik.edu.tr (*Corresponding Author)

Abstract

In the face of increasing energy demands and environmental concerns, the search for sustainable and efficient energy storage technologies has intensified. This review presents a holistic survey of innovative solutions by examining biological approaches. The study proceeds through three thematic sections: Biological Fuel Cells and Battery Systems, Photosynthesis and Solar Energy Storage, and Energy Generation at the Cellular Level. The first section, Biological Fuel Cells and Battery Systems describes the integration of biological processes into energy storage mechanisms. The use of biological systems and their contribution to the development of environmentally friendly and high performance energy storage technologies are discussed. In the 2nd section, Photosynthesis and Solar Energy Storage are very prominent in sustainability and energy efficiency issues in terms of both energy production and energy source food production while reducing carbon dioxide with photosynthesis-based energy storage methods. Energy production at the cellular level is discussed in the last section, Adenosine triphosphate (ATP), which is necessary for the cell to perform processes such as growth, reproduction and response to environmental stimuli, is characterized as the primary fuel. ATP production is carried out by mitochondria in animal cells and chloroplast in plant cells. Energy storage at the cellular level is carried out by molecules such as glycogen and lipids in animal cells and starch in plant cells. Considering all three issues, it has been observed that biological-based energy storage methods have numerous advantages in terms of sustainability and energy efficiency. In application areas where engineering approaches are at the forefront, it is thought that it may be possible to design more sustainable and highly energy efficient energy production systems by gaining new perspectives with biology-based simulation studies.

Keywords: Energy Storage System; Bio-battery; Bio-fuel cell; Photosynthesis Energy; Cellular Level Energy.

1. INTRODUCTION

Energy production, which has been one of the most important issues of the past decades, has emerged as a problem of meeting energy needs with increasing population and developing technology. Therefore, the importance of prioritizing studies on energy storage is gaining interest over the years [1]. To eliminate challenges such as the limited fossil fuel reserves of modern fossil fuel-dependent culture, and global warming caused by the combustion of fossil fuels, many alternative storage systems have been developed considering the storage of energy as biomass [2]. To the best of our knowledge, despite discussions on energy storage occurring across biological, chemical, and physical realms in various studies, there appears to be a notable absence of a comprehensive review specifically

<https://doi.org/10.61150/ijonfest.2024020107>

focusing on the biological aspect in the literature [3]. Hence, integrating biological principles into energy storage systems could offer a novel perspective, making it imperative to conduct further research to broaden the scope of biologically inspired applications, which are currently limited in number.

A battery is a system consisting of one or more electrochemical cells that allow chemically-stored energy [3,4]. Many different research studies have been carried out in battery technology, including reduction-oxidation (redox) reactions in the electrolyte placed between two electrodes, one positive and one negative [4,5]. It is acknowledged that ongoing research endeavors will persist in this domain. The increasing energy demand has led to the concept of renewable batteries with advantages such as energy storage, flexible shape, the ability to use renewable biocatalysts, room temperature operation, and readily available fuel sources. It is known that with the invention of bio-batteries, it is possible to reduce the damage to nature caused by traditional batteries made of metal [6].

The process whereby sunlight is utilized to generate high-energy carbohydrates, which eventually form fossil fuels over millions of years, is referred to as natural photosynthesis. However, energy storage methods are insufficient to meet the growing and diversifying needs of the society. Therefore, new methods for harnessing natural photosynthesis to store, transport, and use energy on demand have become one of the major global focuses [7]. Energy storage methods realized with the help of photosynthesis-based bio-inspired techniques have been extensively studied and have shown promising results in solar cell technology. The future scope of solar energy conversion systems is to adapt the results of bio-inspirations and to further improve the operation and performance of solar cells with the production of solar cells with higher promising incident light absorption and power conversion rates [8].

The last thematic issue that will be discussed in this study the expression of energy storage methods with cellular energy production. When cellular energy production is examined, ATP (Adenosine triphosphate) and ADP (Adenosine diphosphate) conversion should be taken into account. The rate of change between these two concepts according to energy use can be explained similarly to the working principle of a battery. In mammalian cells, ADP and phosphate are converted into ATP by reactions such as glycolysis and oxidative phosphorylation. This conversion of ATP can be described as analogous to the charging of a battery. The conversion of ATP to ADP manages the energy required in the cellular process, can be simulated as the discharge process of the battery [9]. Considering this scenario, it appears feasible to elucidate the cellular energy storage method and conventional energy storage methods in a similar manner.

The motivation of this study can be expressed as a study on biological storage methods, which are mentioned as one of the energy storage methods in the literature but have not been classified in detail [1-3]. In this way, it is thought to classify the micro and macro-scale bio-supported energy storage systems used by comparing them. During literature research, the leading biological energy storage studies are classified as biological battery systems, photosynthetic solar storage, and cellular storage [10,17]. In this study, we discussed the these aforementioned topics and evaluate the concepts of energy efficiency, and sustainability at both micro and macro levels in the context of biological systems. In this way, the comparison of conventional fuel cells and batteries with biological fuel cells, and batteries will provide an overview of the methods of photosynthetic energy storage and the concept of ATP in energy storage at the cellular level.

2. Biological Insights into Energy Storage Technologies

In this section, we will classify energy storage systems from a biological point of view and discuss energy storage mechanisms and energy concepts in detail in sub-headings such as Biological Battery and Fuel Cell Systems, Photosynthesis and Storage with Solar Energy, and Cellular Level Energy Production.

2.1 Biological Fuel Cells and Batteries Systems

In this section, biological fuel cells (bio-fuel cells) and biological batteries (bio-batteries), which have different

working principles but have a lot in common, will be described in detail. In addition, the definitions, mechanisms, and comparisons of electrical conversion systems with conventional methods are shared in detail under different headings in this section.

2.1.1 Description of Bio-Fuel Cells and Bio-Batteries

Bio-batteries and bio-fuel cells operating at low temperatures, which have the potential to be environmentally friendly, and suitable for cooperation with renewable energy sources, have a lot in common due to their reliance on biologically derived materials [10].

Bio-fuel cells are bio-electrolysis-based energy conversion devices that utilize enzymes or microorganisms to convert chemical energy into electrical energy. In these systems, electron transfer can take place directly with the help of enzymes or in different structures supported by electrodes [10]. Bio-fuel cells are highly advanced systems that have been developed in recent years based on the cooperation of microbiological cells, organelles such as mitochondria and enzymes [11,12]. Szczupak [13] obtained a living organism that can generate sustainable electrical energy with the help of biofuel cells placed inside mussels. In this way, electrified mussels integrated into batteries were observed to activate devices using the energy produced live.

Bio-batteries can be defined as systems that use biological materials to mimic the energy generation processes of conventional batteries in living organisms. These systems commonly generate electricity from carbohydrates using enzymes as catalysts [10]. Although agricultural products such as sugar-containing fruits and plants, citrus fruits have been proposed as bioenergy sources, some studies have also suggested the use of plant-based wastes such as non-agricultural fruit and vegetable peels, and corn stalks that do not trigger food consumption-related issues [14,15]. Togibasa [14] aimed to develop a affordable, simple, and practical bio-battery from tropical almonds, which have a low risk of food shortage due to their abundance in the region where they are produced.

2.1.2 Mechanisms of Bio-Fuel Cells and Bio-Batteries

Bio-batteries can be characterized as systems that have anode (-) cathode (+) and electrolyte parts, similar to conventional batteries that produce useful forms of energy using renewable energy technologies [8]. Bio-batteries are designed to generate electricity by considering indirect galvanic cell design. Khan and Obaid [15] used a sugar digesting hydrogenase enzyme containing an anode and an oxygen reducing laccase enzyme containing a cathode in their study.

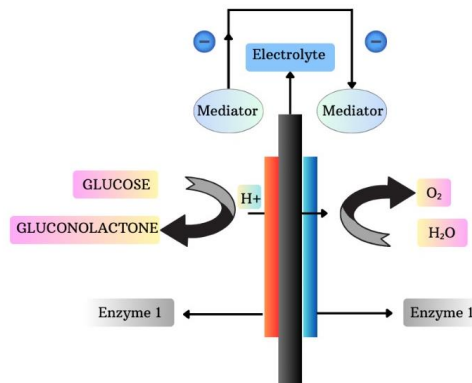


Figure 1. An example of a bio-battery working mechanism.

The working mechanism of the battery starts with the production of hydrogen and electron ions from sugar at the anode. These ions pass to the cathode with the help of the carrier and react with oxygen to form water. Energy is produced thanks to the movement of the released electrons. Figure 1 shows the the working principle of an example bio-battery.

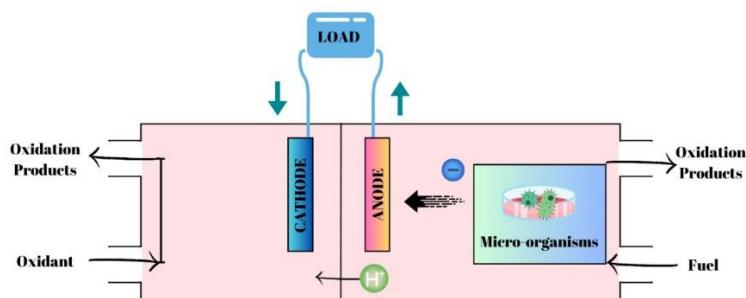


Figure 2. Working mechanism of Bio-Fuel Cells.

The working mechanism of bio-fuel cells is that microorganisms produce electrochemical active materials through fermentation and metabolism and electrons are transported from the anode side to the cathode side with the help of the biocatalytic system. Figure 2 represents the the working mechanism of bio-fuel cells. Energy storage can be achieved through the movement of free electrons. In addition, various types of bacteria and algae such as *Escherichia coli*, *Enterobacter aerogenes*, and *Clostridium butyricum* offer an advantage to the use of hydrogen production in fuel cells [16,17].

2.1.3 Comparison of Bio-Fuel Cells and Bio-Batteries with Conventional Methods

The literature review uncovered that research on applications of bio-fuel cells and bio-batteries is relatively limited, leaving ample room for development in various areas. In both energy storage methods, the concepts of sustainability and energy efficiency emerge when we want to compare bio-based and traditional methods. Since organic materials are used in bio-supported fuel cells and batteries, they do not cause the formation of greenhouse gasses with the use of fossil fuels as in traditional methods. In addition, compared to traditional methods, bio-supported fuel cell and battery systems can be classified under biomass renewable energy technology, which can be expressed with natural and renewable supported organic material. In this context, it can be argued that bio-supported energy storage systems are more prominent in terms of sustainability compared to traditional storage methods. [7,16].

If the concept of energy efficiency is taken into account in traditional methods and bio-assisted methods in fuel cell and battery systems, it will be observed that the amount of energy produced is higher in traditional methods. Since bio-assisted batteries and fuel cells can produce energy directly using biochemical reactions, it can be anticipated that energy efficiency will be higher in bio-assisted systems due to fewer energy losses.

2.2 *Photosynthesis and Storage with Solar Energy*

To date, the type of energy obtained through renewable energy methods is mostly electrical energy. Electrical energy has two disadvantages: the difficulty of storage, and the lower density of stored electricity compared to other fuels. This situation pushes us to design systems that can produce fuel from solar energy. The only biological reaction on our planet that can produce fuel from solar energy is photosynthesis. Photosynthesis refers the synthesis using light. This reaction, which produces carbohydrates and oxygen using carbon dioxide and water, has the potential to be a solution to the greenhouse gas effect and global warming crisis. Produced carbohydrates provide most of the energy needed to support all life on Earth. Moreover, the source of the fossil fuels we currently consume is primitive photosynthetic activities. Currently, photosynthesis is estimated to produce more than 100 billion tons of dry biomass annually, this is equivalent to a hundred times the weight of the total human population on our planet and an average annual energy storage rate [18]. Due to its high energy capacity utilization, scientists are looking for new ways to harness and artificially mimic photosynthesis.

2.2.1 *Natural Photosynthesis*

Photosynthesis is the reaction in which phototrophic organisms such as plants and algae use solar energy to strip electrons from water and reduce carbon dioxide in the air to carbohydrates. Oxygen formed as a result of the oxidation of water makes the air breathable. The fact that we can now breathe is an indication that these reactions continue. Synthesized carbohydrates provide a large portion of the energy needed to support life on Earth. Moreover, the reason for the formation of the fossil fuels we use most is (unfortunately) primitive photosynthetic activity.

We can examine the photosynthesis reaction in two parts. These parts are light-dependent reactions and dark, that is, light-independent reactions. Light-dependent reactions use solar energy to power the synthesis of the energy splitter adenosine triphosphate (ATP) and reduced nicotinamide adenine dinucleotide phosphate (NAPD). Subsequent dark reactions consume these chemicals during the enzymatic reduction of carbon dioxide to carbohydrates. Depending on the dark reaction chain, the efficiency for plants is a maximum of 6%, and for some microalgae grown in small bioreactors, the rate is even higher at 5–7% [19]. Unfortunately, for most crops, actual productivity is often less than 1%. Since the overall efficiency of converting solar energy into electricity with standard silicon-based solar cells is usually 10-20%, instead of producing energy directly using the photosynthesis reaction, we use materials produced as a result of the reaction or develop artificial photosynthesis reactions.

2.2.2 *Energy Storage Via Natural Photosynthesis Method*

Energy storage systems with the natural photosynthesis method use the product resulting from the photosynthetic reaction, that is, the stored form of light energy by phototrophic organisms. The end product of photosynthesis is called Biomass [18]. Wood and other forms of biomass can be converted into other biofuels such as ethanol biogas and syngas and used to generate heat and electricity when needed.

2.2.3 *Artificial Photosynthesis*

Artificial photosynthesis is a technology that mimics the natural process of photosynthesis. In this process, chemical energy is stored using inputs such as sunlight, water and carbon dioxide (CO₂). Artificial photosynthesis is usually carried out by photochemical or electrochemical methods that convert sunlight into electrical energy or chemical bond energy. In energy storage systems in artificial photosynthesis, the products resulting from photosynthesis can be changed by genetic modification to the phototrophic organism, catalysts can be used to increase production or artificial surfaces can be created to imitate the photosynthesis reaction. Among the current projects being worked on in the artificial photosynthesis technique:

In energy storage technologies supported by biological systems, the storage of energy through microalgae

photosynthesis is becoming increasingly significant. Large amounts of biomass and lipid materials such as triacylglycerol can be obtained with microalgae species developed using genetic engineering techniques and metabolic engineering. It has a great impact on improving the economy of microalgae-based biodiesel [20]. Photosynthetic-derived fuel is a promising renewable and carbon-neutral alternative energy reserve. While microalgae provide raw materials for renewable biofuels such as biodiesel, methane, hydrogen, dimethyl furan and ethanol, they can also be used in lands that are not suitable for agriculture by using salt water and wastewater [21]. Many microalgae species are rich in oils, and the biomass of microalgae usually doubles within 24 hours. Effective use of solar energy will provide a great solution to the current energy shortage and environmental pollution caused by non-renewable energy consumption. Therefore, natural simulation of photosynthesis will become an important aspect of using solar energy to produce clean energy. Microalgae can capture solar energy, fix carbon dioxide through photosynthesis, convert light energy into chemical energy and store it in the form of fat in cells [21]. As a result, by using microalgae, we can naturally convert the energy in sunlight into fuel during the photosynthesis process.

The possibility of energy storage through photosynthetic membranes designed by utilizing biological systems is another important issue to be considered. The aim here is to exploit the photocatalytic properties of engineered surfactants in soft (soap film-based) compartments for oxygen-fuel (i.e. carbon monoxide, CO) production and separation.

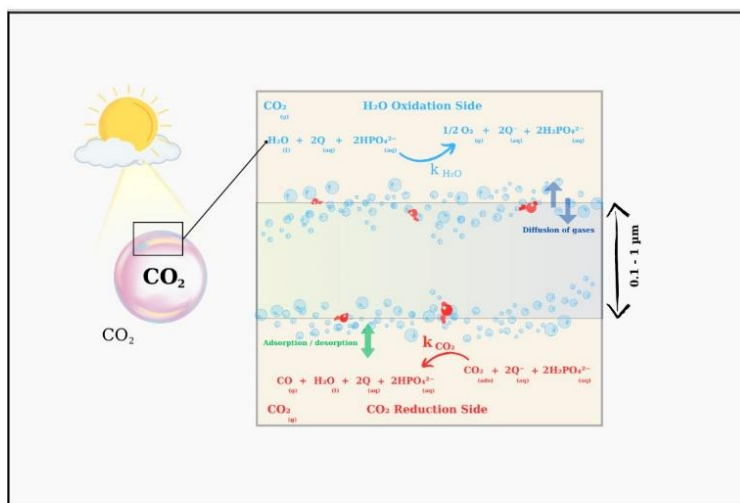


Figure 3. Physicochemical Model of a Reactive Soap Film.

Soap films consist of a water core stabilized by surfactant molecules that self-assemble at gas-liquid interfaces [22]. Figure 3 shows the Physicochemical Model of a Reactive Soap Film. Ideally, a soap film membrane allows molecular catalysts to naturally assemble on the water surface, thus preventing the photocatalytic surface from decreasing in effectiveness due to microbubble formation, thus keeping oxygen and fuel separated for long periods. In the envisioned configuration, the soap film membrane separates two CO₂-filled regions to carry out two half-reactions, the oxidation of water and the reduction of carbon dioxide, in two opposing monolayers of surfactant. These last two half-reactions form part of the desired overall photochemical reaction that converts carbon dioxide into a useful fuel using solar energy.

2.3 Cellular Level Energy Production

Cellular energy production is a fundamental process that fuels the myriad activities of all living organisms, from the simplest to the most complex. Energy production is a cornerstone of life, enabling organisms to carry out certain processes such as growth, reproduction, and response to environmental stimuli. Adenosine triphosphate (ATP) is the primary fuel, also “energy currency”, for that has been efficiently converted via nutrients through a series of intricate biochemical pathways [23]. ATP serves as a versatile energy storing agent owing to the presence of phosphate groups, providing the energy required for cellular processes such as biosynthesis, muscle contraction, active transport, and DNA/RNA synthesis. Cellular level energy production involves multiple interconnected biological pathways, primarily glycolysis, the citric acid cycle (also known as the Krebs cycle), and oxidative phosphorylation [24]. These pathways collectively enable the efficient generation of ATP from substrates such as glucose and fatty acids. Mitochondria are known as the “powerhouse” of the cell and play a central role in maintaining the energy production in normal mammalian cells through cellular respiration. By facilitating glycolysis, the citric acid cycle, and oxidative phosphorylation, mitochondria efficiently generate ATP to meet the energy demands of the cell. ATP synthesis relies on electron flow across the mitochondrial membranes to the specific molecular mechanisms. This electron transfer flow generates a proton gradient across the internal mitochondrial membrane, creating a proton motive force. The flow of protons back across the membrane through ATP synthase drives the synthesis of ATP [25]. The close association between mitochondria and ATP production highlights the importance of these organelles in cellular energy metabolism and overall cellular function. Plants can generate ATP through cellular respiration, similar to mammalian cells. Different than mammalian cells, plants possess electron transport in unique organelles called chloroplast. Electrons enter the chain from the water during photosynthesis, and carbon dioxide reduces to carbohydrates and produces ATP [26]. However, ATP production in plants is complemented by photosynthesis, a process unique to plants and some microorganisms.

In addition to energy production, energy storage is also a critical process in both mammalian cells and plants. ATP cannot be stored in large amounts within the mammalian cells because of the high rapid turnover and demand. Turnover process is tightly regulated via cells to meet the energy demands. In case of excess ATP generation, cells can use glycogen and lipids, high-energy compounds that can quickly regenerate ATP in case of a need [27]. Similar to mammalian cells, ATP is not stored in large quantities within plant cells. Instead, plants maintain a dynamic equilibrium between ATP synthesis and consumption. Excess energy in plants is stored primarily as starch, a polysaccharide composed of glucose molecules. Starch serves as a long-term energy reserve and is stored in specialized storage organs such as tubers, seeds, and roots. Lipids also serve as an energy storage form in plants, particularly in oil-rich seeds and fruits. Triglycerides are stored in lipid droplets and can be mobilized for energy production when needed.

3. CONCLUSION

In this study, the concepts in biological systems are the diversity of energy storage methods, energy efficiency and sustainability, comparison with conventional (physical and chemical) methods, increasing the use of biological approaches, and enabling the understanding of energy storage at the micro-scale as well as at the molecular or cellular level. The problem of the study is that in the literature, energy storage methods are mostly classified and studied as physical storage such as thermal and magnetic kinetic and chemical storage methods such as hydrogen, battery, and fuel. Since biological scale classification and studies on energy storage methods are limited, a classification study was wanted to be carried out in this field.

The overall investigation of biological energy storage systems in terms of sustainability is as follows:

The concept of sustainability is highly important in energy storage systems where environmental damage is reduced, such as the use of clean energy technologies, the protection of natural resources, and the reduction of greenhouse gas emissions. When the concept of sustainability is taken into account in fuel cell and battery systems, it is a negative situation that the production of normal fuel cells and batteries involves production processes that

adversely affect the environment, such as mining. Bio-fuel cells and bio-batteries, on the other hand, are produced from natural and environmentally friendly materials, which is an important advantage in terms of sustainability. In addition, bio-fuel cells and bio-batteries have more sustainable features compared to normal systems, such as the possibility of producing biological organisms with the use of renewable energy sources and containing biodegradable or recyclable materials. The use of agricultural products containing sugar and protein for electricity production in bio-batteries and bio-fuel cells poses a risk for the reduction of food products. However, the use of vegetable wastes such as corn stalks, fruit and vegetable peels for the glucose requirement of batteries contributes to the formation of a sustainable environment as it will reduce the formation of waste.

Energy storage systems based on photosynthesis can store energy in various forms such as electricity, biofuel or chemicals. Carbon neutral systems are available and can be installed in areas that are not suitable for agriculture, such as saltwater and wastewater. Considering these features, photosynthesis-based systems attract attention with their sustainability even among renewable energy systems. Since it uses carbon dioxide as raw material during production, it improves the air quality of the region. It has the potential to be a band-aid against greenhouse gases and global warming, which are the bleeding wounds of our age. Although there are serious problems in studies on living cells such as algae and plants, keeping their living environments at optimum levels and obtaining products from sunlight at levels as low as 7%, it is likely that engineering solutions will be found soon.

In the concept of sustainability at the cellular level, it is thought that concepts such as the use of energy in the cell when needed and the formation of harmful products will be at the forefront. It is known that CO₂, which is the final product of respiration in living cells, creates a greenhouse gas effect. It can be stated that the use of CO₂ as a primary source of photosynthesis performed by plant cells is important for sustainability in terms of both energy source and gas reduction. In addition, with the help of energy storage products such as stored lipids, glycogen, and starch, the sustainability of the energy required for the growth, reproduction and development of the cell is ensured.

The overall investigation of biological energy storage systems in terms of energy efficiency is as follows:

The concept of energy efficiency examines the efficient use of resources in energy storage technologies, less energy losses, less waste, cheaper costs, etc. Reducing energy losses is said to be an important parameter considering the increasing energy demand and cost for more effective storage of energy resources in a highly efficient way. Although bio-fuel cells and bio-batteries have more advantages over conventional batteries in terms of sustainability, the opposite is the case when energy efficiency is taken into account. It can be said that the energy efficiency of conventional fuel cells and batteries are considerably higher than bio-batteries in terms of their higher energy interpretation and longer life.

The sun's rays exceed our current energy needs by 7000 times. Unfortunately, due to the losses incurred in capturing and storing this energy, the energy obtained is far below the current potential. The only biological reaction that can use solar energy is photosynthesis. Although photosynthetic organisms can capture the sun's rays regardless of wavelength, they can only use red photons to reduce carbon dioxide, so other wavelengths of radiation are first reduced to the red wavelength for use. The energy left over from the reduction is converted into heat energy. In the photosynthesis reaction, the efficiency of producing glucose with energy from red photons is 33%. When the energy loss during the conversion of the sun's rays into red photons is taken into account, this rate varies from organism to organism and decreases to approximately 4.5%. The energy stored by photosynthesis on Earth is thought to be quite large, and the global efficiency of natural photosynthetic reactions is 0.1%, given the annual amount of energy that falls on our planet from the sun. The systems studied to increase the efficiency rates are called artificial photosynthesis systems. In the study on genetically modified algae, which is one of the artificial photosynthesis systems, it is seen that this efficiency increases to 7%.

It has been observed that energy efficiency at the cellular level highly depends on the organisms, and the

respective organelle, and the energy storage method. While the organelle that produces energy in animal cells is mitochondria, it is chloroplast in plant cells. As an energy storage method, glycogen can be quickly broken down into smaller branches as glucose in animal cells, and lipid, which can be considered as a long term energy storage unit, and starch can be broken down into glucose when energy is needed, providing a sustainable energy source for the plant. Thus, cellular level energy efficiency can be counted as higher than energy production and storage. While cellular level energy efficiency in biological organisms is indeed remarkable, it's important to recognize that comparing it directly to energy production and storage systems in non-biological contexts may not be entirely straightforward. In conclusion, studying and learning from nature can inspire innovations in energy technology and contribute to more sustainable and efficient energy solutions.

Funding

No funding was received to assist with the preparation of this manuscript.

Conflict of interest

All authors declare that they have no conflicts of interest.

References

- [1] Kalhammer, F. R., & Schneider, T. R. (1976). Energy storage. *Annual Review of Energy*, 1(1), 311-343.
- [2] Goodenough, J. B. (2015). Energy storage materials: a perspective. *Energy storage materials*, 1, 158-161.
- [3] Kozak, M., & Kozak, Ş. (2012). Enerji depolama yöntemleri. *Uluslararası Teknolojik Bilimler Dergisi*, 4(2), 17-29.
- [4] Tamilselvi, S., Gunasundari, S., Karupiah, N., Razak RK, A., Madhusudan, S., Nagarajan, V. M., ... & Afzal, A. (2021). A review on battery modelling techniques. *Sustainability*, 13(18), 10042.
- [5] EFE, Ş., & GÜNGÖR, Z. A. (2021). Geçmişten Günümüze Batarya Teknolojisi. *Avrupa Bilim Ve Teknoloji Dergisi*(32), 947-955. <https://doi.org/10.31590/ejosat.1048673>
- [6] Siddiqui, U. Z., & Pathrikar, A. K. (2013). The future of energy biobattery. *IJRET: International Journal of Research in Engineering and Technology*, 2(11), 99-111.
- [7] Lv, J., Xie, J., Mohamed, A. G. A., Zhang, X., Feng, Y., Jiao, L., ... & Wang, Y. (2023). Solar utilization beyond photosynthesis. *Nature Reviews Chemistry*, 7(2), 91-105.
- [8] Senthil, R., & Yuvaraj, S. (2019). A comprehensive review on bioinspired solar photovoltaic cells. *International Journal of Energy Research*, 43(3), 1068-1081.
- [9] Hardie, D. G., Scott, J. W., Pan, D. A., & Hudson, E. R. (2003). Management of cellular energy by the AMP-activated protein kinase system. *FEBS letters*, 546(1), 113-120.
- [10] Kannan, A. M., Renugopalakrishnan, V., Filipek, S., Li, P., Audette, G. F., & Munukutla, L. (2009). Bio-batteries and bio-fuel cells: leveraging on electronic charge transfer proteins. *Journal of nanoscience and nanotechnology*, 9(3), 1665-1678.
- [11] Bhatnagar, D., Xu, S., Fischer, C., Arechederra, R. L., & Minteer, S. D. (2011). Mitochondrial biofuel cells: expanding fuel diversity to amino acids. *Physical Chemistry Chemical Physics*, 13(1), 86-92.
- [12] Cracknell, J. A., Vincent, K. A., & Armstrong, F. A. (2008). Enzymes as working or inspirational electrocatalysts for fuel cells and electrolysis. *Chemical reviews*, 108(7), 2439-2461.
- [13] Szczupak, A., Halánek, J., Halámková, L., Bocharova, V., Alfonta, L., & Katz, E. (2012). Living battery–biofuel cells operating in vivo in clams. *Energy & Environmental Science*, 5(10), 8891-8895.
- [14] Togibasa, O., Haryati, E., Dahlan, K., Ansanay, Y., Siregar, T., & Liling, M. N. (2019, April). Characterization of bio-battery from tropical almond paste. In *Journal of Physics: Conference Series* (Vol. 1204, No. 1, p. 012036). IOP Publishing.
- [15] Khan, A. M., & Obaid, M. (2015). Comparative bioelectricity generation from waste citrus fruit using a galvanic cell, fuel cell and microbial fuel cell. *Journal of Energy in Southern Africa*, 26(3), 90-99.
- [16] Shukla, A. K., Suresh, P., Sheela, B., & Rajendran, A. J. C. S. (2004). Biological fuel cells and their applications. *Current science*, 87(4), 455-468.
- [17] Song, H. L., Zhu, Y., & Li, J. (2019). Electron transfer mechanisms, characteristics and applications of biological cathode microbial fuel cells—A mini review. *Arabian Journal of Chemistry*, 12(8), 2236-2243.
- [18] Berber, J. (2007). Biological solar energy. *Philosophical Transactions of the Royal Society A: Mathematical, Physical and Engineering Sciences*, 365 (1853), 1007-1023.
- [19] Cogdell, R. J., Gardiner, AT, Molina, P. I., & Cronin, L. (2013). The use and misuse of photosynthesis in the quest for novel methods to harness solar energy to make fuel. *Philosophical Transactions of the Royal Society A: Mathematical, Physical and Engineering Sciences*, 371(1996), 20110603.
- [20] Xie, Y., Khoo, KS, Chew, KW, Devadas, VV, Phang, SJ, Lim, HR, ... & Show, PL (2022). Advancement of renewable energy technologies via artificial and microalgae photosynthesis. *Bioresource Technology*, 363, 127830.

- [21] Fayyaz, M., Chew, K. W., Show, P.L., Ling, T.C., Ng, I.S., & Chang, J. S. (2020). Genetic engineering of microalgae for enhanced biorefinery capabilities. *Biotechnology advances*, 43, 107554.
- [22] Falciani, G., Bergamasco, L., Bonke, S.A., Sen, I., & Chiavazzo, E. (2023). A novel concept of photosynthetic soft membranes: a numerical study. *Discover Nano*, 18(1), 9.
- [23] Rigoulet, M., Bouchez, C. L., Paumard, P., Ransac, S., Cuvellier, S., Duvezin-Caubet, S., ... & Devin, A. (2020). Cell energy metabolism: An update. *Biochimica et Biophysica Acta (BBA)-Bioenergetics*, 1861(11), 148276.
- [24] Al-Khami AA, Rodriguez PC, Ochoa AC. Energy metabolic pathways control the fate and function of myeloid immune cells. *J Leukoc Biol*. 2017 Aug;102(2):369-380. doi: 10.1189/jlb.1VMR1216-535R. Epub 2017 May 17. PMID: 28515225; PMCID: PMC5505747.
- [25] Bergman, J. (1999). ATP: the perfect energy currency for the cell. *Creation Research Society Quarterly*, 36(1), 2-9.
- [26] Bonora, M., Patergnani, S., Rimessi, A. et al. ATP synthesis and storage. *Purinergic Signalling*8, 343–357 (2012). <https://doi.org/10.1007/s11302-012-9305-8>
- [27] Welte, M. A., & Gould, A. P. (2017). Lipid droplet functions beyond energy storage. *Biochimica et Biophysica Acta (BBA)-Molecular and Cell Biology of Lipids*, 1862(10), 1260-1272.



Dynamic simulation of the performance of a solar assisted heat pump in different climates

Bahareh Alipour^a, Maryam Karami^{b*}, Parisa Heidarnejad^c

^a*School of Mechanical Engineering, College of Engineering, University of Tehran, Tehran, Iran, e-mail:bahareh.alipour72@gmail.com*

^b*Kharazmi University, Faculty of Engineering, Tehran, Iran, e-mail:karami@khu.ac.ir (*Corresponding Author)*

^c*Istanbul Gedik University, Department of Mechanical Engineering, Istanbul, Turkey*

Abstract

One method to reduce energy consumption in buildings is using solar-assisted heat pumps, in which the combination of heat pump and solar collector is used to improve the thermal performance. In this paper, TRNSYS and EES software are used to simulate the performance of an indirect expansion solar-assisted heat pump. Dynamic simulation of the system is performed by changing parameters such as the mass flow rate of the collector working fluid and the collector area in five climates including Hot/Dry, Cold/Dry, Moderate/Humid, Hot/semi-Humid, and Hot/Humid. The results show that, in January, the Cold/Dry climate had the lowest free energy ratio (FER) because of the high space heating load. In this month, the Hot/semi-Humid climate has the highest FER, because of the higher solar radiation and no need for space heating. The annual FER in the Hot/Dry zone is 71% which is higher than that of other zones. The lowest FER is related to Moderate/Humid climate due to high humidity and cloudiness.

Keywords: Solar assisted heat pump; Climatic conditions; Dynamic simulation; TRNSYS.

1. INTRODUCTION

One of the methods of energy conservation is the use of solar-assisted heat pumps (SAHP) so that the temperature of the evaporator of the heat pump can be increased using solar radiation. The SAHP is made from a combination of a heat pump and solar collector, which is used as a heat source to increase the coefficient of performance (COP) [1]. In general, SAHPs are divided into two categories, direct expansion SAHP and indirect expansion SAHP based on how the solar collector and evaporator are connected [2]. In the direct expansion system, the refrigerant of the heat pump circulates directly in the solar collector, which acts as the evaporator of the system. The solar energy absorbed in the collector/evaporator is transferred to the load through the heat pump condenser. In the indirect expansion SAHP, an intermediate fluid such as water is heated in the solar system and then enters a heat exchanger for transferring to the refrigerant.

There are numerous studies on the SAHP performance in the literature. Freeman et al. [3] simulated the performance of the SAHP for providing domestic hot water (DHW) space heating (SH) of a residential building using TRNSYS software. They evaluated three modes: parallel, series and combination. The annual coefficient of performance (COP) for parallel, combined, series and conventional heat pump modes was 2, 2.5, 2.8 and 1.2, respectively. Chaturvedi and Abazeri [4] conducted their experimental study to find the steady state efficiency of a

direct expansion SAHP for water heating. Test results showed that in North American winter environmental conditions, the COP for the system was between 2 and 3. The results of the study by Morrison et al. [5] showed that the annual COP of the SAHP was 1.8 to 2.3 times that of the air source heat pump (ASHP), which saved 44 to 56% of the annual energy consumption. Wang et al. [6] compared the performance of a multifunctional indirect SAHP with a domestic HP that has a solar water heater. The results showed that this pump has a better COP than the HP in terms of electrical energy consumption and efficiency. They also evaluated using four heat exchangers for integrating a heat pump air conditioner, a solar water heater and a heat pump water heater. It is found that the novel SAHP is particularly appropriate for the regions with high solar radiation. Cai et al. [7] investigated a multifunctional indirect SAHP consisting of a multifunctional HP and a solar concentrator collector. They reported that as the solar radiation increased from 0 to 800 W/m^2 , the COP increased from 2.35 to 2.75. By using a suitable storage tank, Youssef et al. [8] stated that the indirect SAHP has more stability in different climates. Ma et al. [9] investigated the indirect SAHP using TRNSYS and EES in Toronto, Canada by modeling one-stage and two-stage CO_2 cycle and R410a refrigerant. The comparison of the systems showed that the performance of the two-stage cycle with a smaller compressor capacity is better than other cycles.

Ammar et al. [10] analyzed a photovoltaic/thermal (PVT)-based SAHP in terms of energy and exergy. The results show that the average COP and exergetic COP are 6.14 and 1.49, respectively. Huan et al. [11] proposed a hybrid system of solar heat pump that can work in series or parallel mode. The performance of the proposed system implemented in a university bathroom in Xi'an region. The average annual COP of the proposed system was 5.7, which is higher than the series and parallel modes, which were 3.3 and 4.3, respectively. In a study, Zhou et al [12] investigated PVT based SAHP experimentally and theoretically. The data were analyzed under typical conditions on winter days in Lüliang, China. A simulation model based on real-world conditions was developed to perform the theoretical evaluation. The comparison showed that the experimental and simulation results are in close agreement, the errors are from 4% to 9.1%, and it assures that this model is reasonable for predicting the seasonal performance of the system. The literature review, done by Lazzarin [13], showed that the heating or cooling can be supplied by the heat pump/chiller loop, in which the condenser of the heat pump increases the DHW temperature in summer or recharge the ground. Liu et al. [14] investigated a low-concentrating PVT-based SAHP to meet the electrical and thermal needs of a university building. The maximum electrical and thermal efficiency were 15.2% and 86.7%. The water-to-water heat pump works stably at a COP higher than 4 and the exergy efficiency of 73%. Meena et al. [15] optimized a solar-assisted heat pump system for water heating applications in colder climatic regions receiving least solar radiation. They found that the COP of the SAHP is about 20.1% higher using the collector with double glazing than that using the collector with single glazing. The performance assessment of PVT-based vapor injection HP indicated that the system COP is 4 in cold climate region with the solar irradiation of 500 W/m^2 [16]. Sun et al. [17] used the photovoltaic/photothermal modules in SAHP systems and reported that the power generation and photovoltaic efficiency are both improved significantly. The operational features of the combined solar-ground source heat pump system was studied and optimized by Zihao et al. [18]. The results showed that the average system COP in the winter typical month (January) for the operation of the soil source heat pump was 3.26.

The purpose of this research is to study the effect of climatic conditions on the thermal performance of an indirect expansion SAHP. The study is done numerically based on meteorological data using TRNSYS-EES co-simulator. The effect of various operating parameters such as the collector area and mass flow rate on the system performance is evaluated using the developed model.

2. SYSTEM DYNAMIC SIMULATION

In this study, the thermal performance of an indirect expansion SAHP is investigated to provide DHW and SH for a one-story house with an area of 100 m^2 with 4 occupants. Figure 1 shows the schematic of the investigated system. At first, the working fluid enters into the flat plate solar collector and heated. If the temperature of the water coming out of the collector is below 20°C , the working fluid of the collector goes to the auxiliary heater to increase

the temperature, and after heating, it goes to the heat pump. If the temperature of the fluid is higher than 20 °C, it will directly enter the heat pump. The working fluid inside the tank is heated by receiving heat from the heat pump condenser and then enters the auxiliary heater to reach the desired temperature (70 °C). This fluid supplies DHW and SH for the case study building and then returns to the tank to be heated again by the heat coming out of the condenser and the cycle repeats.

In this study, the effect of climatic conditions on the performance of the SAHP is investigated considering five different climate zones: Hot/Dry, Cold/Dry, Moderate/Humid, Hot/semi Humid, and Hot/Humid. Five cities of Iran including Yazd, Tabriz, Rasht, Abadan, and Bandar Abbas are selected from the climate zones, respectively. Tehran, the capital of Iran, is also selected because of its importance in terms of energy consumption with more than 8.7 million populations and 3.3 million houses. The characteristics of the selected cities are listed in Table 1.

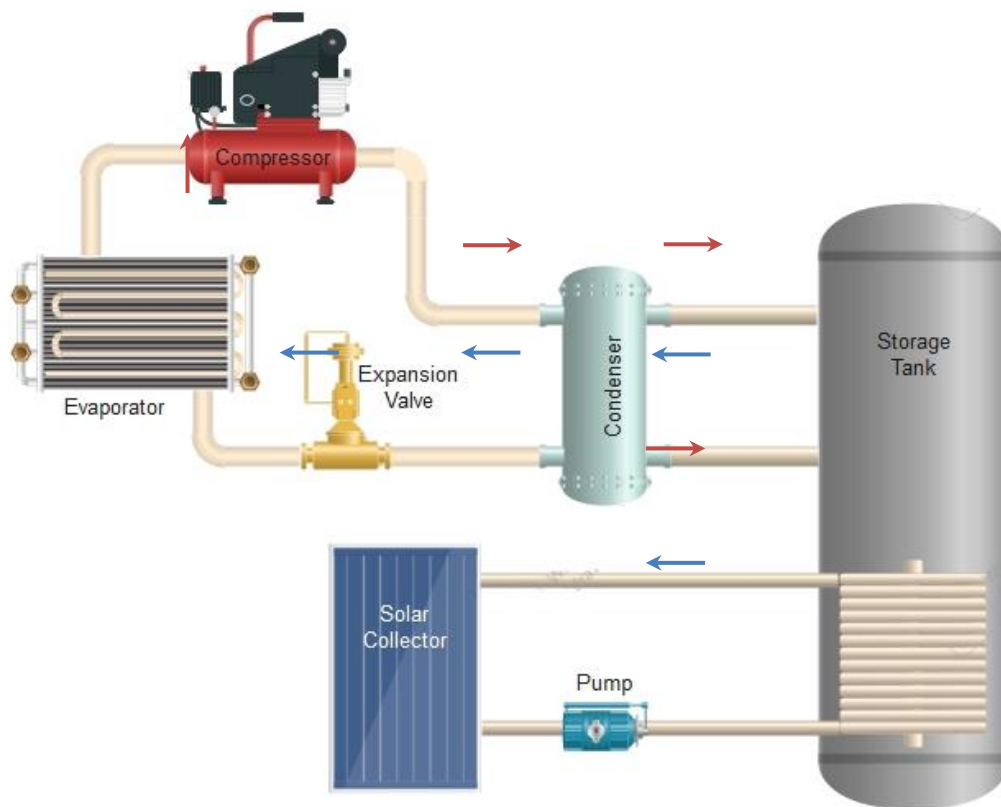


Figure 1. Schematic of the investigated SAHP

Figure 2 indicates the TRNSYS model of the SAHP. It should be noted that system controllers (Type 2b) were used to control the flow rate of the collectors and the storage tanks. For example, if the difference between the outlet and inlet temperature of the collector is less than 5 °C, the collector loop pump will be turned off. Also, if the difference exceeds 10 °C, the pump will turn on. Type 14b is used to simulate the daily DHW demand, of which profile is obtained in Ref. [19]. As mentioned, the cooling and heating loads of the case study building are obtained using Design Builder modeling and the results are coupled with TRNSYS using Type 9e, which calls the calculated thermal and electrical loads by linking to an external excel file.

Since TRNSYS software does not have the ability to simulate the investigated heat pump, the governing equations of the heat pump are coded in EES software and then coupled with the TRNSYS model to determine the amount of heat generated. To write the thermodynamic equations of the heat pump, the temperature and flow rate of

the inlet water are called from TRNSYS model. The refrigerant used in the heat pump is R-134a and the evaporator temperature is considered to be 10°C.

Table 1. Characteristics of the selected cities [20]

| Climate (City) | Longitude (°E) | Latitude (°N) | Outdoor design dry and wet bulb temperature (°C) | | Solar irradiation (kWh/m ² /day) |
|--------------------------|----------------|---------------|--|-------------|---|
| | | | Winter (99%) | Summer (1%) | |
| Hot-Dry (Tehran) | 35.41 | 51.19 | -1.3 | 37.2/18.7 | 5.2-5.4 |
| Hot-Dry (Yazd) | 51.67 | 32.65 | -4.9 | 36.9/15.8 | 5.2-5.4 |
| Cold-Dry (Tabriz) | 46.27 | 38.10 | -8.5 | 34/16.2 | 3.8-4.5 |
| Moderate-Humid (Rasht) | 49.59 | 37.27 | 3 | 29.7/25 | 2.8-3.8 |
| Hot-semi Humid (Abadan) | 48.29 | 30.35 | 6 | 46.7/22.3 | 3.8-4.5 |
| Hot-Humid (Bandar Abbas) | 56.27 | 27.18 | 10.9 | 40.1/25.2 | 4.5-5.2 |

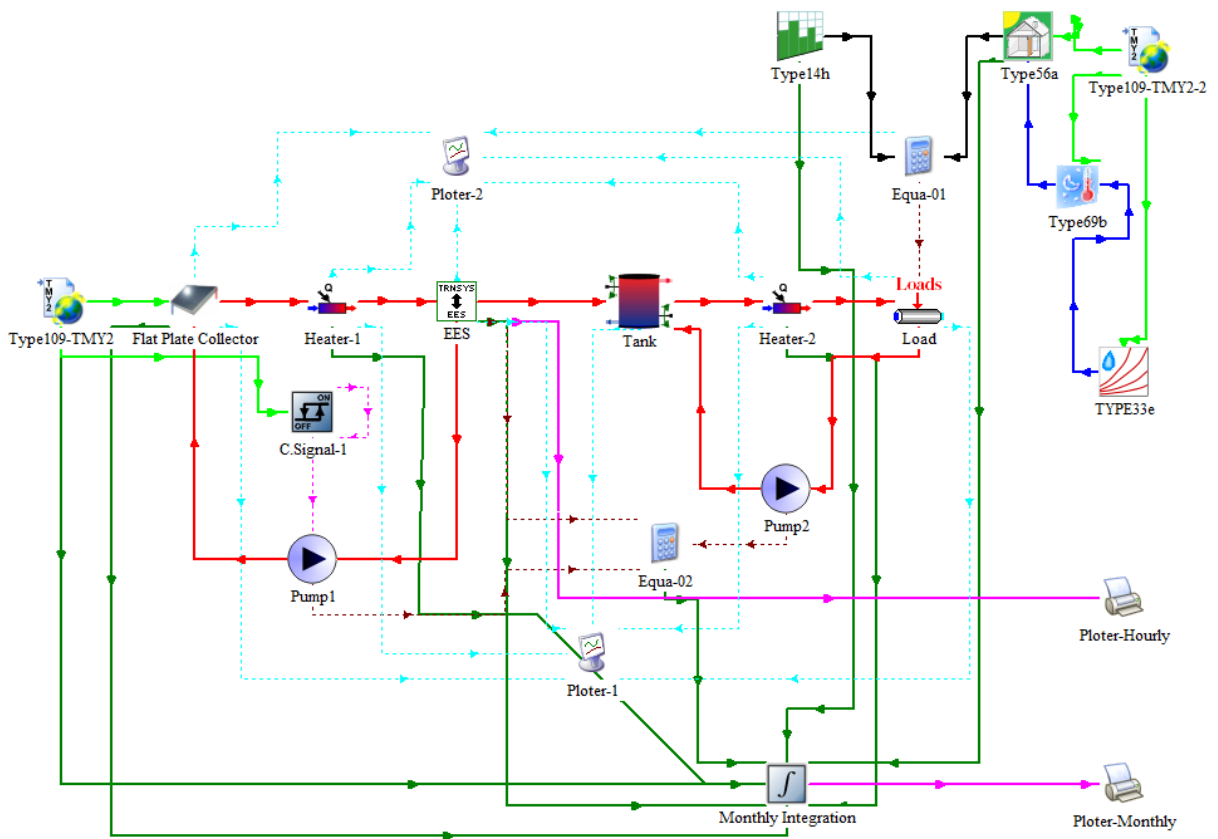


Figure 2. TRNSYS model of the SAHP



Table 2. TRNSYS types and features of the system components

| | |
|--|--|
| Weather Data | <ul style="list-style-type: none"> • Type 109: Weather conditions from METEONORM and solar radiation • Type 66: Sky temperature • Type 33: Psychrometric characteristics |
| Water-to-water heat pump | <ul style="list-style-type: none"> • Type 155 (model for calling MATLAB) |
| Flat plate solar collectors | <ul style="list-style-type: none"> • Type 73 • Area: 5-20 m² • Mass flow rate: 36-144 kg/h • Fluid Type: Water • Maximum efficiency: 0.8 |
| Thermal Storage Tank | <ul style="list-style-type: none"> • Type 4c • Thermal storage tank volume: 0.1 m³ • Thermal storage tank loss coefficient: 2.5 W/m².K • Internal auxiliary heater power: 2.5 kW |
| Circulation Pump | <ul style="list-style-type: none"> • Type 3b • Power coefficient: 0.5 • Maximum power: 1 kw |
| Auxiliary Heater 1 | <ul style="list-style-type: none"> • Type 6 • Heater Efficiency: 0.9 • Maximum heat capacity: 100 kW • Outlet water temperature: 20°C |
| Auxiliary Heater 2 | <ul style="list-style-type: none"> • Type 6 • Heater Efficiency: 0.9 • Maximum heat capacity: 100 kW • Outlet water temperature: 70°C |
| Cooling and Heating Load Module | <ul style="list-style-type: none"> • Type 9e • Type 9e is linked to an external excel file. • Type 682 is used to supply Thermal loads. |
| Control Signal | <ul style="list-style-type: none"> • Type 2d |
| DHW Schedule | <ul style="list-style-type: none"> • Type 14h |
| Diverter Valve and Tee Piece | <ul style="list-style-type: none"> • Type 11f and Type 11h |

2.1. Heat Pump Modeling

Since TRNSYS software does not have the ability to simulate the investigated heat pump, the governing equations of the heat pump are coded in EES software and then coupled with the TRNSYS model to determine the amount of heat generated. To write the thermodynamic equations of the heat pump, the temperature and flow rate of the inlet water are called from TRNSYS model. The refrigerant used in the heat pump is R-134a and the evaporator temperature is considered to be 10°C.

The heat transfer in evaporator is obtained using:

$$\dot{Q}_{evaporator} = \dot{m}_R(h_{R_1} - h_{R_4}) \tag{1}$$

where h_{R_1} and h_{R_4} are the enthalpy of inlet and outlet refrigerant of evaporator and \dot{m}_R is the mass flow rate of the refrigerant in the cycle.

In this study, $\epsilon - NTU$ is used to calculate the heat exchanger effectiveness:

$$\epsilon = \frac{\dot{Q}_{(con.evp)}}{\dot{Q}_{max(con.evp)}} \tag{2}$$

The effectiveness of heat exchangers with phase change such as evaporators and condensers is calculated as follows:

$$\varepsilon_{hx1} = 1 - \exp\left(\frac{-UA}{\dot{m}_{w1} c_{pw}}\right) \quad (3)$$

where UA , \dot{m}_{w1} and c_{pw} is the overall heat transfer coefficient, the collector fluid flow rate, and the collector fluid specific heat, respectively.

The following relations are used to calculate the heat transfer between the refrigerant and the collector working fluid in the evaporator:

$$\dot{Q}_{Wmax} = \dot{m}_{W1} c_{pw} (T_{W1} - T_{R1}) \quad (4)$$

$$\dot{Q}_{water} = \varepsilon_{hx1} \dot{Q}_{Wmax} \quad (5)$$

$$\dot{Q}_{water} = \dot{m}_{W1} c_{pw} (T_{W1} - T_{W2}) \quad (6)$$

$$\dot{Q}_{evaporator} = \dot{Q}_{water} \rightarrow \dot{Q}_{evaporator} = \dot{m}_R (h_{R1} - h_{R4}) \quad (7)$$

Where T_{W1} , T_{W2} , and T_{R1} are the inlet and outlet evaporator temperatures and initial temperature of the refrigerant.

The consumed work by the compressor is obtained by the following relation:

$$\dot{W}_{compressor} = \eta_c \dot{m}_R (h_{R2} - h_{R1}) \quad (8)$$

where η_c is the compressor efficiency.

Regarding the constant enthalpy process in the expansion valve, the heat transfer in the condenser is calculated as follows:

$$h_{R3} = h_{R4} \rightarrow \dot{Q}_{condensor} = \dot{m}_R (h_{R2} - h_{R3}) \quad (9)$$

For calculating the heat transfer from the condenser to hot water storage, the following relations are used:

$$\dot{Q}_{hotwater} = \dot{Q}_{condensor} \rightarrow \dot{Q}_{hotwater} = \varepsilon_{hx2} \dot{Q}_{hotwater_{max}} \quad (10)$$

$$\dot{Q}_{hotwater_{max}} = \dot{m}_{pw} c_{pw} \left(-T_{pw1} + \frac{(T_{R3} + T_{R2})}{2}\right) \quad (11)$$

$$\dot{Q}_{hotwater} = \dot{m}_{pw} c_{pw} (T_{pw2} - T_{pw1}) \quad (12)$$

where \dot{m}_{pw} , c_{pw} , and T_{pw1} are the mass flow rate to hot water storage, the specific heat of the inlet water to the tanks, and the initial water temperature in the condenser, respectively. T_{R2} and T_{R3} are the inlet and outlet refrigerant temperature to/from the condenser.

2.2. Performance Indicators

The COP of the heat pump is the ratio of heat transfer of the condenser to the consumed work by the compressor:

$$COP = \frac{\dot{Q}_{condensor}}{\dot{W}_{compressor}} \quad (13)$$

In this study, the free energy ratio (FER), which is the ratio of the supplied load by the solar energy to the total required load, is used to investigate the system performance:

$$FER = \frac{\dot{Q}_l - \dot{Q}_{aux} - \dot{W}_{comp} - \dot{W}_{pump}}{\dot{Q}_l} \quad (14)$$

where \dot{Q}_l and \dot{Q}_{aux} are the summation of DHW and SH loads and the auxiliary thermal energy supplied by the backup heater.

3. RESULTS AND DISCUSSION

In Figure 3, the monthly variation of system COP for different climates is shown. As can be seen, the maximum COP is about 3.8 and occurred in the Hot/Dry climate (Yazd) in September, because of the low SH load. In warm months, the system COP in Hot/Humid climate (Bandar Abbas) is lower than that in other climate. This is because of the high ambient humidity, which affects the incident solar radiation on the collectors. The annual average COP are 3.3, 3.4, 2.8, 2.6, 2.7, and 2.6, which are respectively obtained in Tehran, Yazd, Tabriz, Rasht, Abadan, and Bandar Abbas. It is found that in humid areas, the COP of the system is minimum, while in dry areas, the maximum COP can be obtained.

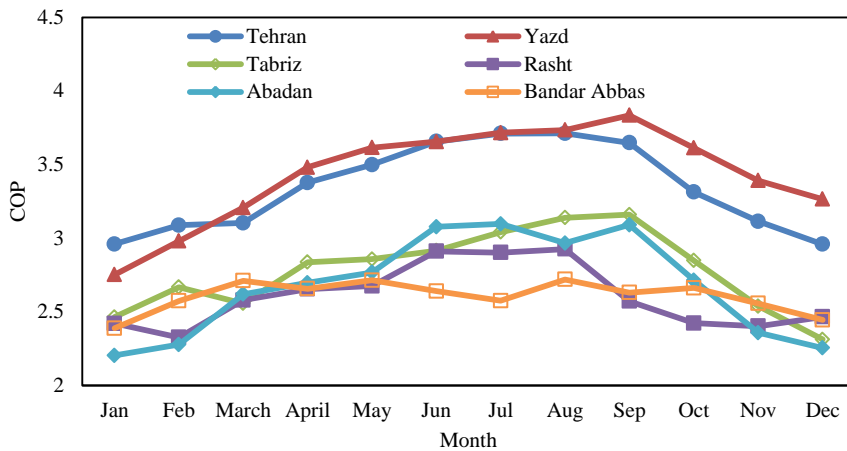


Figure 3. Monthly variation of system COP for different climates

Figure 4 shows the monthly average FER of the system in different climates. As observed from the results, the system works almost the same in the warm months in all cities except Rasht and Bandar Abbas. During this period, due to the high intensity of solar radiation, the use of auxiliary heaters is minimized. In the cold months, the cold weather causes a sharp drop in FER in Tabriz. The reason for the decrease in FER is the using an auxiliary heater in the cold months. Rasht also has the lowest annual FER, which is caused by low radiation and cloudy weather. Due to the high radiation and dry air, Yazd has the highest annual FER among the cities. Although it has a higher geographical latitude than Bandar Abbas and the radiation of Bandar Abbas is more, but it seems that the humidity and air pressure is not ineffective and the duration of cloudiness is an undeniable factor in FER. In January, Yazd has the highest FER with 61%, followed by Bandar Abbas, Abadan, Tehran, Tabriz and Rasht. In July, the FER of all cities except Bandar Abbas and Rasht is almost equal and at the maximum value. In this month, the cities of Bandar Abbas and Rasht have lower FER, which is due to the air humidity in these two cities.

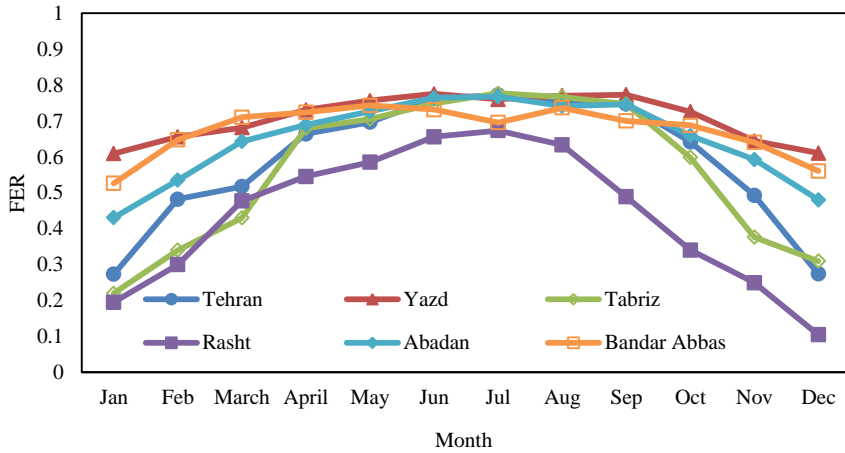


Figure 4. Monthly average FER for different climates

Figure 5 shows the annual average of FER in different climates. Yazd has the highest FER with an annual average of 70%. After that, Bandar Abbas ranks second with an average annual FER of 68% and Rasht has the lowest FER with an annual average of 44%. The reason for the big difference between Rasht and Bandar Abbas is that Rasht is a coastal city that is surrounded by the Caspian Sea on one side and the Alborz mountain range on the other. In this situation, the formation of convective clouds that stay over the city due to its proximity to the mountains makes the sky of this city cloudy in most seasons of the year. The cloud prevents the absorption of maximum radiation and on the other hand it prevents the radiation from the earth to the sky during the night. Humidity itself is one of the important factors in reducing FER. Therefore, the reduction of FER is because of cloudy weather and high humidity. On the other hand, in Bandar Abbas, which is also a coastal city, and there is the Persian Gulf on one side and dry and desert areas on the other, this causes the clouds to easily move in the direction of the wind after the formation in Bandar Abbas and the cloudiness in Bandar Abbas is much lower than in Rasht. This factor causes the air humidity to be high, but the FER rate is much higher compared to Rasht.

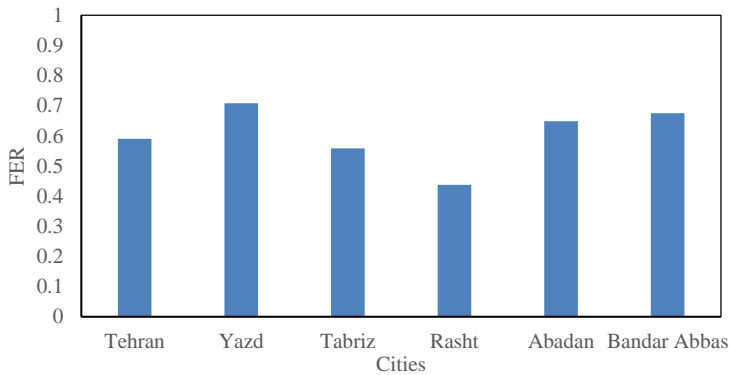


Figure 5. Annual FER for different climates

Table 3 shows the annual FER variations by the collector area in different climates. As can be seen, the largest increase in FER with the increase in the collector area is related to the Rasht by 22.41% for the increase in area from 5 m² to 20 m², which is due to the low solar radiation and cloudy weather of this city. It seems that a collector with an area of more than 15 m² is needed in this city. In Tabriz, with an increase in area from 5 m² to 10 m², the increase

in FER is 16.38%, and with a further increase in area, the FER increases rapidly, so it seems that the collector with an area of 10 m² is more suitable for this city. In other cities, FER changes are less and have almost a constant trend. On the other hand, in Bandar Abbas, there are slight changes with the increase in the collector area, which indicates that the collector area of 5 m² is adequate in this city.

Table 3. Annual FER increase percent with the increase of collector area

| Collector area | Climate zone (City) | | | | | |
|----------------------|---------------------|----------------|-------------------|------------------------|-------------------------|--------------------------|
| | Hot/Dry (Tehran) | Hot/Dry (Yazd) | Cold/Dry (Tabriz) | Moderate/Humid (Rasht) | Hot/semi Humid (Abadan) | Hot/Humid (Bandar Abbas) |
| 5-10 m ² | 9.55 | 10.16 | 16.38 | 21.65 | 11.64 | 3.24 |
| 10-15 m ² | 8.24 | 8.83 | 7.02 | 14.41 | 9.85 | 2.26 |
| 15-20 m ² | 7.49 | 4.23 | 6.13 | 12.34 | 8.85 | 1.07 |

Table 4 shows the annual FER variations due to the increase in the mass flow rate of the collector working fluid in different climates. It can be concluded that the FER increases with the increase of mass flow rate. The increase in the FER with increasing the mass flow rate from 36 kg/h to 72 kg/h in Rasht is very noticeable with an approximate amount of 19% and after that the increase rate decreases. On the other hand, this trend is almost constant in other cities.

Table 4. Annual FER increase percent with the increase of collector mass flow rate

| Mass flow rate | Climate zone (City) | | | | | |
|----------------|---------------------|----------------|-------------------|------------------------|-------------------------|--------------------------|
| | Hot/Dry (Tehran) | Hot/Dry (Yazd) | Cold/Dry (Tabriz) | Moderate/Humid (Rasht) | Hot/semi Humid (Abadan) | Hot/Humid (Bandar Abbas) |
| 36-72 kg/h | 6.55 | 5.18 | 9.92 | 18.98 | 4.98 | 5.42 |
| 72-108 kg/h | 5.48 | 5.95 | 4.08 | 7.52 | 6.41 | 4.10 |
| 108-144 kg/h | 5.86 | 6.27 | 4.21 | 7.92 | 6.81 | 2.89 |

4. CONCLUSION

In this study, the performance of the indirect expansion SAHP using a conventional flat plate collector has been investigated in five climatic conditions. The effect of collector fluid flow rate and area were investigated using the dynamic simulation of the system by TRNSYS. The results indicated that the system in the Hot/Dry zone (Yazd) has the highest FER with an annual average of 70%. In Moderate/Humid zone (Rasht), the system has the lowest FER with an annual average of 44%. Changing the collector area improves the system performance. The average increase of COP and FER for increasing the collector area from 5 to 20 m² in Tehran is 38% and 23%, respectively. The COP and FER increase with the collector mass flow rate. The average increase of COP and FER in Tehran is 40% and 17%, respectively, by increasing the mass flow rate from 36 kg/h to 144 kg/h. It is concluded that considering the system performance and reducing environmental pollution, the use of SAHPs is technically and economically reasonable.

References

- [1] Fu, H.D., Pei, G., Ji, J., Long, H., Zhang, T., Chow, T.T., 2012, Experimental study of a photovoltaic solar-assisted heat pump/heat pipe system, *Appl. Therm. Eng.*40, 343-350.
- [2] Kara, O., Ulgen, K., Hepbasli, A., 2008, Exergetic assessment of direct-expansion solar-assisted heat pump systems: review and modeling, *Renew. Sustain. Energy Rev.*12, 1383-1401.
- [3] Freeman, T. L., Mitchell, J. W., Audit, T. E., 1978, Performance of combined solar-heat pump systems, *Solar Energy*, 22, 125.

- [4] Chaturvedi, S. K., and Shen, J. Y., 1984, Thermal performance of a direct expansion solar-assisted heat pump, *Solar Energy*, 33 (2), 155-162.
- [5] Morrison, G. L., 1994, Simulation of Packaged Solar Heat-Pump Water Heaters, *Solar Energy*, 53 (3), 249-257.
- [6] Wang, Q., Ren, B., Zeng, Z.Y., He, W., Liu, Y.Q., Xiangguo, X., Chen, G.M., 2014, Development of a novel indirect-expansion solar-assisted multifunctional heat pump with four heat exchangers, *Building Serv. Eng. Res. Technol.* 0 (0), 1–13
- [7] Jingyong Cai, Jie Ji, Yunyun Wang, Wenzhu Huang, 2016, Numerical simulation and experimental validation of indirect expansion solar-assisted multi-functional heat pump, *Renewable Energy* 93, 280-290.
- [8] Youssef, W., Ge, Y., Tassou, S. A., 2017, Indirect expansion solar assisted heat pump system for hot water production with latent heat storage and applicable control strategy, 1st International Conference on Sustainable Energy and Resource Use in Food Chains, ICSEF, 180-187, Berkshire, UK.
- [9] Ma, J., Fung, A. S., Brands, M., Juan, N., Moyeed, O.M.A., 2020, Performance analysis of indirect-expansion solar assisted heat pump using CO₂ as refrigerant for space heating in cold climate , *Solar Energy*, 208, 195-205.
- [10] Ammar, A.A., Sopian, K., Alghoul, M.A. et al., 2019, Performance study on photovoltaic/thermal solar-assisted heat pump system. *J Therm Anal Calorim* 136, 79–87.
- [11] Huan, C., Li, S., Wang, F., Liu, L., Zhao, Y., Wang, Z., Tao, P., 2019, Performance Analysis of a Combined Solar-Assisted Heat Pump Heating System in Xi'an, China. *Energies*, 12, 2515.
- [12] Zhou, J., Zhu, Z., Zhao, X., Yuan, Y., Fan, Y., Myers, S., 2020, Theoretical and experimental study of a novel solar indirect-expansion heat pump system employing mini channel PV/T and thermal panels, *Renewable Energy* 151, 674-686.
- [13] R. Lazzarin, 2020, Heat pumps and solar energy: A review with some insights in the future, *International Journal of Refrigeration*, 116, 146-160.
- [14] Liu, Y., Zhang, H., Chen, H., 2020, Experimental study of an indirect-expansion heat pump system based on solar low-concentrating photovoltaic/thermal collectors, *Renewable Energy* 157, 718-730.
- [15] Meena, C.S., Raj, B.P., Saini, L., Agarwal, N., Ghosh, A., 2021, Performance Optimization of Solar-Assisted Heat Pump System for Water Heating Applications. *Energies*, 14, 3534.
- [16] Yao, J., Zheng, S., Chen, D., Dai, Y., Huang, M., 2021, Performance improvement of vapor-injection heat pump system by employing PVT collector/evaporator for residential heating in cold climate region, *Energy*, 219, 119636.
- [17] Sun, T.; Li, Z.; Gou, Y.; Guo, G.; An, Y.; Fu, Y.; Li, Q.; Zhong, X. 2024, Modeling and Simulation Analysis of Photovoltaic Photothermal Modules in Solar Heat Pump Systems. *Energies* 17, 1042.
- [18] Zihao Qi, Yingling Cai, Yunxiang Cui, 2024. Study on optimization of winter operation characteristics of solar-ground source heat pump in Shanghai, *Renewable Energy*, 220, 119517.
- [19] Karami, M., Javanmardi, F., 2020, Performance assessment of a solar thermal combisystem in different climate zones, *Asian Journal of Civil Engineering* 21:751–762.
- [20] Heidarinejad, G., Delfani, S., 2007, Guidelines for the selection of outdoor design conditions for Iranian cities. Tehran: Road, Housing and Urban Development Research Center (BHRC).